FOR REFERENCE

NOT TO BE TAKEN FROM THIS ROOM

FREQUENCY-RESOLVED PHOTOCONDUCTIVITY STUDIES IN AMORPHOUS CHALCOGENIDE FILMS

by

Ercüment Akat

BS. in Physics, Boğaziçi University, 1987

MS. in Physics, Boğaziçi University, 1993

Submitted to the Institute for Graduate Studies in

Science and Engineering in partial fulfillment of

the Requirements for the degree of

Doctor

of

Philosophy

Bogazici University Library

39001100867491

14

Boğaziçi University

2000

ACKNOWLEDGEMENTS

I should like to thank Prof. Dr.Gülen Aktaş, my thesis supervisor, whose criticisms at the sessions held in her office and friendly guidance both during the preparation of the article and in the course of the thesis were invaluable; and whose help was at a *demarcation level,* where she neither boosts the researcher to the end, not to hamper his/her individual work, nor leaves him/her muddled in the process. I should also admit that her way of viewing things, related with or without physics has given me insight.

I acknowledge the generous assistance of my dear friends, Aydın Akkaya with the mounting of the setup, introduction of the system and preparation of the films I measured, and Korel Eraybar with the pictures drawn in computer.

I am under special obligations to Prof.Dr.Durul Ören and Prof.Dr.Emel Çıngı, respectively the former and present Chairs of my affiliate, the Physics Department of Yildiz Technical University who, as a part of a long-time tradition, have kindly loosened my departmental duties during the thesis period.

I would also like to present my sincere thanks to Prof.Dr.Yani Skarlatos who read thoroughly the article and shared his opinion with me.

My sincere thanks go to Prof.Dr.Surkay Akbarov and Asst.Prof.Nazmiye Yahnioğlu who open heartedly helped the copies of the thesis be printed by their own machines.

Last but not least, I should express my genuine appreciation to my mother Mukaddes Akat for the basis she established, her support and patience through the years, and my wife Sezer Akat who has painstakingly helped me at every stage of preparation of the thesis in raw form and never given up her stimulating demeanour in the seemingly long course of the study.

ABSTRACT

FREQUENCY-RESOLVED PHOTOCONDUCTIVITY STUDIES IN AMORPHOUS CHALCOGENIDE FILMS

Frequency-resolved photocurrent measurements (FRPC) were carried out on amorphous chalcogenide films such as AsSeSb AsSe and AsSeTe, by a method called *frequency-resolved spectroscopy (FRS)* as a function of temperature (between 230 K and 395 K), of excitation intensity (between 40 $Watts/m^2$ and 600 $Watts/m^2$) and in the frequency range of 10 Hz to $1.1x10^4$ Hz, yielding the lifetime distribution directly. The results indicate that the recombination is through *distant pairs*, since the lifetime does depend on the excitation intensity, through $\tau = AG^{\nu}$; as $\tau \propto G^{-0.46}$ at 295 K and $\tau \propto G^{-0.77}$ at 395 K, rather than by *geminate* (twin) pairs. It can also be concluded that there is a continuous distribution of states in the mobility gap implied by the value of the exponent 0.72 (in $I_{ph} \propto G^{0.72}$), which is between 0.5 and 1.0, the figures that according to Rose (1978), correspond respectively to monomolecular and bimolecular recombination. The temperature exponent n in the relationship $I_{ph} \propto T^n$ has turned out to be between 7 and 10 for a frequency of some ω_0 (=200 Hz); and 11 and 13 for $17\omega_0$ (=3322 Hz); the value of the exponent showing a diminishing behaviour as the generation rate (intensity of excitation) is elevated.

Finally, the exponent s in the relationship $I_{ph} \propto \omega^s$ is found to depend on both temperature T and the generation rate G in a manner such that the photocurrent will be more sensitive (inversely) to the frequency of excitation as either one of the above variables or both are lowered.

ÖZET

AMORF KALKOJEN FİLMLERDE FREKANS TEPKİLİ FOTOİLETKENLİK ÇALIŞMALARI

AsSeSe, AsSe ve AsSeTe gibi amorf kalkojen filmlerde, fotoiletkenlik ölçümleri, *frekansa bağımlı spektroskopi* yöntemiyle, sıcaklığın (230 K ile 395 K arasında) ve ışık şiddetinin (40 $Watts/m^2$ ile 600 $Watts/m^2$ arasında) bir fonksiyonu olarak, 10 Hz ile $1.1x10^4$ Hz lik frekans aralığında, yaşam süresi dağılımını doğrudan verecek şekilde yapılmıştır. Elde edilen sonuçlar, yaşam süresinin uyarma şiddetine $\tau = AG^{\nu}$ (τ yaşam süresini, G uyarma şiddetini gösterirken A ve ν birer sabit) formülüyle bağımlı olmasından ötürü (295 K de $\tau \propto G^{-0.46}$, 395 K de ise $\tau \propto G^{-0.77}$), birleşme mekanizmasının *ikiz çiftler* değil, *uzak çiftler* yoluyla olduğunu göstermektedir. Ayrıca, bulunan üs değeri olan 0.72 nin, Rose'a (1978) göre, sırasıyla *tekmoleküllü* ve *çiftmoleküllü* birleşmelere karşılık gelen 0.5 ve 1.0 değerleri arasında yer alması nedeniyle, mobilite aralığında sürekli bir durum dağılımı bulunduğu sonucu çıkarılabilir. $I_{ph} \propto T^{n}$ (I_{ph} fotoakımı, T de sıcaklığı gösteriyor) bağıntısındaki üs n'nin, ω_0 (=200 Hz) gibi bir frekans için 7 ile 10 arasında; $17\omega_0$ (=3322 Hz) için ise 11 ile 13 arasında olduğu ve uyarma şiddeti arttıkça azalan bir davranış sergilediği bulunmuştur.

Son olarak, $I_{ph} \propto \omega^{s}$ (ω frekansı gösteriyor) bağıntısındaki üs s'nin hem sıcaklık T' ye hem de uyarma şiddeti G' ye; fotoakım frekansa, bu değişkenlerin biri ya da her ikisi de azaldıkça (ters olarak) daha duyarlı olacak şekilde bağlı olduğu anlaşılmıştır.

TABLE OF CONTENTS

ACKNOWLEDGEMENTS.....iii

ABSTRACT.....iv

ÖZET.....v

LISTOF FIGURES.....vii

LIST OF TABLES.....ix

1. INTRODUCTION.....1

2. THEORY.....4

2.1. Amorphous Solids.....4

2.1.1. Covalent Bond.....4

2.1.2. Semiconductors.....5

2.1.3. Multicomponent Chalcogenide Glasses.....10

2.1.4.Hopping Conductivity.....12

2.1.5.Classification of Amorphous Materials.....14

2.1.6. A Distinction Between two Classes of Materials.....16

2.1.7. Electrical Properties of Chalcogenide Glasses.....16

2.1.8. Density of States.....17

2.1.9. Fermi Energy.....19

2.2. Photoconductivity.....21

2.2.1. Optical Absorption.....21

2.2.2. Photoconductivity in Amorphous Substances.....26

2.3. Recombination and Minority Carrier Injection.....27

2.3.1. Direct and Indirect Recombination.....27

2.3.2.Demarcation Levels....29

2.3.3. Equilibrium and Nonequilibrium Carriers; Nonequilibrium Conductivity....32

2.3.4. Energy Distribution of Nonequilibrium Carriers....37

2.4. Lifetime of Nonequilibrium Carriers....39

2.4.1. Linear and Quadratic Recombination....43

2.4.2. Determination of the Principal Parameters β and τ 47

2.4.3. Frequency Dependence of Photoconductivity and Phase Shift Compensation Method, Sinusoidal Modulation....47

2.4.4. System With One Type of Trap, Steady-State Case....48

2.4.5. TRS and FRS....53

2.4.6. Geminate Pairs....54

2.4.7. Distant Pairs....56

3. EXPERIMENTAL DETAILS....58

3.1. Sample Preparation....58

3.2. Lock-in amplifiers....61

3.3. Experimental Results and Discussion....64

3.4. Dependence of Lifetime on Generation and Temperature....74

3.5. Dependence of Photocurrent on Generation, Temperature and Frequency....81

3.6. Dependence of Frequency Exponent on Generation and Temperature....89

4.CONCLUSION....95

APPENDIX....97

REFERENCES.....101

REFERENCES NOT CITED.....103

LIST OF FIGURES

Figure 2.1. Orbiting of the electrons forming the covalent bond.....5

Figure 2.2. Formation of an electron-hole pair, upon the *arrival* of an incident photon.....6

Figure 2.3. Schematic density of states diagrams for amorphous semiconductors. a-The CFO model, b-the Davis-Mott model, c-modified Davis-Mott model and d-a *real* glass with defect states.....13

Figure 2.4. The possible transitions and recombinations indicating the variations of charges.....22

Figure 2.5.Possible ways of recombining of a free electron with a free hole by way of traps.....23

Figure 2.6. As a result of the incident photon, an e-h pair forms and the electron, after the thermalization and several trapping-detrapping stages, recombines with a hole in the ground state of a luminescent centre.....25

Figure 2.7. The scheme showing the most important transitions in a semiconductor having a wide forbidden band and traps of one type.....46

Figure 3.1. The simplified block diagram for a single phase lock-in amplifier, which measures the component of the signal at a single phase with respect to the reference.....63

Figure 3.2. A schematic representation of the setup used in the measurements.....64

Figure 3.3. Frequency-resolved photocurrent (FRPC) response of an a-AsSeSb sample at the excitation intensities of 600, 200 and 40 Watts/m^2 and for a fixed temperature of 120 C.....68

Figure 3.4. Frequency-resolved photocurrent (FRPC) response of an a-AsSeSb sample at temperatures of 40, 80 and 120 C and for the fixed illumination level of 600 Watts/m^2.....69

Figure 3.5. Frequency-resolved photocurrent (FRPC) response of an a-AsSe sample at the excitation intensities of 600, 200 and 40 Watts/m^2 and for a fixed temperature of 70 C.....70

Figure 3.6. Frequency-resolved photocurrent (FRPC) response of an a-AsSe sample at temperatures of 40, 80 and 140 C and for the fixed illumination level of 200 Watts/m^2.....71

Figure 3.7. Frequency-resolved photocurrent (FRPC) response of an a-AsSeTe sample at temperatures of 40, 70 and 90 C and for the fixed illumination level of 200 Watts/m^2.....72

Figure 3.8. A comparison of the frequency-resolved photocurrent (FRPC) responses of samples of AsSeTe, AsSeSb and AsSe, at a temperature of 60 C and for the fixed illumination level of 40 Watts/m^2.73

Figure 3.9. Photocurrent lifetime versus excitation intensity in an a-AsSeSb sample at 295K and 390 K.....76

Figure 3.10. Photocurrent lifetime versus 1000/T in an a-AsSeSb sample, at two excitation intensities, 600 and 200 Watts/m^2.....77

Figure 3.11. Photocurrent lifetime versus 1000/T in an a-AsSeTe sample, at two excitation intensities, 200 and 40 Watts/m^2.....78

Figure 3.12. Photocurrent lifetime versus 1000/T in an a-AsSe sample, at two excitation intensities, 600 and 200 Watts/m^2.....79

Figure 3.13. Photocurrent lifetime versus ln(T) in an a-AsSe sample, at three excitation intensities, 600, 200 and 40 Watts/m^2.....80

Figure 3.14. Temperature dependence of photocurrent in an a-AsSeSb sample for three excitation intensities, 600,200 and 40 Watts/m^2, taken at $\omega = 200$ Hz.....82

Figure 3.15. Temperature dependence of photocurrent in an a-AsSe sample at the excitation intensity of 600 Watts/m^2 and taken at four different frequencies.....85

Figure 3.16.Temperature dependence of photocurrent in an a-AsSeTe sample at the excitation intensity of 600 Watts/m^2 and taken at four different frequencies..... 86

Figure 3.17. Frequency dependence of photocurrent in a-AsSeTe at –110 C, a temperature which is extremely difficult to get any sensible data for the other two, namely AsSe and AsSeSb, whose photoconductivities are much below that of AsSeTe.....87

Figure 3.18. A comparison of the photocurrents in the three types of films, at the excitation intensity of 600 Watts/m^2 and ω=1529 Hz.....88

Figure 3.19. The temperature dependence of the exponent ν (in $I_{ph} = AG^{\nu}$) for AsSeSb, at frequencies of 200 and 3322 Hz.....91

Figure 3.20. The temperature dependence of the exponent n (in $I_{ph} \propto T^n$) for AsSeSb, at frequencies of 200 and 3322 Hz.....92

Figure 3.21. The temperature dependence of the exponent s (in $I_{ph} \propto \omega^s$) for AsSeSb, at excitation intensities of 600, 200 and 40 Watts/m^2.....93

Figure 3.22. The temperature dependence of the exponent s (in $I_{ph} \propto \omega^s$) for AsSe, at excitation intensities of 600, 200 and 40 Watts/m^2.....94

LIST OF TABLES

Table 3.1. The exponent n in the relation $I_{ph} \propto T^n$, for AsSeSb films, as a function of both the generation rate G and the frequency of excitation ω, within respectively 15-fold and 54-fold ranges.....83

Table 3.2. The exponent n in the relation $I_{ph} \propto T^n$, for AsSeTe films, as a function of both the generation rate G and the frequency of excitation ω, within respectively 15-fold and 200-fold ranges.....84

LIST OF SYMBOLS

a	Bohr radius
c	Speed of light
d	Average separation of a geminate pair
D	Diffusion coefficient
D_n	Electron demarcation level
D_p	Hole demarcation level
e	Electronic charge
E	An energy level
E_a	Activation energy
E_A	Extent of the conduction band
E_B	Extent of the valence band
E_C	Bottom of the conduction band
E_F	Fermi energy
E_{F0}	Fermi energy at $0K$
E_{Fn}	Quasi Fermi level for electrons
E_{Fp}	Quasi Fermi level for holes
E_g	Energy gap or band gap
E_T	Energy of the traps
E_V	Top of the valence band
$f(E)$	Fermi distribution function
$g(E)$	Density of states at E
G	Rate of generation
h	Planck's constant
I	Illumination intensity
k	Coefficient of proportionality
k_B	Boltzmann's constant

m_e	Mass of the electron
m_h	Mass of the hole
m	Density of the trapped states
M	Density of the trapping states
n	Density of free electrons
n_0	Density of electrons in equilibrium
n_r	Density of filled recombination centres
n_t	Density of trapped electrons
Δn	Density of excess electrons
Δn_{St}	Steady-state value of the non-equilibrium electron density
N_C	Effective density of states in CB
N_{CM}	Effective density of states in CB *reduced* to trap level M
p	Density of free holes
p_0	Density of holes in equilibrium
p_r	Density of unfilled recombination centres
p_t	Density of trapped holes
Δp	Density of excess holes
Δp_{St}	Steady-state value of the non-equilibrium hole density
P_V	Effective density of states in VB
P_{VM}	Effective density of states in VB *reduced* to trap level M
$P(\tau)$	Distribution of lifetimes
q_n	Cross section for capturing a free electron
q_p	Cross section for capturing a free hole
r	Distance separating two localized states
t_d	Detection time
T	Temperature
T_S	Deposition temperature
V	Potential
W	Energy difference between two states

α_L	Localization parameter
β	Quantum yield
χ	Electron affinity
ϕ	Phase shift
γ	Exponent of generation
γ_{pk}	Recombination coefficient
λ_C	Critical wavelength
$\mu(E)$	Mobility at energy E
μ_n	Mobility of an electron
μ_p	Mobility of a hole
ν_n^*	Product of the highest lattice frequency and a factor ≤ 1
σ	Conductivity
σ_0	Conductivity prefactor
σ_C	Conductivity due to CB states only
σ_D	Dark conductivity
σ_L	Conductivity due to illumination
σ_{Ph}	Photoconductivity
σ_V	Conductivity due to VB states only
σ_{St}	Steady state conductivity
$\Delta\sigma$	Excess conductivity
τ_0	Lifetime prefactor (~10^{-8} sec)
τ	Lifetime of carriers or mean time between two successive collisions
τ_n	Lifetime of electrons
τ_p	Lifetime of holes
τ_{On}	Response time
τ_{nk}	Lifetime for the recombination of electron with the k th type of hole
υ_n	Thermal velocity of electrons

υ_p	Thermal velocity of holes
ω	Modulation frequency
$\psi(x)$	Wavefunction

1. INTRODUCTION

Amorphous semiconductors of which chalcogenide films (such as a-AsSe, a-AsSeSb or a-AsSeTe) are a member have become increasingly important and have aroused much interest in the last three decades, due to the applications (e.g. optical switching and memory devices) of these films whose technological aspects can be roughly divided into two classes [1].

i- Hydrogenated amorphous silicon (a-Si:H) type alloys, the applications of which include inexpensive solar cells, thin film transistors, image scanners, electrophotography, optical recording and gas sensors; and

ii- Amorphous chalcogenides, whose applications include electrophotography, switching and memory elements.

One should investigate and understand throughly their bandgaps full of localized states which in turn are thought to control the excess carrier processes and thereby determine the photocurrent response in the chalcogenide films. The method of *frequency-dependent photocurrent* measurements is a good way of understanding the recombination kinetics that is supposed to clarify the localized gap states in these films. Under conditions of thermal equilibrium, the thermally generated carriers in a solid are distributed between available energy states according to Fermi statistics (see Section 2.1.9). A certain fraction of these electrons and holes are in conduction states and determine the dark electrical conductivity of the solid which can only be measured if the measurement technique does not itself perturb the thermal equilibrium, e.g. by injection of charge from applied electrodes. The absorption of light which involves the photogeneration of free carriers disturbs the thermal equilibrium and leads to an enhanced number of electrons and holes in conduction states [2]. Under constant illumination a steady-state photocurrent will be reached in which the rate of photogeneration is equalled by the various recombination processes through which the carriers are restored to the normal equilibrium conditions. This disturbance of the

equilibrium distribution of carriers by photoexcitation is the phenomenon of *photoconductivity.*

Among the detailed knowledge for these films required by their technological applications are also their speed, namely the response time of the devices and the lifetimes of the carriers. Besides the technological perspective, we are interested in the chalcogenide materials, either in thin film or in bulk form, from a purely physical point of view.

Some sort of response time can be obtained from a measurement in frequency domain as a phase shift where an excitation light which varies sinusoidally with time is used [3]. The photocurrent induced by such a periodical excitation is named as the *modulated photocurrent.* A phase shift appears between the excitation and the modulated photocurrent, depending on the experimental conditions and the nature of the localized states.

When the excitation light has a photon energy greater than the band gap, an electron can be excited not only to the conduction band but also to localized states just below the band edge. But the density of states of the conduction band is much greater than those of localized states and so it is reasonable to assume that the photocarrier generation is dominated by the band-to-band excitation. One of the two methods that try to study the kinetics is the **time-resolved spectroscopy (TRS)** where the luminescence from the sample excited by a single excitation pulse (in fact a δ-function light pulse) is detected during an infinitely narrow boxcar gate set at some time t_d after the pulse [4]. However, for systems whose recombination kinetics are second order and thus lifetimes vary with the excitation intensity or with the carrier density during decay, TRS may give the relaxation of the system to a metastable excited state rather than the ground state, a situation that generally arises if the system has lifetime components longer than the pulse repetition interval.

Therefore, in this work, due to the mentioned drawbacks, in contrast to (TRS), the **frequency-resolved spectroscopy (FRS)** method was used, where the amplitude of the excitation pulse is modulated and the lifetime distribution is observed directly [5].

To detect only those components close to the modulation frequency, the method requires the use of sine wave modulated excitation and lock-in detection in exact quadrature. Since the recombination rate decreases exponentially with separation, in distant pair systems, it turns out that at moderate or low excitation intensities, the probability of recombination of an electron with a hole, other than the nearest neighbour is very small [6]. In the distant pair model where the recombining electrons and holes are localized at binding centres that display a random distribution throughout the sample, the recombination is bimolecular (see Section 2.4.7) at high excitation densities, monomolecular at low densities, and the photoluminescence lifetime τ distribution is always dependent on excitation density G, shifting to shorter τ with increasing G.

As a result of applying a sinusoidal excitation to the samples of amorphous materials (chalcogenide films in our case), and observing the phase shift between the signal applied and the photocurrent arising through a lock-in detector, hence using the so called *quadrature frequency resolved spectropy (QFRS)*, one can decide whether the recombination is carried out through *geminate* (i.e. twin) or *distant pair* kinetics.

In the thesis we will touch basically the following points:

Amorphous semiconductors,

Photoconductivity,

Concept of demarcation levels,

Equilibrium and nonequilibrium carriers,

Lifetime of nonequilibrium carriers,

Linear and quadratic recombination,

Geminate and distant pairs,

Time and frequency resolved spectroscopies (TRS) and (FRS),

Lock-in amplifiers,

Experimental results and discussion.

2. THEORY

2.1. Amorphous Solids

2.1.1. Covalent Bond

As it is well known, around the nucleus of the atom in which all the protons and neutrons are held together by the *strong force*, (which is a powerful, fundamental, natural force between particles and has a very short range of influence typically less than 10^{-15}m and which overcomes the electrostatic repulsion between the protons and keeps the nucleus intact) the electron is constantly moving in an orbit with a given radius, over a long time period (perhaps 10^{-12} sec. on the atomic time scale) and would appear as a spherical negative charge cloud around the nucleus and not as a single dot representing a finite particle. We can therefore view the electron as a charge contained within a spherical shell of a given radius. The shells and subshells are spatial regions around the nucleus where the electrons are most likely to be found [7].

When two atoms are brought together, the valence electrons interact with each other and with the neighbour's positively charged nucleus, as a result of which is often formed a bond between the two atoms, producing a molecule. The *covalent bond* results from the sharing of valence electrons to complete the subshells of each atom. In a covalent bond, as illustrated in Figure 2.1, electrons 1 and 2 must orbit both atoms, therefore cross the overlap region more frequently, indeed twice as often. Thus, electron sharing results in a greater concentration of negative charge in the region between the two nuclei, which keeps them bonded to each other. Furthermore, by synchronizing their motions, electrons 1 and 2 can avoid crossing the overlap region at the same time. For example, when electron 1 is at the far right (or left), electron 2 is in the overlap region; later the situation is reversed.

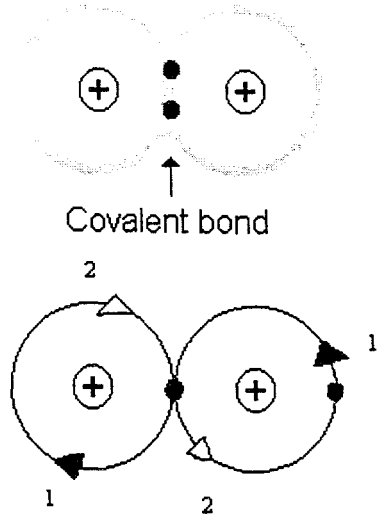

Figure 2.1. Orbiting of the electrons forming the covalent bond.

Since a covalently bonded material is very resistant to crystallization, it is reasonable as a first hypothesis, to assume that the multicomponent chalcogenide glasses are essentially covalent in nature and that all bonding requirements of each constituent atom are *locally* satisfied. Replacement of the weak *van der Waals* bonds present in materials like Se and As_2Se_3, by covalent bonds in the multicomponent glasses should lead to sharp increases in microhardness and stability, in accordance with observation

2.1.2. Semiconductors

At temperatures above absolute zero and in the absence of radiation, we know that the atoms (of Si for instance) in the crystal lattice will be constantly vibrating due to thermal energy with a distribution of energies. There is thus an electron-hole generation process going on in the sample as a result of *thermal generation*. Even though the average energy of the vibrations is at most 3 kT , a value incapable to break

the Si-Si bond, a few of the lattice vibrations in certain crystal regions may nonetheless be sufficiently energetic to *rupture* a Si-Si bond, in such a way that a bond becomes overstretched, disrupting and hence releasing an electron into the conduction band where the electron effectively becomes *free*. So that it can wander around the crystal and contribute to the electrical conduction when an electric field is applied, because there are plenty of neighbouring empty energy levels. Under the action of some electric field (E_x for instance), the electron in the conduction band moves in the opposite direction (then –x) and immediately starts gaining energy from the field.

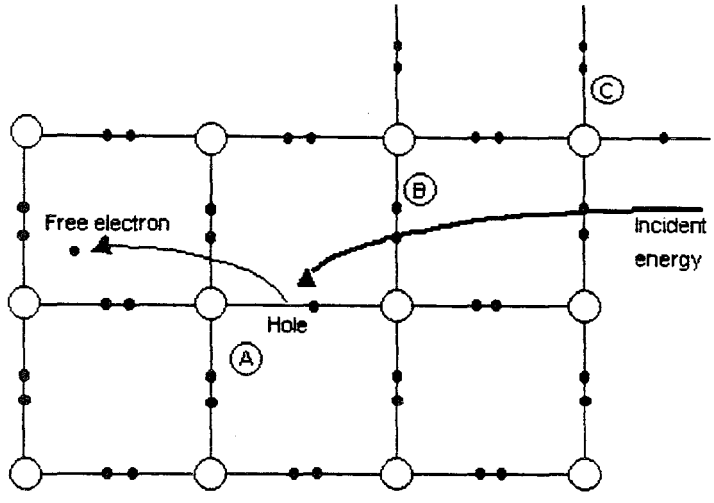

Figure 2.2.Formation of an electron-hole pair, upon the *arrival* of an incident photon.

When the electron collides with the thermal vibration of an atom (a *phonon*), it loses some of this energy and thus falls down in energy in the conduction band. After the collision the electron starts to accelerate again until the next collision, and so on. The region remaining around the hole in the valence band is positively charged because a charge of –e has been removed from an otherwise neutral region of the crystal. An electron in a neighbouring bond can readily tunnel into this broken bond and fill it, thereby effectively causing the hole to be displaced to the original position of the electron. By electron tunnelling from a neighbouring bond, holes are therefore also free to wander around the crystal (in the opposite direction) and also contribute to electrical conduction in the presence of an applied field. We also know that when a hole gains energy, it moves *down* in the valence band because the potential energy of the hole is

the hole is of opposite sign to that of the electron. An intrinsic semiconductor differs from an extrinsic semiconductor in the sense that the number of thermally generated electrons is equal to the number of holes (broken bonds) in the first, while in the latter, as its name implies, impurities are added to the semiconductor that can contribute either excess electrons or excess holes. It is also possible to obtain, as an example, both an *n-type* and a *p-type* Si crystal depending respectively on whether the electrical conduction will be mainly due to the motion of electrons or holes.

In the energy representation of the semiconductors, the conduction band whose width is called the *electron affinity* χ is separated from the valence band by an energy gap E_g, called the *band gap.* The bottom of the conduction band and the top of the valence band are denoted respectively by E_C and E_V. An electron in the valence band, however, is not localized to an atomic site but extends throughout the whole solid. Although the electrons might be thought to be localized at the bonding orbitals between the host atoms, this is not, in fact, true. In the crystal, the electrons can tunnel from one bond to another and exchange places. If we were to work out the wavefunction of a valence electron in the crystal, we would find that it extends throughout the whole solid which means that the electrons in the covalent bonds are indistinguishable, hence we cannot label an electron from the start and say that this electron is in this covalent bond between these two atoms.

The electronic conductivity of a substance depends on two factors, the number of current carriers per unit volume and the ease with which the carriers move through the substance under an applied electric field. The latter, known as the carrier *mobility* and generally tending to decrease as the temperature is raised, especially at high temperatures, is a more fundamental concept than localization and this accounts for the decrease in conductivity of metals with increasing temperature. In a perfectly periodic crystal (although in reality there is no such thing), for which the *Bloch* wavefunctions [of the form $\psi_k(x)=U_k(x)\exp(ikx)$ where $U_k(x)=U_k(x+a)$ (a being the lattice constant), is a periodic function] are valid, all states are delocalized, and the mobility of any state is almost infinite. In real crystals, however, the mobility is limited by scattering arising from deviations from perfect periodicity. In highly disordered

systems, intense scattering due to large fluctuations in the one-electron potential can reduce the mobility to quite small values, despite the delocalized nature of the states. A metal is a conductor with essentially a constant number of current carriers but a pure semiconductor is one in which the number increases as the temperature is raised. The mobility of the states in an amorphous solid sensitively depends on the density of states, $g(E)$ (see Section 2.1.8); where the density of states is large, the mobility can be finite; where the density of states is small (i.e. in the band tails), the mobility is essentially zero. *Mott* suggested that at the transition from extended to localized states the mobility should drop by several orders of magnitude producing a mobility edge. Indeed, the concept of localized states implies that the mobility is zero at $T = 0K$. The interval between the energies E_C and E_V acts as a pseudogap and is defined as the *mobility gap* [8]. The existence of mobility edges then shows, for $kT < (E_C - E_V)$, that the conductivity takes the form

$$\sigma = \sigma_C \exp\left[-\frac{(E_C - E_F)}{kT}\right] + \sigma_V \exp\left[-\frac{(E_F - E_V)}{kT}\right] \tag{2.1}$$

At $T = 0K$ we must have

$$E_F = \frac{1}{2}(E_V + E_C) \tag{2.2}$$

An important result is that the Fermi energy (see Section 2.1.9) at $T = 0K$, is halfway between the valence and conduction band edges, not halfway between the mobility edges. Thus, in general, if the mobilities in the delocalized parts of the valence and conduction bands are not too different, the conductivity will be dominated by either holes or electrons even in the intrinsic range, depending only on whether it is the conduction or valence band tail which is more extensive. This is simply a consequence of the fact that a faster particle is always scattered less by a fixed potential than a more slowly moving particle, and is an effect already evident in the *Kronig-Penney* model.

The *activation energy* in an amorphous semiconductor is the difference between the conduction band mobility edge and the Fermi energy which, as is said above, is not

necessarily in the centre of the mobility gap; under an applied stress there will be not only a change in the relative separation of the valence and conduction bands, but also a significant shift of the individual mobility edges relative to the band edges. In a pure crystal the optical and electronic energy band gaps are equal, whereas in an amorphous material the electronic properties are described by a mobility gap and the optical properties can be related to an optical band gap that is generally greater than the mobility gap.

Once $g(E)$, the single particle density of states (DOS) and the corresponding mobility $\mu(E)$ are known, we can analyze the electrical properties of the material conductivity, thermoelectric power, Hall effect, magnetoresistance, etc. The same information enables us to predict the optical properties, i.e. absorption, reflectivity, photoemission, photoconductivity and so forth. It is important to note that

i-the states in the gap represent bound states;

ii-consequently they are localized around the imperfections; and

iii-the remaining states in the valence and conduction band are, in general, still delocalized, unless the perturbing potential is extremely large.

The band tailing should not be very extensive in, for example, amorphous Ge and Si, but, on the other hand, we should expect enormous tailing in the multicomponent chalcogenide glasses which contain states that arise from regions of the material in which the density is anomalously low. If *dangling bonds* exist, that arise when one of the two electrons that make up the covalent bond is missing, perhaps because of the particular method of preparation of the material, then some donor or acceptor states will be present, and the concentrations of the two types of charged ions need not be equal. The positive and negative ions act as effective traps for electrons and holes respectively, and also behave as scattering centres that could limit the mobility of free carriers. Because of this, mobility might be expected to enhance with increasing energy above the edges. The temperature dependence of the mobility follows two distinctly different temperature variations. In the high temperature region, the drift mobility is observed to be limited by scattering from lattice vibrations.

2.1.3. Multicomponent Chalcogenide Glasses

The study of the electrical properties of glasses begins with the work of the Leningrad school under *Kolomiets* on the chalcogenide glasses which appear to behave, whether in the glassy or liquid state, as intrinsic semiconductors with a band gap of less than 2 eV. A very important property established by this school, which differentiates them sharply from crystalline materials of similar composition, is that their conductivity depends little on purity or stoichiometry; for them the familiar shallow donors and acceptors of crystalline semiconductors do not seem to exist. This property has the result that the conductivity increases by many orders of magnitude when they crystallise, which is certainly the reason why chalcogenide glass switches show a memory effect. One of the widest present uses of amorphous solids is for their dielectric properties. They make particularly good insulators, probably because, the transport of charge through them occurs less readily than in crystalline materials. Dielectrics that can, of course, also be produced from the vapour and in thin film form find areas of application in integrated circuits and microelectronics.

The discovery of nondestructive fast electrical switching in thin films of multicomponent chalcogenide glasses reported by *Ovshinsky* in 1968, a phenomenon that was observed in experiments where the voltage-current characteristics were measured as a function of increasing electric field applied has been one of the great milestones in the history of amorphous materials. For low electric fields, the current is ohmic and the material is in an almost nonconducting state, in which the resistivity is typically in the range of 10^8-10^{10} ohm-cm at room temperature. When a certain critical voltage is reached, the resistance drops drastically and the material is converted in a very short time, from a highly resistive into a highly conductive state. When the voltage is decreased, this state may be maintained, or the material may revert back to its original state, depending on the type of glass used.

Amorphous chalcogenide films, which are sulphur, selenium or tellurium based materials and whose properties are generally different from those of the tetrahedrally bonded amorphous semiconductors such as silicon, have applications in electrophotography, optical recording, lithography, bias-induced switching or memory

devices and are in thin film geometries. The optical energy gap is approximately twice the thermal activation energy, a result typical of amorphous chalcogenide semiconductors, which are usually p-type in nature.

In amorphous semiconductors $n \neq p$ because of the much larger number of electrons and holes in localized tail states and gap states. A numerical example illustrates this: For a mobility gap of $E_C - E_V = 1$ eV and E_F, more likely determined by the gap and tail states and staying in the gap centre, one obtains $n \approx 10^{10}\,\mathrm{cm}^{-3}$ at 300 K and because a wide range of amorphous semiconductors exhibit the intrinsic slope of the conductivity curve down to 150 K or lower, $n \approx 10^{3}\,\mathrm{cm}^{-3}$ at 150 K. Since there are certainly more than 10^3 localized tail and gap states present, one can conclude that the equation $n = p$ cannot be valid at these low temperatures.

A characteristic property of the crystal structure is its periodicity and degree of symmetry. For each atom, the number of neighbours, also called the *coordination number* and their exact orientations are well-defined, otherwise the periodicity would be lost. There is therefore a *long-range order* resulting from strict adherence to a well-defined bond length and relative bond angle. Many substances exist in a noncrystalline or amorphous form, due to their method of formation. As we move away from a reference atom, after the first and perhaps the second neighbours, random bending and twisting of the bonds are sufficient to destroy long-range order. For an amorphous structure, although the coordination of each atom is specified, since each and every atom ought to satisfy its chemical bonding requirement, the whole structure lacks long-range order and is therefore called a *continuous random network* of atoms (often called *CRN*) which is impossible to build on a macroscopic scale, and an amorphous sample would never have a homogeneous atomic network. These materials can only be produced as thin films, because a bulk sample would eventually break down due to the stresses in the bonds [9]. It is also expected that the overall resistivity of the thin film to be greater than that of a bulk sample, due to the fact that the electron can also become scattered from the surfaces.

2.1.4. Hopping conductivity

Cohen, Fritzsche, and *Ovshinsky (CFO)* suggested that in cases of extreme disorder, e.g. the chalcogenide glasses, it is possible that the valence and conduction band tails actually overlap in what formerly was the energy gap. Such a situation preserves a gap between the valence and conduction band mobility edges, and it is the very existence of this mobility gap, $E_C - E_V$, that leads to semiconducting rather than metallic behaviour.

The hopping of carriers between localized states situated in the mid-gap region $E_A \langle E \langle E_B$, as is seen in Figure 2.2, occurs either at low T or in materials with a high defect density but at high T. The probability that a carrier jumps from one localized state to another state of higher energy will depend upon:

i- $\exp\left(-W/kT\right)$ where W is the energy difference between the two states;

ii- ν_{ph}, the phonon spectra ; and

iii- $\exp(2\alpha_L r)$, the overlap of the wavefunctions, where α_L is the localization parameter and r is the distance separating the two localized states.

The bottom of the conduction band in some semiconductors occurs at $k = 0$. Such semiconductors as GaAs, InP, InGaAs, etc., are called direct bandgap materials and are optically active. In other semiconductors, the bottom of the conduction band does not occur at the point $k = 0$ but at certain other points. Such semiconductors as Si, Ge, AlAs, etc., are called indirect semiconductors. These materials have very weak interactions with light and cannot be used for efficient optical devices. The reasons are based on momentum conservation in optical transitions that make it difficult to have strong transitions in indirect semiconductors.

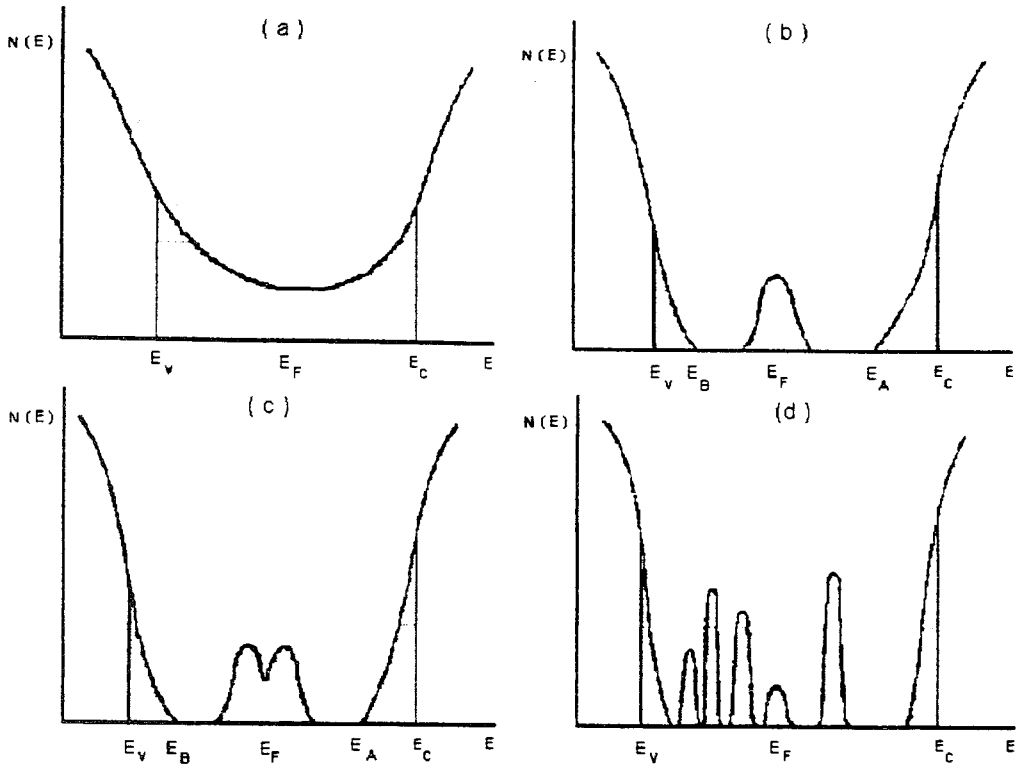

Figure 2.3. Schematic density of states diagrams for amorphous semiconductors. **a**-The CFO model, **b**-the Davis-Mott model, **c**-modified Davis-Mott model and **d**-a *real* glass with defect states.

For strong localization (i.e. $\alpha_L r >> 1$), nearest neighbour hopping is to be expected, however, in the weak localization case, the electrons will have more choices of centres to hop to. At those values of temperatures for which kT is smaller than the bandwidth at E_F, the thermal energy that the electrons are to receive, might not be enough to allow to pass on to the nearest neighbour, in this case the few electrons taking part in conduction will transmit to farther states of energies comparable to their own. In this case called the *variable range hopping*, the hopping distance r increases with decreasing temperature since the electrons will have a higher probability of jumping to a more distant site where W is smaller.

2.1.5. Classification of Amorphous Materials

In crystalline solids the five major classes are
a-ionic, **b**-covalent, **c**-metallic, **d**-van der Waals and **e**-hydrogen bonding.
Since the first subdivision of type **b** materials that includes the tetrahedrally bonded materials (such as Si and Ge) in which there is only positional disorder are materials of little technological use due to their inherently high density of localized states. It is only with the addition of H and/or halogen atoms that the density of states is reduced to a point where device possibilities emerge.

The second subdivision of covalently bonded materials includes S, Se and Te, which are two-fold coordinated and where we expect positional disorder. Multicomponent glasses such as As_2S_3, As_2Se_3, SiTeAsGe or GeTe will possess compositional as well as positional disorder. It is important to understand that amorphous semiconductors are metastable thin solid film materials, whereas a glass is a viscous liquid that is normally formed by the continuous hardening of a cooled liquid. An ideal glass or an amorphous material is a solid in internal equilibrium in which there is, just as in crystalline solids, a definite set of equilibrium positions about which the atoms oscillate.

2.1.6. A Distinction Between Two Classes of Materials

When one comes to consider specific defects and energy levels in amorphous semiconductors, it is convenient, by two criteria, to distinguish two classes of materials: *Ge type* and *Se type*. From the point of view of the network flexibility, the coordination numbers of Ge and Se are, as in the crystalline, *four* and *two* respectively, in accordance with the 8-N rule. Four-fold coordination means symmetrical bonding and the formation of rigid structures hence, a continuous random network (CRN) with tetrahedral bonds can be constructed with negligible density deficit and very little possibility for local reorganization of atoms. On the other hand, two-fold coordination is very asymmetrical and model structures must necessarily be fairly open (unless the chains are folded back and forth in a very tightly ordered arrangement, in which case one has the trigonal crystalline phase) and have a greater degree of flexibility. As a

2.1.4. Hopping conductivity

Cohen, Fritzsche, and *Ovshinsky (CFO)* suggested that in cases of extreme disorder, e.g. the chalcogenide glasses, it is possible that the valence and conduction band tails actually overlap in what formerly was the energy gap. Such a situation preserves a gap between the valence and conduction band mobility edges, and it is the very existence of this mobility gap, $E_C - E_V$, that leads to semiconducting rather than metallic behaviour.

The hopping of carriers between localized states situated in the mid-gap region $E_A \langle E \langle E_B$, as is seen in Figure 2.2, occurs either at low T or in materials with a high defect density but at high T. The probability that a carrier jumps from one localized state to another state of higher energy will depend upon:

i- $\exp\left(-W/kT\right)$ where W is the energy difference between the two states;

ii- ν_{ph}, the phonon spectra ; and

iii- $\exp(2\alpha_L r)$, the overlap of the wavefunctions, where α_L is the localization parameter and r is the distance separating the two localized states.

It is obvious that the magnitude of this conduction should depend on the ratio of the levels that are occupied and free (due to compensation). In the absence of electrons at the donor levels (complete compensation) there is no hopping conduction. As the electron density at the donors increases (degree of compensation decreases), the hopping conduction should be higher. However, when the electron density becomes greater than about half the density of donors, further increase of the electron density should reduce the conductivity because then the hopping conduction is restricted by the diminishing number of vacant levels.

2.1.7. Electrical Properties of Chalcogenide Glasses

Electrical conductivity of both bulk samples and thin films of amorphous As_2Se_3 has been measured often. Bulk samples exhibit a conductivity (of the order of 10^{-12} $(ohmcm)^{-1}$) that is ohmic for applied fields of up to 10^5 V/cm at $300K$ but obeying the ordinary semiconductor relation in the temperature range of 300 to $450K$.

$$\sigma = \sigma_0 \exp\left(-\frac{E_A}{kT}\right) \tag{2.3}$$

where E_A is the activation energy and σ_0 is the value of conductivity at $0K$. If the carriers move by hopping in the localized states, the conductivity varies nearly exponentially with temperature (apart from a small temperature-dependent preexponential term), and the measured activation energy is the sum of the activation energies for carrier creation and for hopping. The AC conductivity of several chalcogenide glasses has been found to be quite dependent on the composition being investigated. The crystalline-to-amorphous transition in As_2Se_3 removes the anisotropy and leaves the carrier mobility, but essentially preserves the energy gap.

On the basis of the *Davis – Mott* model, there can be three processes leading to conduction in amorphous semiconductors, their relative contribution to the total conductivity predominating in different temperature regions.

i- At very low temperatures conduction can occur by thermally assisted tunnelling between states at the *Fermi level*,

ii- as one goes up to higher temperatures charge carriers are excited into the localized states of the band tails; carriers in these localized states can take part in the electric charge transport only by hopping and

iii- at still higher temperatures carriers are excited across the mobility edge into the extended states, where the mobility is much higher than in the localized states [10].

Optical absorption measurements made on amorphous semiconductors have shown that the band gap decreases with increasing temperature. As the temperature is lowered, the number and energy of phonons decrease, and the more energetic phonon-assisted hops

will progressively become less favourable. Carriers will then tend to hop to larger distances in order to find sites which lie energetically closer than their spatially nearest neighbours, with the condition that the number of accessible sites should at least be one. This mechanism is the so-called *variable range hopping*.

2.1.8. Density of States

Amorphous semiconductors are prepared from a nonequilibrium situation and are therefore metastable. Consequently, their DOS depends upon their details of preparation conditions. Several factors that determine the DOS for a given material consist of, among others, the coordination number, the interatomic distance and the type of chemical bonding. Above the melting point where the periodicity is lost and yet there is no observed change in resistivity, a material has long-range positional disorder, but again short-range order; a point valid for all amorphous solids that appear to have approximately the same conductivity as the corresponding crystalline material; however, the resistivity does vary where the *density* of the material changes markedly. Thus, the long-range periodicity is apparently not of great importance, because the general electrical characteristics of the material remain unaltered. The lack of long-range order inherent in amorphous solids results in conduction band and valence band tails, the extent of which depend upon the amount of inherent disorder.

$$g(E)=\left(8\pi 2^{1/2}\right)\left(\frac{m_e}{h^2}\right)^{3/2}E^{1/2} \tag{2.4}$$

From Eq. (2.4) it is seen that the density of states increases proportionately to $E^{1/2}$ with energy from the bottom of the energy band. As we approach the top of the band, $g(E)$ decreases with the energy as $(E_C - E)^{1/2}$, so that as $E \to E_C$, $g(E) \to 0$. The variation of $g(E)$ with energy in a band can therefore be described as a square root dependence on the energy from the band edge. These models were appropriate to multicomponent chalcogenide glasses that show positional disorder in addition to the compositional disorder, with the result that there is a large DOS in the mid-gap region. The large

number of experimental papers on amorphous As_2Se_3 enable us to reach the following tentative conclusions:

i- The short-range orders of the crystalline and amorphous solids are essentially identical and this structure meets all of the covalent bonding requirements of the constituent atoms, and still depends on van der Waals interactions to fill three-dimensional space. However, the anisotropy of the crystal is removed in the amorphous phase where the direction would not matter.

ii- Formation of nonstoichiometric glasses, with either excess As or excess Se, does not have much effect on the electrical conductivity. Yet even small concentrations of certain impurities induce large changes in conductivity, and these changes are correlated with variations in the activation energy rather than arising from mobility effects. Although the decrease in activation energy might represent impurity lowering of the mobility gap, it could possibly be due to bond breaking and the consequent formation of deep traps in the gap. Then, the traps, rather than being clustered at a well-defined level, must be distributed throughout a region of energy in the band gap, a phenomenon that can be observed in photoconductivity, thermally stimulated conductivity and photoluminescence experiments and for which there is a great deal of evidence. Electrons are localized predominantly where there are few holes and holes which are the dominant current carriers in chalcogenide alloys are localized at places relatively farther from electrons. The density of gap states is probably higher in evaporated and sputtered films than in *annealed* bulk samples because annealing, that is, keeping the sample at a temperature lower than the melting temperature helps get rid of most of the defects and micro vacancies that are in fact the localized states and hence, increase the density of the material. In chalcogenide alloys $g(E_F)$~$5x10^{18}cm^3eV^{-1}$. Previous studies of the arsenic chalcogenides, however, indicate that the local coordination of chalcogenide atoms about arsenic atoms is threefold as in the crystal forms. It is therefore to be expected that the fundamental structural unit of these glasses is similar to that of the crystal, namely, a shallow pyramid with an arsenic atom at the apex and chalcogenide atoms at the corners of the triangular base. This basic asymmetry of the structural unit contrasts sharply with the tetrahedral glasses.

2.1.9. Fermi Energy

To determine the probability $f(E)$ of finding an electron at an energy level E, we must consider what is called *particle statistics*, a topic that is key to understanding the behaviour of semiconductor devices. The probability of the occupation of energy levels with energy E, by electrons is given by the Fermi function

$$f(E) = \frac{1}{1 + \exp\left[\left(E - E_F\right)/kT\right]} \tag{2.5}$$

Calculations show that the total densities of free electrons and holes are respectively,

$$n_0 = \frac{2}{h^3}(2\pi m_e kT)^{3/2} \exp\left(\frac{E_F}{kT}\right) = N_C \exp\left(\frac{E_F}{kT}\right) \tag{2.6}$$

$$p_0 = \frac{2}{h^3}(2\pi m_h kT)^{3/2} \exp\left(\frac{-E_F - E_g}{kT}\right) = P_V \exp\left(\frac{-E_F - E_g}{kT}\right) \tag{2.7}$$

In calculating the density we can replace the whole conduction band by energy states coinciding with its lower edge, the density of such states being assumed to be N_C, which, for this reason is frequently called the *effective density of the electron states* in the conduction band. The *Fermi energy* E_{F0} is that energy for which the probability of finding an electron at $0K$, for $E < E_{F0}$ is unity, while for $E > E_{F0}$, is zero. Although the Fermi energy depends on the properties of the energy band, to a good approximation it is only weakly temperature-dependent.

There is a deep significance of the Fermi energy E_F, which should at least be mentioned. For a given metal the Fermi energy that represents the free energy per electron, called the *electrochemical potential* μ, is a measure of the potential of an

electron to do electrical work $(=V\Delta Q)$ or nonmechanical work, through chemical or physical processes. As a corollary, we note that when electrical work is done on the system, for example, when a battery is connected to a semiconductor, then E_F is not uniform throughout the whole system and a change ΔE_F in E_F within a system that is equivalent to electrical work per electron is the energy expended in taking an electron through the semiconductor. A photon must have at least some amount of energy E_g, equal to the band gap value, to excite an electron from the valence band to the conduction band where the electron can drift; but photons having less energy do not get absorbed, because their energy would place the electron in the band gap where there are no states (for a crystal).

Density of states $g(E)$, represents the number of states per unit energy per unit volume. We assume that, the valence band states are filled and the conduction band states are empty since the number of states in the conduction band is overwhelmingly larger than the number of electrons in this band (that is $n \langle\langle N_C$) where one could use the Maxwell-Boltzmann statistics, due to the huge number of states not filled by free electrons. This is contrary to the case of *degenerate semiconductors* for which $n \approx N_C$, as a result of excessively high doping and where one should use Fermi-Dirac statistics.

The bottom of the conduction band in some semiconductors occurs at $k = 0$. Such semiconductors as GaAs, InP, InGaAs, etc., are called direct bandgap materials and are optically active. In other semiconductors, the bottom of the conduction band does not occur at the point $k = 0$ but at certain other points. Such semiconductors as Si, Ge, AlAs, etc., are called indirect semiconductors. These materials have very weak interactions with light and cannot be used for efficient optical devices. The reasons are based on momentum conservation in optical transitions that make it difficult to have strong transitions in indirect semiconductors.

2.1. Photoconductivity

2.2.1. Optical Absorption

One of the most important roles of information processing devices is to detect information. In electronics, the presence or absence of information is detected by devices such as field effect transistors, bipolar transistors, diodes and so on. The absorption of light can occur for a variety of reasons, including absorption by impurities in the material or intraband absorption which is the most important optoelectronic way in semiconductors as far as devices are concerned. Since the photon momentum is extremely small on the scale of the electron momentum, the conservation of momentum requires that the electron-hole transitions are vertical in k space.

As is seen in Figure 2.2, initially an incident photon of energy $h\nu$ greater than E_g absorbed in a semiconductor excites a valence band electron to the conduction band where the electron can drift freely and where the average (kinetic) energy of electrons is $(3/2)kT$ above E_C, which means that the electrons are very close to E_C. If the photon energy is much larger than the band gap energy E_g, then the excited electron is not near E_C and has to lose the extra energy $(h\nu - E_g)$ to lattice vibrations as heat, as the electron is scattered from one atomic vibration to another, a process called *thermalization.*

As Figure 2.4 indicates, in **a** and **c**, the electrons in the conduction band and the holes in the valence band recombine respectively with the electron and hole traps and hence reduce the number of carriers, while in **b** and **d**, the electrons and holes trapped temporarily at E_T are excited, by the help of appropriate phonons, respectively to the conduction and valence bands, leaving behind positive and negative charges at these traps and causing the number of free carriers to rise.

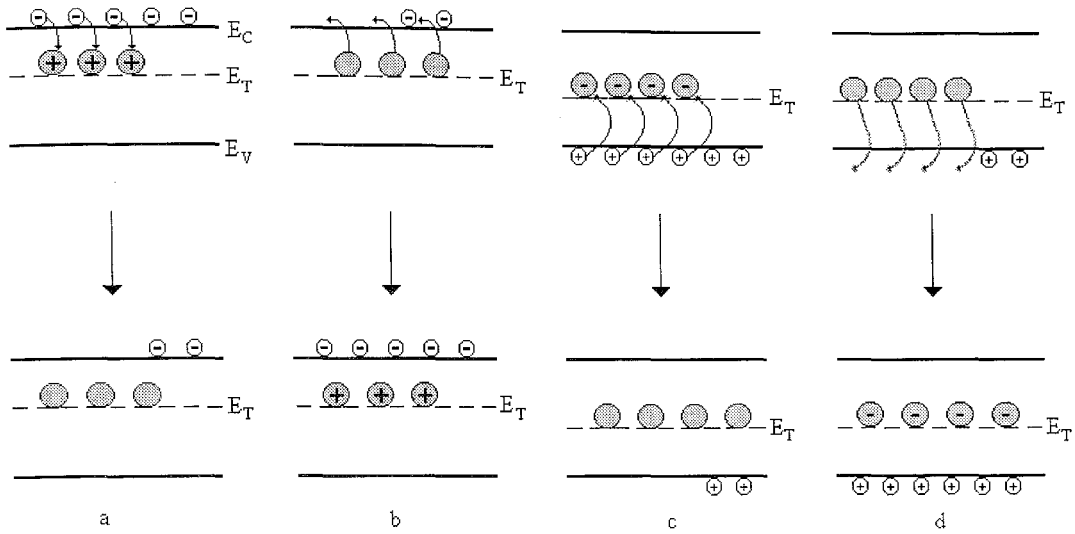

Figure 2.4. The possible transitions and recombinations indicating the variations of charges.

Materials like GaAs, InP, InGaAs have strong optical absorption at the bandedges because the optical absorption can occur without a phonon participation. On the other hand, Si and Ge have an indirect bandgap, and the absorption strength is weak near the bandedge. Yet, although these materials cannot be used as lasers, they can be fabricated as detectors.

As Figure 2.4 indicates, in **a** and **c**, the electrons in the conduction band and the holes in the valence band recombine respectively with the electron and hole traps and hence reduce the number of carriers, while in **b** and **d**, the electrons and holes trapped temporarily at E_T are excited, by the help of appropriate phonons, respectively to the conduction and valence bands, leaving behind positive and negative charges at these traps and causing the number of free carriers to rise.

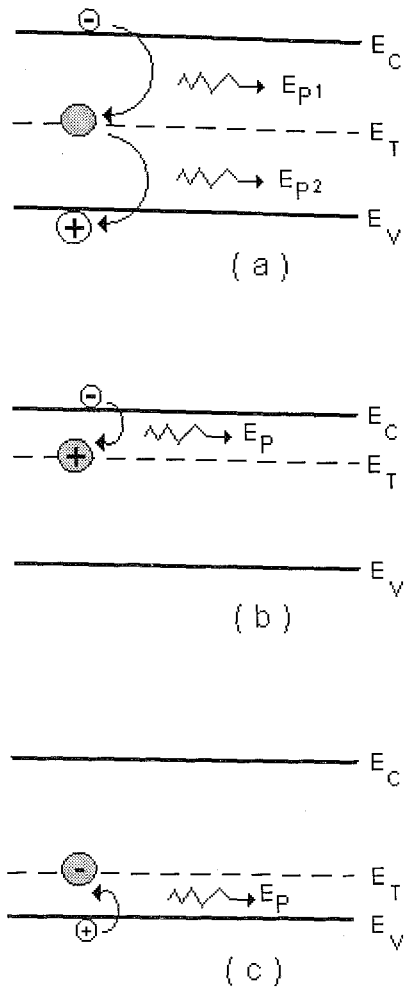

Fig 2.5. Possible ways of recombining of a free electron with a free hole by way of traps.

Direct recombination of mobile electrons and holes across the mobility gap, process **a**, has a large cross section and must be an important mode of decay. Process **b**, recombination of a free electron with a localized hole, trapped below the Fermi energy has a somewhat smaller cross section, and is unlikely to dominate direct recombinations. But if a sufficiently large density of positively charged electron traps exists above the Fermi energy, process **c** can be the predominant decay mode, despite the smaller cross section compared to that of direct recombination.However, process **c**

results in an electron being trapped above the Fermi energy, a nonequilibrium situation. Once trapped, the electron is highly localized and can only escape with the assistance of phonons.

As the electron wanders in the conduction band, it becomes captured by a trap at E_T where it remains captured until a strong lattice vibration excites it back into the conduction band. The time the electron spends trapped at E_T depends on the energy depth of the trap from the conduction band, $E_C - E_T$, that is, the deeper is the trap, the longer it will take the electron to be *reexcited* to the conduction band, hence be free. The electron wanders around again in the conduction band and eventually becomes trapped in an excited state of a luminescent centre or
an activator. Typically, luminescent centres are intentionally added impurities or crystal defects such as interstitials or vacancies. The electron then falls down in energy to the ground state of the activator, releasing a photon. Later, the electron at the ground state recombines with a wandering hole in the valence band, thus the activator acts as a radiative recombination centre. But with some impurities, the energy that is released when the electron falls down to the ground state is in the form of lattice vibrations, so that the impurity acts as a nonradiative recombination centre. The time interval between photogeneration and recombination can be quite long if the electron remains captured at E_T for a considerable length of time. In fact, the electron may become trapped and detrapped a great many times before it finally recombines, so the emission of light can persist for a relatively long time after the cessation of excitation. Since the probability of photon absorption depends on the densities of both valence band and conduction band states, the photon absorption process intensifies when there are more valence band states available, for more electrons can be excited. We also need available conduction band states into which the electrons can be excited, otherwise the electrons would have difficulty to find empty states to fill.

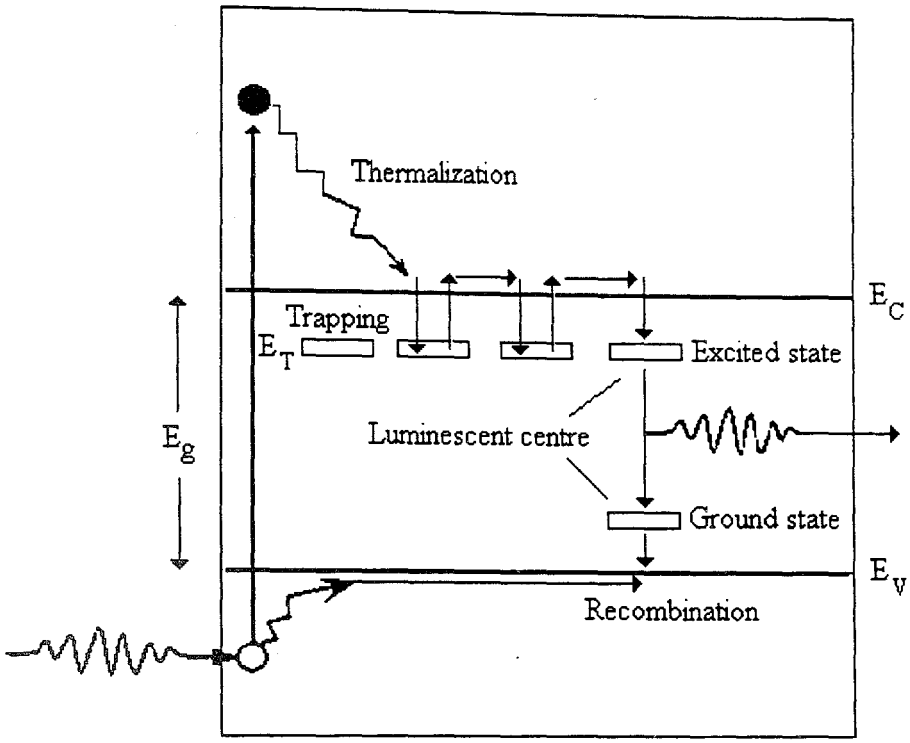

Figure 2.6. As a result of the incident photon, an e-h pair forms and the electron, after the thermalization and several trapping-detrapping stages, recombines with a hole in the ground state of a luminescent centre.

If on the other hand, the photon energy $h\nu$ is less than the band gap energy, the photon will not be absorbed and we can say that the semiconductor is transparent to wavelengths longer than some critical $\lambda_C \left(=\frac{hc}{E_g}\right)$, provided that there are no energy states in the band gap to host the electron temporarily.

BOĞAZİÇİ ÜNİVERSİTESİ KÜTÜPHANESİ

2.2.2. Photoconductivity in Amorphous Substances

There are a number of applications for devices which change their resistance when exposed to light, such as light detectors for various purposes, exposure meters for cameras, optical signalling systems etc. Considerations in choosing a photoconductor for a given application include the sensitive wavelength range, time response and optical sensitivity of the material. In general, semiconductors are most sensitive to photons with energies equal to the band gap or slightly more energetic than band gap.

Photoconductivity is the change in the electrical conductivity when a material is exposed to electromagnetic radiation (e.g. light, injection, strong field etc.). It has been commonly observed in chalcogenide glasses, and the major results appear to be essentially independent of composition. Holes rather than electrons always appear to dominate the photocurrent, in agreement with the thermoelectric results. At $300K$, the photocurrent is proportional to the light intensity, while at, as low as $70-80K$, the photocurrent is proportional to the square root of the intensity. Thus, it can be concluded that bimolecular recombination processes predominate at low temperatures, whereas monomolecular processes are valid at high temperatures (see Section 2.4.7).

However, at intermediate temperatures, the intensity dependence of the photocurrent is intermediate between square root and linear, indicative of a continuous distribution of traps in the gap. This result is contrary to the results on amorphous As_2Se_3, in which the transition from bimolecular to monomolecular recombination is rather abrupt.

2.3. Recombination and Minority Carrier Injection

2.3.1. Direct and Indirect Recombination

When a free electron, wandering around in the conduction band of a crystal, *meets* a hole, it falls into this low-energy, empty electronic state and fills it. This process is called **recombination** which intuitively corresponds to the free electron finding an incomplete bond with a missing electron.The electron then enters and completes this bond. The excess energy of the electron is lost as a photon of energy $h\nu(=E_g)$. In fact, it is *this* type of recombination that results in the emitted light from light emitting diodes (LEDs). In elemental semiconductor crystals, (such as Si and Ge), electrons and holes usually recombine through recombination centres that increase the probability of meeting, because they can *take up* any possible momentum difference between a hole and an electron. The electron, then localized and bound to this centre, *waits* there for a hole with which it can recombine. In this recombination process, the energy of the electron is usually lost to lattice vibrations (as *sound*) by way of the *recoiling* of the third body. Emitted lattice vibrations are called **phonons** that are quanta of energy associated with atomic vibrations in the crystal analogous to the photon.

Let us assume that we have weak illumination, which causes, say, only a 10% change in n_0, that is, $\Delta n = 0.1n_0 = 0.5x10^{13}\,\text{cm}^{-3}$ then $\Delta p = \Delta n = 0.5x10^{13}\ \text{cm}^{-3}$ and hence, $p \approx \Delta p$, which shows that although n changes by only 10%, p changes drastically, that is, by a factor of $\approx 10^{13}$. Obviously when the light is switched off, the condition $p = \Delta p$ must eventually revert back to the dark case where $p = p_0$. In other words, the excess minority carriers, Δp, and excess majority carriers, Δn must be removed by recombination. Excess holes recombine with the electrons available and disappear, a process however, that takes time because the electrons and holes have to find each other. The mean time between collisions, τ, has further significance, its reciprocal $1/\tau$ representing the *mean frequency of collisions* or *scattering events*; is the

mean probability per unit time that the electron will be scattered. In order to describe the rate of recombination, we introduce a temporal quantity, denoted by τ_h and called the **minority carrier lifetime (mean recombination time),** which is defined as follows: τ_h is the average time a hole exists in the valence band from its generation to its recombination, that is, the mean time the hole is free before recombining with an electron. An alternative and equivalent definition is that $1/\tau_h$ is the average probability per unit time that a hole will recombine with an electron. We must remember that the recombination process occurs through recombination centres, so the recombination time, τ_h, will depend on the concentration of these centres and their effectiveness in capturing the minority carriers. Once a minority carrier has been captured by a recombination centre, there are many majority carriers available to recombine with it, so τ_h, in an indirect process, is independent of the majority carrier concentration. This is the reason for defining the recombination time as a minority carrier lifetime. If the minority carrier recombination time is, say, 10 seconds and if there are some 1000 holes, then it is clear that these excess holes will be disappearing at a rate of 100 (=1000/10) per second. The rate of recombination of excess minority carriers is simply $\Delta p / \tau_h$. At any instant, therefore,

(rate of increase in excess hole concentration) = (rate of photogeneration) – (rate of recombination of excess holes) (2.8)

If G is the rate of photogeneration, then clearly the net rate of change of Δp is

$$\frac{d\Delta p}{dt} = G - \frac{\Delta p}{\tau_h} \tag{2.9}$$

to which, by some intuition,

$$\Delta p(t) = G\tau_h + \Delta p(0)\exp\left(-t/\tau_h\right) \tag{2.10}$$

is found to be the solution. Whether or not a defect with a trapped charge acts as a recombination centre depends on the level of G and the temperature T. Higher G increases n and p, making recombination more likely and resulting in greater trapped quasi-Fermi level splitting. Reducing T lowers the emission probability of the trapped

charge, leading to increased recombination at shallower states and, as before, a greater trap quasi-Fermi level splitting. Most traps would not contain trapped charge if $n = p$ and the gap state distribution is symmetrical.

2.3.2. Demarcation levels

It is known that insulators have a more or less continuous distribution of defect states throughout the forbidden zone and also of these states, some may be overwhelmingly crowded. Whether one grants the quasi-continuum or not, there is a sufficient scattering of states throughout the forbidden zone to justify the development of a quantitative criterion for distinguishing traps from recombination centres. The energy level at which an electron will have equal probabilities of being excited into the conduction band and of capturing a free hole is the **demarcation level** for electrons such that states lying above this level will act predominantly as traps and those below predominantly as recombination centres [11].

Here the states are assumed to be of one class, in the sense of having a common cross section q_n for capturing a free electron and a common cross section q_p for capturing a free hole, even though these states may be distributed in energy. The electron demarcation level D_n is defined by the following equality

$$\nu_n^* \exp\left(-\frac{|D_n - E_C|}{kT}\right) = \rho v q_p \tag{2.11}$$

The left hand side is the rate of thermal excitation of an electron into the conduction band, ν_n^* is often regarded as the product of the highest lattice frequency and a constant less than or equal to unity, expressing the probability that an electron excited energetically to the conduction band will *actually* pass into the conduction band.
By an argument of detailed balance

$$\nu_n^* = N_C v q_n \tag{2.12}$$

then substituting this expression in Eq (2.11),

$$|D_n - E_C| = kT \ln\left[\frac{N_C q_n}{p q_p}\right] \tag{2.13}$$

$$n = \frac{G}{p_r v q_n} \qquad \text{and} \qquad p = \frac{G}{n_r v q_p} \tag{2.14}$$

dividing them through

$$\frac{p}{n} = \frac{q_n p_r}{q_p n_r} \tag{2.15}$$

then

$$|D_n - E_C| = kT \ln\left\{\frac{N_C q_n}{\left[\frac{n q_n p_r}{q_p n_r}\right] q_p}\right\} \tag{2.16}$$

$$|D_n - E_C| = kT \ln\left[\frac{N_C n_r}{n p_r}\right] \tag{2.17}$$

also from the definition of the steady-state Fermi level for electrons

$$n = N_C \exp\left[-\frac{|E_{Fn} - E_C|}{kT}\right] \tag{2.18}$$

$$|D_n - E_C| = kT \ln\left\{\frac{N_C n_r}{N_C \exp\left[-\frac{|E_{Fn} - E_C|}{kT}\right] p}\right\} \tag{2.19}$$

$$|D_n - E_C| = kT\left\{\ln[N_c n_r] - \ln\left[N_C \exp\left[-\frac{|E_{Fn} - E_C|}{kT}\right] p_r\right]\right\}$$

$$|D_n - E_C| = kT\left\{\ln[N_C n_r] - \ln N_C - \ln p_r + \frac{|E_{Fn} - E_C|}{kT}\right\}$$

$$|D_n - E_C| = kT\left\{\ln n_r - \ln p_r + \frac{|E_{Fn} - E_C|}{kT}\right\}$$

$$|D_n - E_C| = |E_{Fn} - E_C| + kT \ln\left[\frac{n_r}{p_r}\right] \tag{2.20}$$

Eq. (2.20) states that to a first approximation the electron demarcation level, D_n, is located at the steady-state Fermi level E_{Fn}. In the second approximation the demarcation level is displaced from the Fermi level by the correction term $kT \ln\left[\frac{n_r}{p_r}\right]$. Obviously, since when $n_r \cong p_r$ holds, the correction term is negligible, Eq. (2.20) can also be written with the help of the equation

$$\frac{p}{n} = \frac{q_n p_r}{q_p n_r} \qquad \text{in the form}$$

$$|D_n - E_C| = |E_{Fn} - E_C| + kT \ln\left[\frac{nq_n}{pq_p}\right] \tag{2.21}$$

Also by a parallel argument, beginning with

$$\nu_p^* \exp\left[-\frac{|D_p - E_V|}{kT}\right] = nvq_n \tag{2.22}$$

to find the demarcation level D_p, for holes, we obtain

$$|D_p - E_V| = |E_{Fp} - E_V| - kT \ln\left[\frac{n_r}{p_r}\right] \qquad \text{or}$$

$$|D_p - E_V| = |E_{Fp} - E_V| - kT \ln\left[\frac{nq_n}{pq_p}\right] \tag{2.23}$$

Let us now explore the meaning and the utility of the demarcation levels. For definiteness we have chosen $n_r \gg p_r$ and have accordingly displaced the demarcation

levels downward from their respective Fermi levels. Although in reality $q_n \neq q_p$, we take them to be equal. States lying at D_n have equal roles as traps and recombination centres, since an electron in one of these states is equally likely to be thermally excited into the conduction band and to capture a free hole. States lying above D_n rapidly take on a predominantly trap character, since the rate of thermal exchange with the conduction band increases exponentially by the Boltzmann factor at a rate of about 100 (at room temperature) for each ~0.12 V displacement above D_n and since the probability for capturing a hole does not change with a shift in energy, a state ~0.12 volt above D_n is acting 99% of the time as a trap and 1% of the time as a recombination centre. In other words, for each 100 times an electron falls into such a state from the conduction band, 99 times the electron is thermally reexcited into the conduction band and only once (on the average) does it capture a free hole. For a state ~0.24 volts above D_n, the ratio of its trap to recombination role is almost 10^4 to 1. By this argument it is clear that states above D_n are in thermal contact with the conduction band and their occupancy is given by the Fermi function centred on E_{fn}. By parallel arguments, the states lying between D_p and the valence band act predominantly as hole traps and their occupancy is given by the Fermi function centred on E_{fp}. The occupancy of states lying between D_n and D_p is governed by the kinetic processes of capturing free electrons and free holes and this occupancy is uniform, that is, the same at all energies lying between D_n and D_p and further they are predominantly recombination centres.

2.3.3. Equilibrium and Nonequilibrium Carriers; Nonequilibrium Conductivity

The process of formation of free charge carriers requires energy for overcoming the energy gaps between allowed bands or between local impurity levels and these bands, that is energy, normally drawn from the reservoir of thermal energy present in

the crystal where the electrons interact very strongly with the atoms (or ions) of the crystal lattice and therefore under normal conditions the temperatures of the lattice and of the electrons become practically identical. Free electrons and holes, liberated by *thermal ionization* and denoted respectively by n_0 and p_0 having densities corresponding to thermal equilibrium (i.e. between electrons and the lattice) will be called *equilibrium* carriers. In contrast to the thermal energy that remains practically unaffected and is saved by the crystal lattice, the energy used to generate excess carriers is retained mainly by the electrons and causes the thermal equilibrium between the lattice and electrons to be disturbed. Therefore, carriers formed in some way other than by thermal ionization are called *nonequilibrium* carriers. Following the cessation of the external excitation (e.g. light, injection, strong field etc.), the thermal equilibrium between the lattice and electrons will (after a time) be reestablished. Nonequilibrium carriers whose number is usually not very large and whose excess energy is small compared with the thermal energy of the crystal lattice, may be generated as the result of internal ionization in a semiconductor on absorption of radiation, or by the disturbance of the equilibrium distribution by a strong field, injection, extraction and so on (when current passes through an inhomogeneous system, for example through a p-n junction).

Taking this into account, we may assume that the application or removal of an excitation (for example, illuminating a semiconductor or placing it in darkness) changes the density of nonequilibrium carriers without affecting that of equilibrium ones, and therefore the total density (n or p) is simply the sum of the equilibrium (n_0, p_0) and nonequilibrium ($\Delta n, \Delta p$) carrier densities:

$$n = n_0 + \Delta n$$
$$p = p_0 + \Delta p \qquad (2.24)$$

An excess conductivity $\Delta\sigma$ appears if, under the action of absorbed light, the densities of the charge carriers n and p increase compared with their values at thermal equilibrium:

$$\Delta\sigma = e(\Delta n\mu_n + \Delta p\mu_p) \tag{2.25}$$

At low temperature the values Δn and Δp may be considerably higher than the corresponding equilibrium densities n_0 and p_0. The presence of nonequilibrium carriers alters the conductivity of a semiconductor and in the general case this can be written in the form

$$\sigma_L = (ne\mu_n + n_0 e\mu_n) + (pe\mu_p + p_0 e\mu_p) \tag{2.26}$$

where e is the electronic charge, and μ_n and μ_p are respectively the electron and hole mobilities which are determined by the nature of the interaction of carriers with the lattice, and they depend, in particular, on the energy distribution of the carriers in the bands. In writing down the above equations we ascribed the same mobilities to equilibrium and nonequilibrium carriers. When a semiconductor is illuminated with light of wavelengths lying in the fundamental absorption region, the absorption of light quanta produces electron transitions from the valence band to the conduction band and consequently generates myriads of nonequilibrium electrons and holes.

The total number of photoexcited carriers is given in the form

$$n = G\tau \tag{2.27}$$

where τ, the lifetime can depend upon the level of excitation G and also upon the absolute temperature . Moreover, variations in material preparation can yield a range of values for τ extending as it does for CdS, from 10^{-2} to 10^{-10} sec. The lifetimes of electrons and holes which are generally independent of each other may approach equality under conditions of high excitation or extreme purity of material conditions that are generally assumed to hold for transistor materials and are controlled by recombination centres, while response times by the combined effects of recombination centres and traps. The temperature dependence of photoconductivity has little or no connection with the temperature dependence of the conductivity in the dark.

Let a sample of semiconductor be exposed to light of intensity I, then the amount of light energy absorbed per unit time per unit area of a layer of thickness dx (x is the direction of propagation of light) is proportional to I and the layer thickness dx:

$$-dI = (kI)dx \tag{2.28}$$

where k is a coefficient of proportionality, known as the *optical absorption coefficient*. The optical energy absorbed per unit time in unit volume is

$$\frac{dI}{dx} = -kI \tag{2.29}$$

Thus

$$\Delta n' = \Delta p' = \beta kI \tag{2.30}$$

where β is a coefficient of proportionality. If I represents the number of quanta per second, then β stands for the *quantum yield*, i.e., the number of pairs formed by a single quantum which usually cannot exceed unity. However, in case that the energy of the quantum exceeds *double* the width of the forbidden band, the carriers generated may possess sufficient kinetic energy to form additional nonequilibrium pairs by *impact ionization*, thereby leading to $\beta > 1$.

$$\Delta n = \Delta p = \beta kIt \tag{2.31}$$

It is known from experiments that in fact, after a certain time from the beginning of illumination, a constant (steady-state) photoconductivity $\Delta\sigma_{st}$ is established corresponding to steady-state values of the nonequilibrium carrier densities Δn_{st} and Δp_{st}. It follows therefore that as well as the process of *generation* of free carriers there should also be a converse process of carrier *annihilation* and the rates of both processes must be equal when the steady-state is reached. Otherwise, the number of free carriers would increase indefinitely which would be an unphysical situation.

Each nonequilibrium carrier liberated by light exists in the free state until it recombines with a hole, for a certain time (the so called *free-state lifetime*) which may of course be different for different carriers. Hence, we introduce the concept of the *average lifetime*, denoted by τ. The value of this average lifetime varies within wide limits (usually from ~10^{-2} to 10^{-7} sec) depending on the substance.

$$\Delta n_{st} = \beta k I \tau_n \tag{2.32}$$

Similarly for holes

$$\Delta p_{st} = \beta k I \tau_p \tag{2.33}$$

Substituting Eqs. (2.32) and (2.33) into Eq. (2.25), we obtain

$$\Delta\sigma_{st} = \Delta\sigma_n + \Delta\sigma_p = e\beta k I\left(\mu_n\tau_n + \mu_p\tau_p\right) \tag{2.34}$$

If one of the terms in parentheses in the above equations outweighs the other (originating from a large difference in the mobilities or in the lifetimes of electrons and holes or both), then we have *unipolar* nonequilibrium conductivity due to carriers of one sign only:

$$\Delta\sigma_{st} = e\mu\tau\beta k I \tag{2.35}$$

In this case the steady-state nonequilibrium conductivity is governed by four parameters: β, k, μ and τ. The first two of this quartet (β and k) represent the interaction of light with matter and govern the process of the generation of nonequilibrium carriers, while the latter pair (μ and τ) describe the interaction of carriers with matter and represent the processes of motion and recombination of nonequilibrium carriers.

2.3.4. Energy Distribution of Nonequilibrium Carriers

Immediately after ionization, the energy of a nonequilibrium electron or a hole, formed by a photon of sufficient energy $h\upsilon$, may be considerably greater than the average energy of the equilibrium carriers, which is of the order of kT. However, as the result of interaction with phonons and lattice defects (also called *thermalization*), the kinetic energy of the nonequilibrium carriers rapidly drops to the equilibrium value, that is, nonequilibrium carriers attain the temperature of the lattice. A calculation has shown that an electron with energy of about 1 eV loses its excess energy after $\sim 10^3$ collisions implying that an electron having a mean free path of $\sim 10^{-6}$cm and a velocity of 10^7cm/sec (in fact the average velocity is moderately higher) loses its excess energy in $\sim 10^{-10}$sec.

We have already pointed out that the lifetime of nonequilibrium carriers in the bands amounts to $10^{-2} - 10^{-7}$sec, a period considerably longer than the time necessary to lose the excess energy. The recombination time is by definition long and in the neighbourhood of milliseconds while the trapping time is likely to be microseconds or shorter. Consequently, a nonequilibrium carrier exists for a large part of its lifetime in a state with the same average kinetic energy (hence temperature) as the equilibrium carriers. In the great majority of cases therefore, we may assume that the energy distributions of the nonequilibrium and equilibrium carriers in the band are identical. We also know that the equilibrium carrier density is determined uniquely (at a given temperature) by the position of the Fermi level.

$$n = n_0 + \Delta n = N_C \exp\left(\frac{E_{Fn}}{kT}\right) \tag{2.36}$$

$$p = p_0 + \Delta_p = P_V \exp\left(\frac{-E_{Fp} - E_g}{kT}\right) \tag{2.37}$$

The levels with the energies E_{Fn} and E_{Fp} are called *quasi Fermi levels*. At equilibrium, the Fermi level is the same for electrons and holes in the bands or at local

states but the quasi Fermi levels are different for the conduction and valence bands and have separate values for each type of local energy state. Two assumptions can be made:

i- The electrons are essentially in thermal equilibrium in the conduction band and the excess holes are in equilibrium in the valence band.

ii- The electron-hole recombination time is much larger than the time for the electron and holes to reach equilibrium within the conduction and valence band, respectively. At equilibrium $E_{Fn} = E_{Fp}$. If excess electrons and holes are injected into the semiconductor, the electron Fermi level E_{Fn} moves towards the conduction band, while the hole Fermi level E_{Fp} moves towards the valence band. The ability to define the quasi Fermi levels provides us with a powerful approach to solve nonequilibrium problems which are, of course, of greatest interest in devices.

In particular, the equilibrium and nonequilibrium carriers have the same average probability of recombination, and in the absence of degeneracy, not only the equilibrium carriers but also the nonequilibrium ones satisfy the Einstein relationship between the mobility μ and the diffusion coefficient D:

$$\frac{D}{\mu} = \frac{kT}{e} \tag{2.38}$$

At high electric fields the mobility decreases as an inverse of the electric field because of the decrease in the scattering time. The diffusion coefficient also diminishes at high fields where the Einstein relation does not hold as well as it does at low fields, since the electron distribution function is quite complicated.

2.1. Lifetime of Nonequilibrium Carriers

Each nonequilibrium carrier, for example an electron, takes part in thermal motion, and consequently, while moving in a band it has a definite probability of meeting a hole and of recombining with it or, as it is sometimes expressed, of being *captured* by a hole. In general, a given semiconductor may contain several *types* of holes (free holes in the valence band, holes localized at various impurity levels or structure-defect levels and so forth). Evidently, the probability of an electron meeting holes of a given type is proportional to the density of these holes and to the average relative, thermal velocities of motion of the electrons and the holes, v_n and v_p which are assumed to be equal. If we introduce a concept of *capture cross section* (or *recombination cross section*) q_n for the capture of an electron by holes of a certain type the density of which is p, then obviously the average time between two meetings of the electron with these holes τ_n is, from

$$n = G\tau_n = \frac{G}{p_r v q_n} \tag{2.39}$$

and

$$p = G\tau_p = \frac{G}{n_r v q_p} \tag{2.40}$$

$$\tau_n = \frac{1}{p_r v q_n} \tag{2.41}$$

and is independent of and consequently, in general not equal to the lifetime of a free hole

$$\tau_p = \frac{1}{n_r v q_p} \tag{2.42}$$

The lifetimes τ_n and τ_p can readily be written, because the assumption of free carrier densities small compared with recombination centre densities means that the occupancy of the recombination centres is substantially the same after illumination as it was in the dark. We can conclude that the lifetimes are constant in the range of carrier densities from about 10^6 cm^{-3} (that is the upper limit of densities assumed for thermal carriers) to about 10^{16} cm^{-3} (the density of recombination centres lying near the Fermi level). Further, except for the slow dependency of thermal velocity on temperature, the lifetimes should be insensitive to temperature, if the capture cross sections are temperature-insensitive. In this model where there are no trapping states, the response time of the photoconductivity, which is equal to the lifetime of its majority carrier, is the time for the photocurrent to reach a steady-state (or some appropriate fraction of steady-state, like 0.5) after initiation of the light. This is also the time required for the photocurrent to decay to the same fraction of its steady-state value after the light is interrupted. The lifetimes τ_n and τ_p are invariant with light intensity and insensitive to temperature.

The response time is now no longer equal to lifetime but is greater than that by the factor $\left(1+\frac{n_t}{n}\right)$ for electrons and $\left(1+\frac{p_t}{p}\right)$ for holes. The response time, designated by τ_{0n} or τ_{0p} is dominated by the majority carriers (the carrier with the longer lifetime). If we wish to double the number of free electrons by an increase in light intensity, then we will have to double the number of electrons in traps as well. Hence, an additional time $\left(\frac{n_t}{n}\right)\tau_n$ is required to excite enough electrons to double the number of trapped electrons and the total response time is

$$\tau_{0n}=\left(1+\frac{n_t}{n}\right)\tau_n \tag{2.43}$$

On interrruption of the light we must wait not only for the free electrons to be captured into the recombination states but also for the trapped electrons to be emptied into the recombination states, by way of thermal excitation into the conduction band

and subsequent capture; because the trapped electrons do not have direct access to the recombination states due to the existence of the discrete states in the forbidden zone at physically different places and more than a few lattice spacings removed from each other. The recombination centres are located so far from the band edges that thermal excitation to the band edges from them could obviously be neglected in comparison with rates of kinetic capture of free electrons and holes. By contrast, the trapping states are located close enough to a band edge that thermal exchange of electrons or holes with the band edge far exceeded the rate of capture of carriers from the opposite band edge.

The steady-state Fermi level for electrons, E_{Fn}, is defined as that Fermi level consistent with the density of electrons in the conduction band. Its energetic distance from the conduction band is given by

$$n = N_C \exp\left[-\frac{|E_{Fn} - E_C|}{kT}\right] \tag{2.44}$$

Similarly the energetic distance from the valence band of the steady-state Fermi level for holes, E_{Fp}, is given by

$$p = N_V \exp\left[-\frac{|E_{Fp} - E_V|}{kT}\right] \tag{2.45}$$

Since in fact each such meeting ends with the capture of the electron by a hole, the time τ_n is essentially the average electron lifetime before being captured by holes of the given type. If the semiconductor contains k *types* of hole which capture electrons, then for each of them we can introduce the lifetime τ_{nk} and τ_{pk}:

$$\tau_{nk} = \frac{1}{p_k q_{nk} v_{nk}} \tag{2.46}$$

$$\tau_{pk} = \frac{1}{n_k q_{pk} \upsilon_{pk}} \tag{2.47}$$

The product of the cross section and the velocity, averaged for all the carriers in the band,

$$\overline{q_{pk} v_{pk}} = \gamma_{pk} \tag{2.48}$$

is called the recombination (capture) coefficient and represents the recombination rate when the densities n_k and Δp are equal to unity. Similarly

$$\overline{q_{nk} v_{nk}} = \gamma_{nk} \tag{2.49}$$

From Eqs.(2.46) and (2.47) we find that the values of the average lifetime of all the carriers in the bands (for which we retain the previous notation τ_{nk} and τ_{pk}) can be written in the form

$$\tau_{nk} = \frac{1}{\gamma_{nk} p_k} \tag{2.50}$$

$$\tau_{pk} = \frac{1}{\gamma_{pk} n_k} \tag{2.51}$$

Concluding, we note that since the values of the lifetimes τ_{nk} and τ_{pk} depend respectively on the densities p_k and n_k respectively, they are not only variable for a given material, but can also vary with time (under nonsteady-state conditions), with temperature, or intensity of illumination and so on.

2.4.1. Linear and Quadratic Recombination

i-The rate of recombination (capture) is proportional to the first power of the nonequilibrium carrier density. This case is realized, for example, when there are holes of only one type which recombine with the nonequilibrium electrons, and the density of these holes p is very high and practically independent of the illumination. Then, in accordance with Eq. (2.50), $\tau_n = \left(1/\gamma_n p \right) = cons.$ and the rate of recombination (capture) of electrons, equal to $\Delta n/\tau_n$, is directly proportional to the density. This case will be called *linear recombination.*

ii-The rate of recombination is proportional to the square of the nonequilibrium carrier density. This happens, for example, when the density of equilibrium carriers is almost zero and on ionization, the electrons are transferred from a lower to an upper band; then the densities of nonequilibrium electrons and holes are equal and the rate of recombination

$$\gamma \Delta n \Delta p = \gamma (\Delta n)^2 \tag{2.52}$$

This case will be called *quadratic recombination.* Only in the special case of linear recombination does the instantaneous value of the lifetime remain the same for the whole process of relaxation. Due to the fact that the number of holes is very small when the number of electrons is also very small, it is not surprising that when $t = 0$ in the rise case and $t \to \infty$ in the decay case, i.e., when $\Delta n \to 0$, the instantaneous value of τ tends to infinity. In the linear case, τ_{st} is a constant independent of the intensity of illumination, and consequently the steady-state nonequilibrium density is proportional to the illumination intensity:

$$\Delta n_{st} \approx I \tag{2.53}$$

In any nonlinear recombination case τ_{st} depends on the illumination intensity and thus, there is no longer a linear relationship between Δn_{st} and I. In particular, in the quadratic recombination case

$$\tau_{st} = \frac{1}{\sqrt{\gamma\beta kI}} \tag{2.54}$$

and finally

$$\Delta n_{st} \approx \sqrt{I} \tag{2.55}$$

Thereby, the linear recombination case is characterized by a linear dependence on the intensity of illumination and the nonlinear recombination case by a nonlinear characteristic and the concepts of *linear* and *nonlinear* nonequilibrium conductivity are frequently used.

It should be pointed out that since each absorbed quantum necessarily excites one electron (unless the photon has an energy greater than *twice* that of the band gap), then the quantum yield of a single microscopic absorption process is identically equal to unity. The coefficients β_n and β_p have a meaning only because absorption processes which produce free electrons and holes may coexist with competing absorption mechanisms which are accompanied by electron transitions or by such transitions as do not produce free carriers. It should also be mentioned that these competing absorption mechanisms are not necessarily due to some foreign *occlusions* in the material (impurities, defects, grain boundaries in polycrystals, and so forth). In principle, even a perfect single crystal which is absolutely free of impurities may exhibit such absorption. For example, absorption in the fundamental band may produce electron transitions from the valence band to the conduction band (Fig.2.7, transition 1), but some absorbed quanta may be used for transitions within the allowed bands (transitions 2 and 3). In the presence of local impurity centres we can also have transitions 4 and 5, each of which leads to the generation of carriers of one sign only. The transitions 2, 3, 4, and 5, which compete with transition 1, may obviously reduce β_n and β_p , the quantum yields of free electron and hole generation, to below unity. In the lower part of Figure 2.7 the transitions represented by letters a, b, c, d, e correspond respectively to

$$a \rightarrow \beta kI$$

$$b \rightarrow \gamma_n n(M-m)$$

$$c \rightarrow \gamma_n m N_{cM}$$

$$d \rightarrow \gamma_p pm$$

$$e \rightarrow \gamma_p (M-m) P_{VM}$$

Recombination may be divided into three main categories such as, direct recombination, recombination through traps and surface recombination. In the first of these, the electrons and holes recombine through an electron dropping from a state in the conduction band to an empty state in the valence band in a single transition. An amount of energy in excess of ΔE must be disposed of by some means, and the simplest process by which this can be done is by radiation which may or may not also involve the emission or absorption of phonons. Another means of disposing of the energy ΔE in a single event is to transfer it to another electron in the conduction band or hole in the valence band, thus creating a highly energetic charge carrier which will soon, however, share its energy with other carriers in the band. This process is known as *Auger* recombination since it is similar in principle to the well-known Auger effect whereby an atom may make a transition to a lower state, the energy being emitted in the form of an electron rather than as radiation. This type of recombination was once thought to be too unlikely to be of importance in semiconductors but it is now known that this is not so.

A third process whereby the energy ΔE may be disposed of is for it to be transferred to a number of phonons. Even the most energetic phonons (the optical phonons) have energies of the order of $0.1\,eV$ so that about ten would be required for $\Delta E = 1eV$. The emission of so many phonons in a band-to-band transition is thought to be very unlikely, but if the process is carried out by way of electron or hole traps multi-phonon processes may be important. The probability of a radiative transition decreases rapidly as the energy radiated is increased, so that, by making the transition in two steps, the energy to be disposed of at each step is considerably reduced and this type of process may be much more probable than the single-step process.

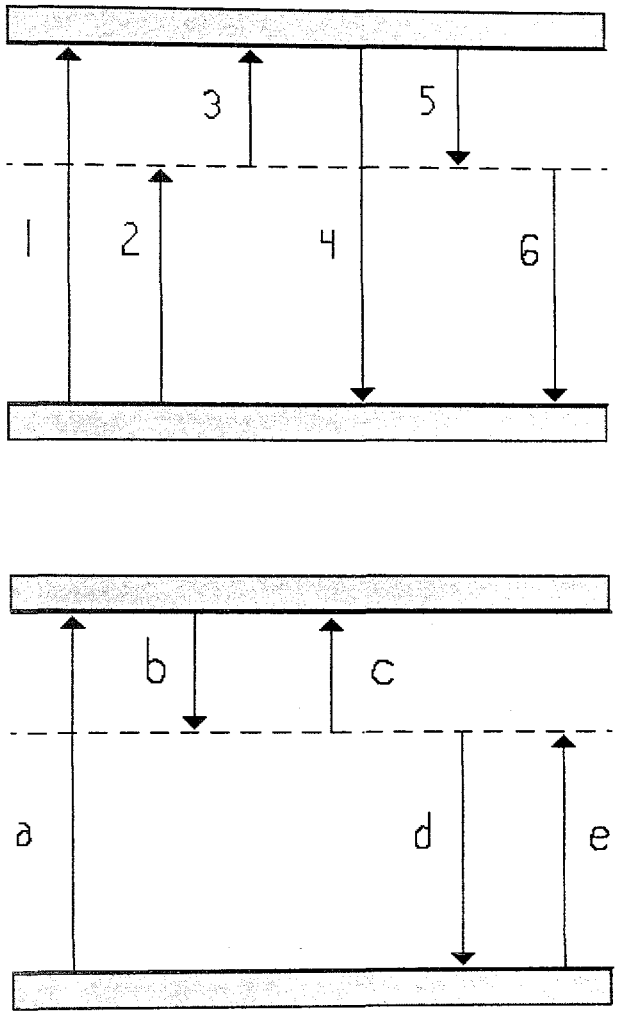

Figure 2.7. The scheme showing the most important transitions in a semiconductor having a wide forbidden band and traps of one type.

2.4.2. Determination of the Principal Parameters β and τ

i-Methods for the determination of β and τ by investigating the *frequency dependence* [i.e., the dependence of the amplitude of the alternating component of the photoconductivity on the frequency of chopping (modulation)].
ii-Methods for the determination of τ by compensating the phase difference between the modulated exciting light beam and the photoconductivity. Essentially the methods of both the first and the second groups are suitable only for studies of linear photoconductivity.

2.4.3. Frequency Dependence of Photoconductivity and Phase Shift Compensation Method, Sinusoidal Modulation

The alternating component of the photoconductivity measured using chopped illumination depends not only on the chopping frequency but also on the form of modulation of the light beam intensity. In the case of sinusoidal modulation we have a phase shift ϕ between the exciting signal and the alternating component of the photoconductivity, depending on the relationship between τ and the modulation frequency ω

$$\phi = \tan^{-1}(2\pi\omega\tau) \qquad (2.56)$$

It follows that by measuring ϕ at a given ω, we can determine τ.The simplest method of measuring the phase shift ϕ is the compensation method. Although other factors may affect, the probability of a phototransition is related to the density of states in both bands rather than in only one of them. If the recombination act is accompanied by the appearance of a light quantum, that is, the energy liberated appears as luminescence, the interpretation of the recombination mechanism presents no difficulties. Thus, for example, in pure germanium (where $\Delta E \approx 0.7$ eV) at room temperature.

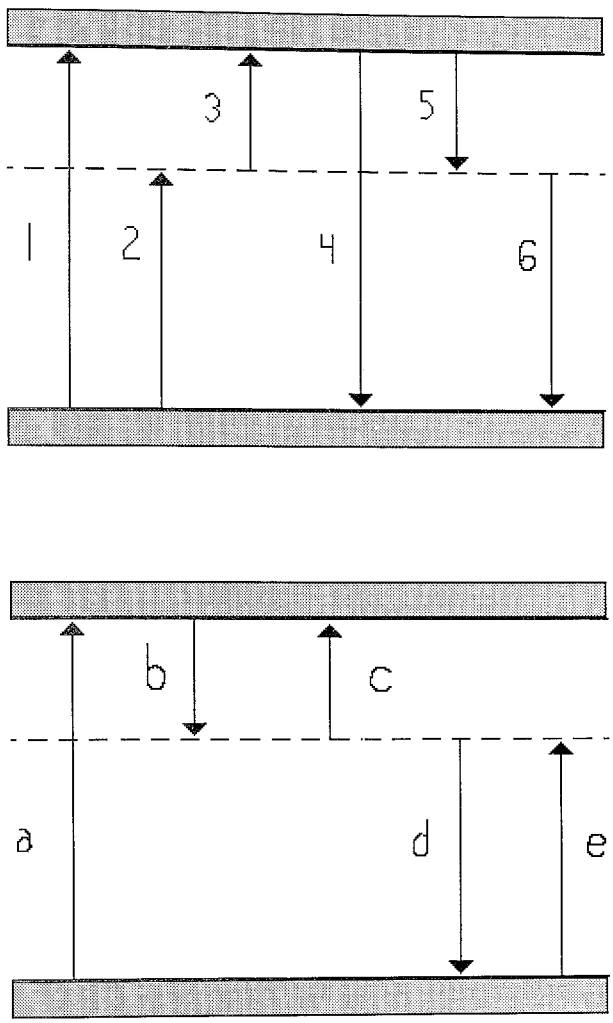

Figure 2.7. The scheme showing the most important transitions in a semiconductor having a wide forbidden band and traps of one type.

$$\gamma_n[n(M-m)-mN_{CM}]=\gamma_p[mp-(M-m)P_{VM}] \tag{2.60}$$

$$\gamma_n[n(M-m)-mN_{CM}]=\beta kI \tag{2.61}$$

$$\gamma_p[mp-(M-m)P_{vM}]=\beta kI \tag{2.62}$$

$$m[\gamma_n n+\gamma_n N_{CM}+\gamma_p p+\gamma_p P_{VM}]=M[\gamma_n n+\gamma_p P_{VM}] \tag{2.63}$$

then the number of trapped electrons

$$m=M\left[\frac{\gamma_n n+\gamma_p P_{VM}}{\gamma_n(n+N_{CM})+\gamma_p P_{VM}}\right] \tag{2.64}$$

and the number of trapped holes

$$M-m=M\left(1-\frac{m}{M}\right) \tag{2.65}$$

$$=M\left[1-\frac{\gamma_n n+\gamma_p P_{VM}}{\gamma_n(n+N_{CM})+\gamma_p(p+P_{VM})}\right]$$

$$=M\left[\frac{\gamma_n(n+N_{CM})+\gamma_p(p+P_{VM})-\gamma_n n-\gamma_p P_{VM}}{\gamma_n(n+N_{CM})\gamma_p(p+P_{VM})}\right]$$

$$=M\left[\frac{\gamma_n N_{CM}+\gamma_p p}{\gamma_n(n+N_{CM})+\gamma_p(p+P_{VM})}\right] \tag{2.66}$$

substituting the above values for m and $M-m$ into Eq 2.61 or Eq 2.62,

$$\gamma_n\left\{nM\left[\frac{\gamma_n N_{CM}+\gamma_p p}{\gamma_n(n+N_{CM})+\gamma_p(p+P_{VM})}\right]-M\left[\frac{\gamma_n n+\gamma_p P_{VM}}{\gamma_n(n+N_{CM})+\gamma_p(p+P_{VM})}N_{CM}\right]\right\}=\beta kI \quad (2.67)$$

$$M\left[\frac{\gamma_n\gamma_p(np-N_{CM}P_{VM})}{\gamma_n(n+N_{CM})+\gamma_p(p+P_{VM})}\right]=\beta kI \quad (2.68)$$

Since it is difficult to calculate the steady-state lifetime τ using Eq. 2.68 in the general case, it is more practical to consider the limiting cases of *low* and *high* trap concentrations.In the presence of photoexcitation, the conductivity, σ_L, can be written as in Eq. (2.26)

$$\sigma_L=(ne\mu_n+n_0e\mu_n)+(pe\mu_p+p_0e\mu_p) \quad (2.26)$$

where n and p are the electron and hole carrier concentrations under optical excitation respectively, n_0 and p_0, the thermal equilibrium concentrations in the dark, and μ_n and μ_p the conductivity mobilities of electrons and holes. The photoconductivity, σ_{ph}, is defined as

$$\sigma_{ph}=\sigma_L-\sigma_D \quad (2.69)$$

Photoconductors in general exhibit $\sigma_{ph}\propto G^{\gamma}$ where γ can be unity, greater than unity, less than unity, or equal to 0.5 (Rose, 1960). Amorphous Si as an example, has exhibited all these characteristics. Large changes in photoconductivity occur, for instance, when the deposition temperature, T_s is altered. Therefore, the differences in σ_{ph} are associated with deeper lying states, which control the lifetime of electrons (τ_n) and holes (τ_p). For electrons, τ_n can be written as

$$\tau_n = \frac{1}{\nu[q_{n1}p_{r1} + q_{n2}p_{r2}]} \tag{2.70}$$

Because of the continuous distribution of states in amorphous semiconductors, the occupancy of states, n_{r1} and n_{r2} will depend on the level of excitation. This leads to a nonlinear dependence of σ_{ph} on the generation rate G, and represented by

$$\sigma_{ph} = AG^{\gamma} \tag{2.71}$$

where A is a constant. The exact value of γ will depend on the details of the distribution of states. The density of trapped electrons within the semiconductor is given by,

$$n_t(E) = N_t(E)\exp\left[\frac{(E_t - E_{Fn})}{kT}\right] \tag{2.72}$$

where we use the quasi-Fermi level, E_{Fn}, rather than E_F, since we now have a nonequilibrium situation. It should be recognized that the shallow trapped electrons do not directly influence the recombination mechanism. However, the transient response is affected by these states since the termination of illumination involves not only the return of the free electrons to thermal equilibrium, but also the return of all the trapped carriers. If the recombination rate $\left(n/\tau_n\right)$ is less than the emission rate, the time taken to decay to half its value, τ_0, is given by,

$$\tau_0 = \left(1 + \frac{n_t}{n}\right)\tau_n \tag{2.73}$$

Photoconductivities with $\gamma = 1.0$ have been associated with monomolecular recombination and observed in a wide variety of undoped a-Si:H films (Zanzuchi *et al.*,1977; Loveland *et al.*,1973). $\gamma = 0.9$ has been obtained over many orders of

illumination intensity (or equivalently generation rate) G, indicating that τ_n remains essentially constant over a wide range of E_{Fn}.

Bimolecular recombination between either trapped or free carriers is reflected by a value of $\gamma = 0.5$ and has been observed in both rf and dc GD a-Si:H films. This occurs when the density of electrons trapped in shallow states begins to exceed the density of recombination centres. At the root of the increase in σ_{ph} with a decrease in $(E_C - E_F)$ lies the fact that there are fewer donor states for electrons to recombine with. Supralinearity, corresponding to $\gamma > 1$, has also been observed, the electron lifetime can, in principle, be elongated by orders of magnitude by the addition of recombination centres. This increase occurs at the expense in the lifetime of the other type of carrier. Now we have three sets of states in the energy gap:

i-hole traps in thermal contact with the valence band that have a small capture cross section for electrons;

ii-recombination centres near the middle of the gap with a large capture cross section for electrons and electron traps;

iii-states in thermal contact with the conduction band.

At low levels of illumination the quasi Fermi level for free holes is situated between **i** and **ii**, so that most of the holes recombine with the more efficient electron recombination sites near **ii**. At higher light levels, E_{Fn} and E_{Fp} move apart sufficiently to encompass state **ii**. The result of incorporating states of type **i** is that there is a transfer of holes from **ii** to **i**. Since $\gamma_{n1} \langle\langle \gamma_{n2}$, this leads to longer lifetimes and higher sensitivities. This supralinear dependence occurs only in the narrow region of temperature where holes are being transferred from state **ii** to state **i**. The photocurrent is frequently found to increase as some high power (greater than unity) of the light intensity over a short range of light intensities, although before and after the transition, it may vary approximately linearly with light intensity.

2.4.5. TRS and FRS

One of the two methods that try to study the kinetics is the **time-resolved spectroscopy (TRS)** where the luminescence from the sample excited by a single excitation pulse (in fact a δ-function light pulse) is detected during an infinitely narrow boxcar gate set at some time t_d after the pulse. However, for systems whose recombination kinetics are second order and thus lifetimes vary with the excitation intensity or with the carrier density during decay, the carriers due to one pulse may not decay completely before the next pulse, and so the decay following an excitation pulse may reflect not the density of carriers created during the pulse but the one already existing, a situation that generally arises if the system has lifetime components longer than the pulse repetition interval. TRS may then give the relaxation of the system to a metastable excited state rather than the ground state [12].

Therefore, in this work, due to the mentioned drawbacks, in contrast to (TRS), the **frequency-resolved spectroscopy (FRS)** method was used, which measures, not the lifetime distribution created by a pulse, but essentially that present during continuous excitation (cw) and gives results that can be interpreted quite straightforwardly. In this method which requires the use of sine wave modulated excitation and lock-in detection in exact quadrature, the lifetime distribution for only those components of the emission which have lifetimes

a-less than

b-greater than or

c-near the inverse modulation frequency

is observed directly by a suitable choice of detector, no matter how broad it is. For **a**, lock-in detection in phase with the modulation detects all components faster than the modulation frequency and sine wave modulation of the laser using a photo acoustic modulator is used. For **b**, all components slower than the modulation may be measured using a boxcar to detect the photoluminescence during the *off* period of a square wave chop, while method **c** uses sine wave modulation and lock-in detection in exact quadrature to detect only those components close to the modulation frequency.

2.4.6. Geminate Pair

The idea of *geminate pair* is frequently invoked for amorphous semiconductors, although the evidence for the concept is not overwhelming. In this model, it is assumed that the electron and hole remain close together following photo-excitation, because of the short thermalization time and low mobility of the carriers. *Tsang and Street (1978)* [13] have proposed that all the PL decay at times down to a few microseconds is due to nonradiative tunnelling by one or both carriers to defect states, followed by slow ($\sim 30\,\mu$sec.) radiative decay. They also described in their recombinational model, a process in which each carrier of an e-h pair, after the formation, diffuses apart at most to a distance of ~50 A and eventually recombines with its original partner, that is, with the hole with which it was created (*geminate* meaning *twin*). There are two important parameters in geminate recombination: r_0, the average distance over which the photoexcited electron moves away from the hole before it thermalizes and which clearly depends upon the frequency of the exciting light; r_c, the effective range of the Coulombic attraction between the e-h pair. Since the photoexcited electron can escape from the Coulomb field of the hole if it has energy within kT of the conduction band edge, then r_c is given by

$$r_c = \frac{e^2}{4\pi\varepsilon kT} \tag{2.74}$$

The activation energy for the photogeneration, $e^2/4\pi\varepsilon r_0$, should depend upon the frequency. There are three criteria that determine when geminate recombination is important:

i- a rapidly increasing photoconductive yield saturating at $\beta = 1$ as the frequency of light rises,

ii- a decreasing activation energy for the photoconduction as the frequency of light rises;

iii- an increase in photoconductive yield at applied fields in excess of 10^3 V/cm at room temperature or 10^4 V/cm at 100 K.

From their TRS results, *Tsang* and *Street* have reported that if the excitation density is sufficiently low for monomolecular recombination, for instance less than some carrier density of about $10^{18} cm^{-3}$, then the PL lifetime distribution is independent of excitation density, depending solely on temperature and as a result, $P(\tau)$ does not vary with the density of the generated pairs, an observation considered to be strong evidence for the geminate model of recombination. Meanwhile, above the critical value of $\sim 10^{18} cm^{-3}$ that represents only the crossover point at which the number of carriers excited in the pulse exceeds the number present at the beginning of the pulse, the geminate pairs are supposed to overlap and recombination kinetics become dependent on the pair density.

It is generally assumed that the photocreated carriers thermalize in their respective band tails by hopping processes. The radiative lifetime of an electron-hole pair recombining by a tunnelling process is given by

$$\tau = \tau_0 \exp\left(\frac{2r}{a}\right) \tag{2.75}$$

where r denotes the intrapair separation. The prefactor is normally assumed to be $\tau_0 \approx 10^{-8}$ sec. and the localization length of the electrons in the conduction band tail states has been estimated to be $a \approx 10-12A$. Both efficiency and spectral distribution are independent of the defect concentration, as long as the defect density does not exceed about $10^{17} cm^{-3}$. In the geminate model, it is assumed that the generated electron-hole pairs do not separate during thermalization and that therefore recombination occurs between the localized geminate carriers. The observed broad distribution of lifetimes $P(\tau)$ in this view is interpreted by the distribution of intra-pair separations which arises from the random walk of the carriers during thermalization.

2.4.7. Distant Pair

In the *distant pair* model, where the recombination is assumed to be carried out between *nearest available neighbours nongeminately*, one cannot talk about the previous mechanism. Since the recombination rate decreases exponentially with separation, in distant pair systems, it turns out that at moderate or low excitation intensities, the probability of recombination of an electron with a hole, other than the nearest neighbour is very small [6]. The characteristic property of the distant pair approach is that the distribution, in contrast to the geminate pair approach; *does* depend on excitation power density to the lowest powers measurable and the recombining electrons and holes are localized at binding centres that form a random distribution throughout the sample. In this model, the recombination is *bimolecular* at high excitation densities, *monomolecular* at low densities, and the photoluminescence lifetime τ distribution always depends on excitation density G, shifting to shorter τ with increasing G.

According to Rose (1978), an exponent of 1.0 in the relationship $I_{ph} \propto G^{\gamma}$, suggests that the recombination kinetics be **monomolecular,** while a 0.5 implies a **bimolecular** recombination. If the intensity dependence of the photocurrent is intermediate between 0.5 (*square root*) and 1.0 (*linear*) (such as 0.72 as we found for AsSeSb), then it is indicative of a continuous and probably exponential distribution of traps in the gap. Now a short explanation of the monomolecular and bimolecular recombination will be in order.

Monomolecular is used here to mean that the probability of recombination between a given electron and some single hole is close to one; the probability of recombination with any other hole is small, whereas *bimolecular*, despite that the prefix *bi* implying *two*, is used to signify that there is more than one hole (not necessarily two), with which a given electron has a significant probability of recombining. When electrons and holes are distributed at random spatially, bimolecular recombination occurs only at very high carrier densities.

We may distinguish three regions of excitation power giving different kinetics[6]:

i-At very low power, such that the average separation of a geminate pair, d, is less than the average separation between pairs, $\rho^{-1/3}$, the decay curve will be independent of excitation power and will be determined not by the statistics of a random spatial distribution of carriers but simply by the physics of diffusion. Thus for $d < \rho^{-1/3}$ the kinetics are *geminate monomolecular*.

ii-At intermediate excitation power, $d > \rho^{-1/3}$, we have *monomolecular distant pair* kinetics.

iii-At sufficiently high power, a carrier has some choice of recombination path and the kinetics are *bimolecular*. This occurs for $\rho > \sim \alpha^3$ at short times (a few τ_0).

The results obtained show conclusively that in any experiment, pulsed or continuous, that lasts long enough to accumulate the permanent population, recombination is through *distant pairs*, and interpretation of, for example, ODMR data, or thermal quenching data, must be carried out in a distant pair framework.

3. EXPERIMENTAL DETAILS

3.1. Sample Preparation

The materials whose lifetimes, photocurrents and their dependences on temperature, rate of generation and frequency of the modulated signal are measured and whose recombination kinetics are deduced are AsSeSb, AsSe and AsSeTe thin films. Of these, *arsenic* (As) and *antimony* (Sb) are Group V, while *selenium* (Se) and *tellurium* (Te) are Group VI elements. The atomic configuration of As is $1s^2 2s^2 2p^6 3s^2 3p^6 3d^{10} 4s^2 4p^3$, whereas that of Se ends with $4p^4$. Since the other two are in Group VI, their atomic configurations end with $5p^3$ for Sb and $5p^4$ for Te.

Arsenic (As) has a coordination number of three, a density of 5.72 gm/cm^3, a bond angle and a bond length that vary respectively between 94.1^0-98.5^0 and $2.49A^0$-$2.51A^0$. From As which is in the liquid phase for temperatures above 613 ^{0}C, both bulk samples and thin films can be made by such processes as evaporation, sputtering or glow-discharge decomposition from the AsH_3 gas. It occurs in many forms but its main use is in the manufacture of insecticides (many As compounds are poisonous). Every As atom can form a covalent bond with three different atoms. The As lattice is made up of sextuple chains interconnected with weak van der Waals bonds. For a-As, which behaves as a semiconductor, a mobility gap of ~1.0 eV was recorded and at room temperature and below, a conductivity of the type of *variable range hopping* was observed [14].

Selenium (Se) that has a density of 4.79 gm/cm^3 and melting and boiling temperatures of respectively 217 ^{0}C and 685 ^{0}C allows us to make a-Se samples both in bulk and thin film form. a-Se exhibits a high photoconductivity even at low energies and thanks to its high electrical and optic characteristics, finds a vast area of application in semiconductor technology as rectifier and solar cell and also in the manufacture of vidicon tubes in Tv sets, AC-DC converters and xerography. Se is

also used in making red glass for the signal light. Se, which, when added to glass in smaller amounts, neutralizes the green colour due to iron in the glass, can also be added to rubber to make it flame-resistant and long-wearing and be used in the production of some stainless steel and special copper alloys.

Tellurium (Te) that possesses structural characteristics similar to those of Se has a density of $6.24\,gm/cm^3$, melting and boiling temperatures of respectively 449.5 ^{0}C and 989.8^{0}C. Like Se, Te too, has metallic, crystalline and amorphous phases and participates in organic and inorganic compounds, lead and copper alloys as a component and both are semimetals. It is used in different areas of industry, especially in semiconductor technology. Antimony (Sb) has an atomic radius of 1.41 A^0, melting and boiling temperatures of respectively 630.5 ^{0}C and 1325 ^{0}C. That also exists in several forms, the most familiar being the brittle, silvery and metallic form. This element that has an important use in making printing type expands when it solidifies from the molten state. When it is added to a lead type metal, it makes the lead type expand when it cools in the moulds to make for sharper and cleaner type.

The samples measured were thin films of amorphous AsSeSb, AsSe and AsSeTe prepared by thermal evaporation, the material used being of 99.999% purity, after which aluminium contacts were also evaporated in a coplanar configuration and copper wires soldered. The films are also annealed for an hour. Since the current-voltage measurements carried out between ± 50 V revealed that the contacts were perfectly ohmic in this region, a voltage of 30 V has been applied to the contacts by a voltage source (Keithley 487 picoammeter), for all measurements. This limit was not exceeded in order not to overexcite the electrons and therefore overshadow the effect of the modulated light.

The *quadrature frequency-resolved photocurrent (QFRPC)* response of the samples in the frequency interval between 10 Hz and 40 kHz, was measured as a function of the intensity of the excitation light and of temperature by a lock-in amplifier, because this frequency-locked AC measurement rejects stray light, dark

current and other unmodulated signals. The photocurrent was excited by a solid state type laser beam with an intensity of 5 mW and wavelength of 635 nm, hence corresponding to an energy of 1.95 eV which is sufficiently higher than the optical band gap of the material and the beam was modulated by driving the laser with a function generator.

The temperature was controlled up to two decimal places, by a 330 Heater and Autotuning Temperature Controller (Lakeshore) and for cold measurements the samples were immersed in a tank that contains liquid nitrogen and its vapour (Figure 3.2). In order not to let contamination by water vapour, the films were immersed gradually, that is, the temperature of a sample was dropping in a single measurement. As the temperature reached under –40C approximately, especially when the excitation level is low, the lock-in did not give satisfactory results except the AsSeTe case whose photoconductivity is considerably higher than that of the other two and which allowed us to measure even at as low as –110C.

The level of filtering of one of the two filters in the process was varying as it was rotated around its axis, while that of the other was fixed. The level of illumination has been measured by a luxmeter and three trustable values, namely 600, 200 and 40 Watts/m^2, (a 15-fold range) has been chosen.

3.2. Lock-in Amplifiers

Lock-in amplifiers are used to detect and measure accurately, very small AC signals, down to a few nanovolts, even when the small signal is obscured by noise sources thousands of times larger than the signal of interest. Lock-in amplifiers, rejecting the noise signals at frequencies other than the reference frequency, use a technique known as *phase-sensitive detection* to single out the component of the signal at a specific reference frequency and phase. Phase sensitive synchronous detection is a powerful method for the recovery of small signals which may be obscured by interference which is much larger than the signal of interest. In a typical

application, a continuous wave (cw) laser which induces the signal of interest is modulated by an optical chopper. The lock-in amplifier is used to measure the amplitude and phase of the signal of interest relative to a reference output from the chopper.

This type of measurements require a frequency reference. An experiment is excited at a fixed frequency (from an oscillator or a function generator) and the lock-in detects the response from the experiment at the reference frequency. As an example, let the reference signal be a square wave at frequency ω_r. This might be the synchronous output from a function generator. If the sine output from the function generator is used to excite the experiment, then the response might be

$$V_{sig}\sin(\omega_r t + \theta_{sig}) \tag{3.1}$$

where V_{sig} is the signal amplitude, ω_r is the signal frequency and θ_{sig} is the signal's phase. Lock-in amplifiers generate their own internal reference signal, (which, in this case is $V_L\sin(\omega_L t + \theta_{ref})$) usually by a phase-locked-loop locked to the external reference. The lock-in amplifies the signal and then multiplies it by the lock-in reference using a phase sensitive detector or multiplier. The output of the PSD is then simply the product of two sine waves.

$$V_{PSD} = V_{sig}V_L\sin(\omega_r t + \theta_{sig})\sin(\omega_L t + \theta_{ref}) \tag{3.2}$$

$$V_{PSD} = \left(\frac{1}{2}\right)V_{sig}V_L\cos[(\omega_r - \omega_L)t + \theta_{sig} - \theta_{ref}] - \left(\frac{1}{2}\right)V_{sih}V_L\cos[(\omega_r + \omega_L)t + \theta_{sig} + \theta_{ref}] \tag{3.3}$$

The PSD output is two AC signals, one at the difference frequency $(\omega_r - \omega_L)$ and the other at the sum frequency $(\omega_r + \omega_L)$. Although when the PSD output is passed through a low-pass filter the AC signals are removed and generally nothing

remains, if $\omega_r = \omega_L$, then the difference frequency component will be a DC signal proportional to the signal amplitude and the filtered PSD output will be

$$V_{PSD} = \left(\frac{1}{2}\right) V_{sig} V_L \cos(\theta_{sig} - \theta_{ref}) \tag{3.4}$$

Fourier's theorem basically states that any input signal can be represented in the *frequency domain*, as the sum of many sine waves of differing amplitudes, frequencies and phases. However, normal oscilloscopes display the signal in the *time domain* which, except in the case of clean sine waves, does not convey much information about the various frequencies making up the signal. Since a lock-in multiplies the signal by a pure sine wave at the reference frequency, all components of the input signal are therefore multiplied by the reference simultaneously. Mathematically speaking, sine waves of differing frequencies are *orthogonal*, that is, the average of the product of two sine waves is zero unless the frequencies are exactly the same. The product of this multiplication yields a DC output signal proportional to the component of the signal whose frequency is exactly locked to the reference frequency. The low-pass filter that follows the multiplier provides the averaging which removes the products of the reference with components at all other frequencies.

A lock-in amplifier, because it multiplies the signal by a pure sine wave, measures the single Fourier (sine) component of the signal at the reference frequency. As an example, suppose that the input signal is a simple square wave at frequency ν, which is composed of a great number of sine waves at multiples of ν with carefully related amplitudes and phases. A $2V_{PP}$ square wave can be expressed as

$$S(t) = 1.273\sin(\omega t) + 0.4244\sin(3\omega t) + 0.2546\sin(5\omega t) + \ldots \tag{3.5}$$

where $\omega = 2\pi\nu$. The lock-in, locked to ν, will single out the first component and thus, the measured signal will be $1.273\sin(\omega t)$, rather than the $2V_{PP}$ that one would measure on a scope.

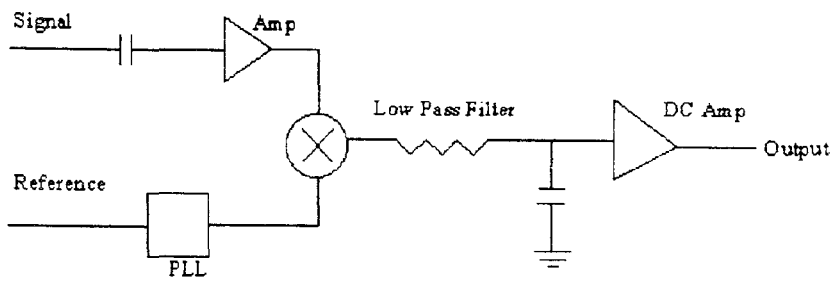

Figure 3.1. The simplified block diagram for a single phase lock-in amplifier, which measures the component of the signal at a single phase with respect to the reference.

In the general case, the input consists of signal plus noise which is represented as varying signals at all frequencies. The ideal lock-in only responds to noise at the reference frequency and the noise at other frequencies is removed by the low-pass filter following the multiplier.

This *bandwidth narrowing* being the primary advantage of a lock-in amplifier, only inputs with frequencies at the reference frequency result in an output. In Figure 3.1 is shown the lock-in amplifier block diagram.

3.3. Experimental Results and Discussion

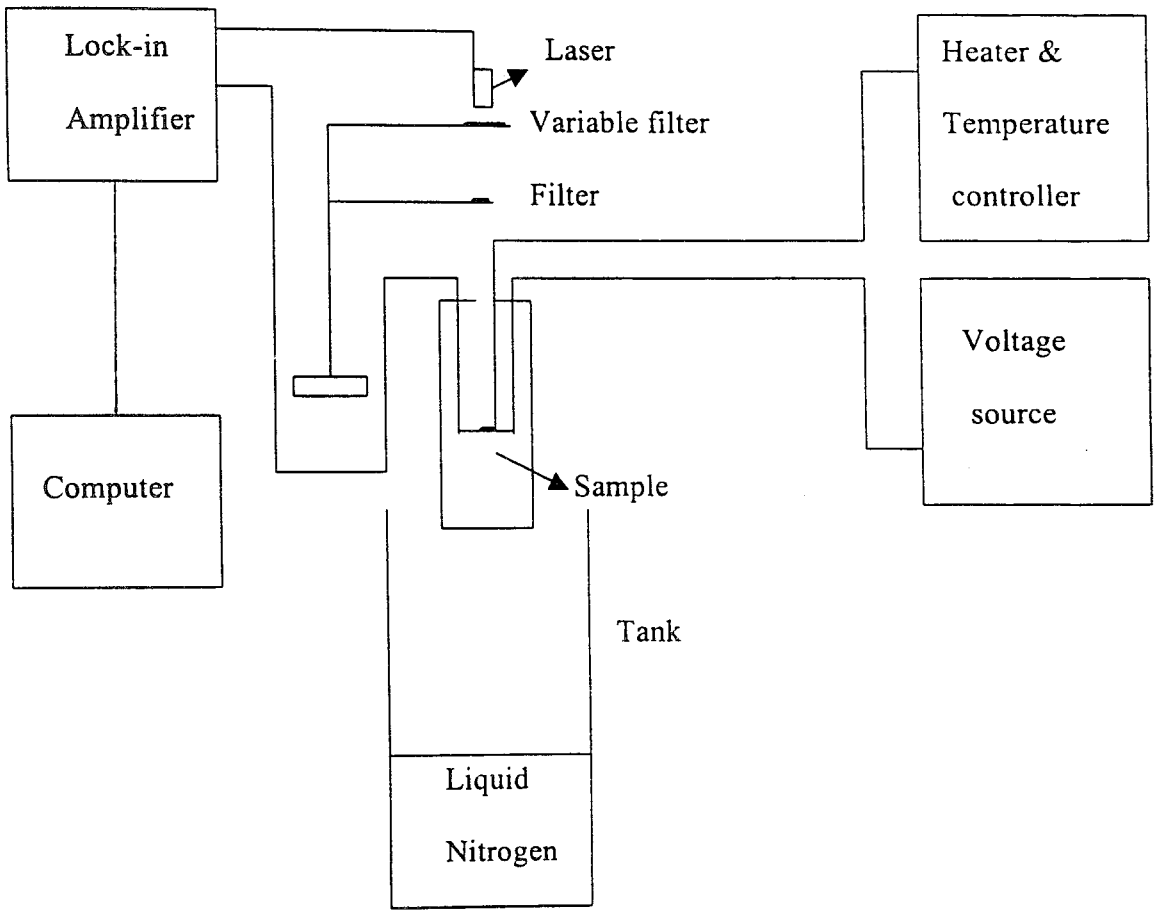

Figure 3.2. A schematic representation of the setup used in the measurements.

As was mentioned above, the results presented here are derived from quadrature frequency-resolved photocurrent (QFRPC) response measurements performed on the samples of AsSeSb, AsSe and AsSeTe thin films. Since the energy of the excitation

light is high enough for the carriers to be photoexcited, surmounting the optical band gaps of their energy scale, we can assume that they move up to extended states and a trap-limited recombination holds.

For each step of the frequency ω of the modulated excitation, the values of both the photocurrent and the phase angle were recorded by the lock-in amplifier in an excel file in the computer. As the frequency, starting from 10 Hz rose up to higher than 10 kHz, each step of frequency being, on the average, 14% larger than the previous, so that the whole frequency range is swept in 65 steps; the photocurrents normally exhibited a continual drop, while the phase angle underwent a gradual rise in most of the range swept, then an almost abrupt fall. While processing the data, what we were involved for each set was the product of the photocurrent (normalized to the maximum value for *that* pair of temperature and excitation level) and the sine of the phase angle [6]. This product (in arbitrary units), when plotted against ω showed a *Lorentzian-type* of distribution of lifetimes for that modulation frequency whose peak value gives the dominant value of the lifetime which is equal to the inverse of ω_{peak}

$$\tau = \frac{1}{2\pi\upsilon_{peak}} \tag{3.6}$$

As can be seen from Figure 3.3, the spectra of AsSeSb films contain a broad single peak, shifting to lower frequencies (that is longer lifetimes) as the intensity decreases while temperature is held fixed. The same behaviour is observed in Figure 3.4 that depicts the ω dependence of the FRPC response for the same material, as the temperature diminishes and intensity held constant. Figure 3.3 displays the FRPC response vs. frequency curves for three different illumination (also called excitation or generation) levels at a constant temperature of 120 C, while Figure 3.4 shows the same response vs. frequency for three different temperatures and at a constant illumination level of 600 Watts/m^2. Almost the same trend can be observed in Figures 3.5 and 3.6 for the AsSe and in Figure 3.7 for the AsSeTe films.

In the *donor-acceptor (DA)* model (Searle, Nashashibi, Austin, Devonshire and Lockwood, 1979),

$$\tau = \tau_0 \exp(\alpha r) \tag{3.7}$$

where τ is the lifetime (sec), $\alpha(=2/a)$ is the localization parameter, $a(=10-12\text{A})$ is the Bohr radius, $\tau_0 \cong 10^{-8}$ sec and r is the diffusion length over which the recombination is assumed to take place. In amorphous materials, both the localization parameter α and the tunnelling distance may vary, giving a distribution of radiative lifetimes. One can conclude from Figure 3.3 and using Eq. (3.6) that the lifetime of carriers shortens as the intensity of illumination enhances, a conclusion plausible, considering the formula for the average time (that is *lifetime*) between two meetings of an electron with holes

$$\tau_{nk} = \frac{1}{p_k q_{nk} v_{nk}} \tag{2.46}$$

where q_{nk} and v_{nk} are respectively the capture cross section of an electron by holes and the average relative velocity of the carriers. Both of these quantities remain roughly constant upon a variation in the intensity, that may in turn greatly increase the number of nonequilibrium carriers (n and p) and the quasi Fermi level E_{Fn}. One can also deduce from Figure 3.4 that the peak (that is the lifetime) shifts to higher temperatures indicating that as one increases the temperature at fixed illumination, the lifetime drops. For band tail states in amorphous and heavily doped crystalline semiconductors, since α increases steadily for states deeper in the gap, this can provide a mechanism in which recombination is faster at higher energies for a fixed electron-hole separation. The geminate model predicts that $P(\tau)$, the probability of recombining at time τ, at any separation r, is independent of the generation rate, whereas according to the distant pair model the $P(\tau)$ distribution should shift continuously to shorter times when the generation rate increases and since we observed a similar tendency in all the samples, we can state that the recombination in these samples is through distant pairs [6]. In Figure 3.8, where a comparison between the (FRPC) responses of samples of

AsSe, AsSeSb and AsSeTe is made at a temperature of 60 C and for a fixed illumination level of 40 Watts/m^2, it is seen that the lifetimes of carriers in the first two are almost the same, while that of the AsSeTe is somewhat longer.

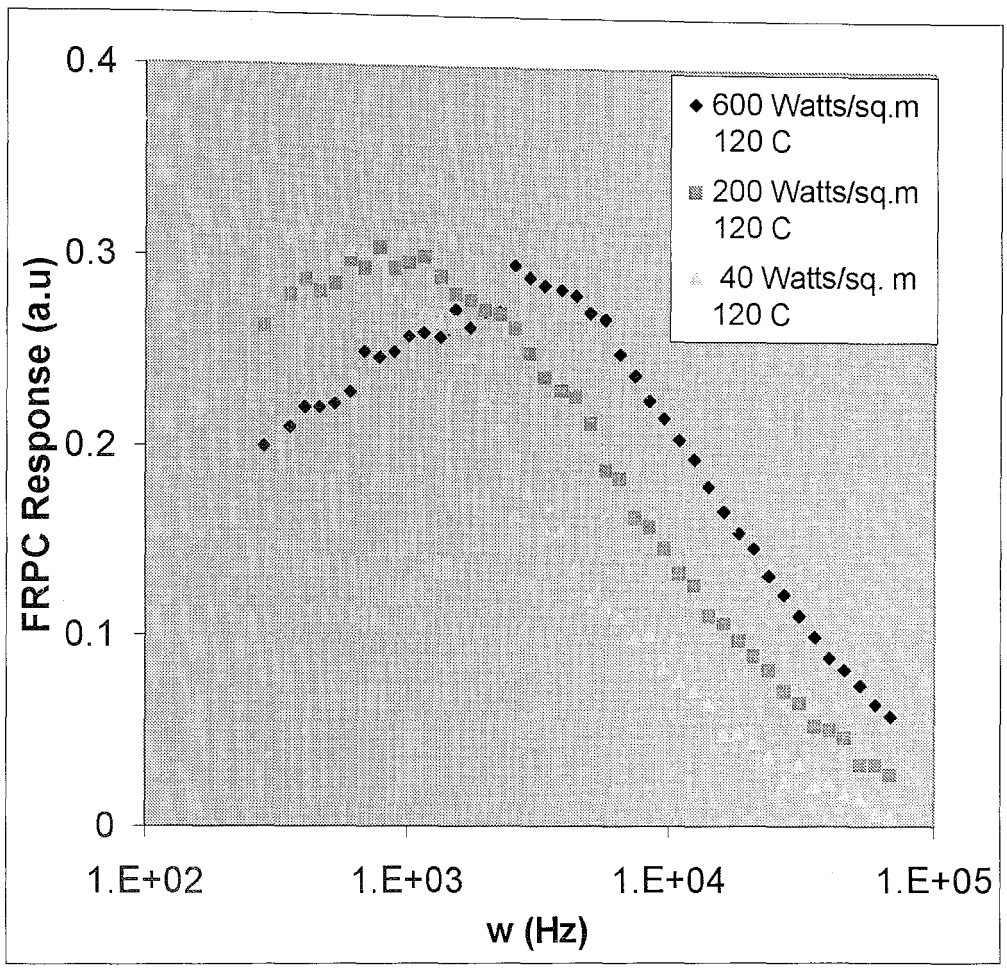

Figure 3.3. Frequency-resolved photocurrent (FRPC) response of an a-AsSeSb sample at the excitation intensities of 600, 200 and 40 Watts/m^2 and for a fixed temperature of 120 C.

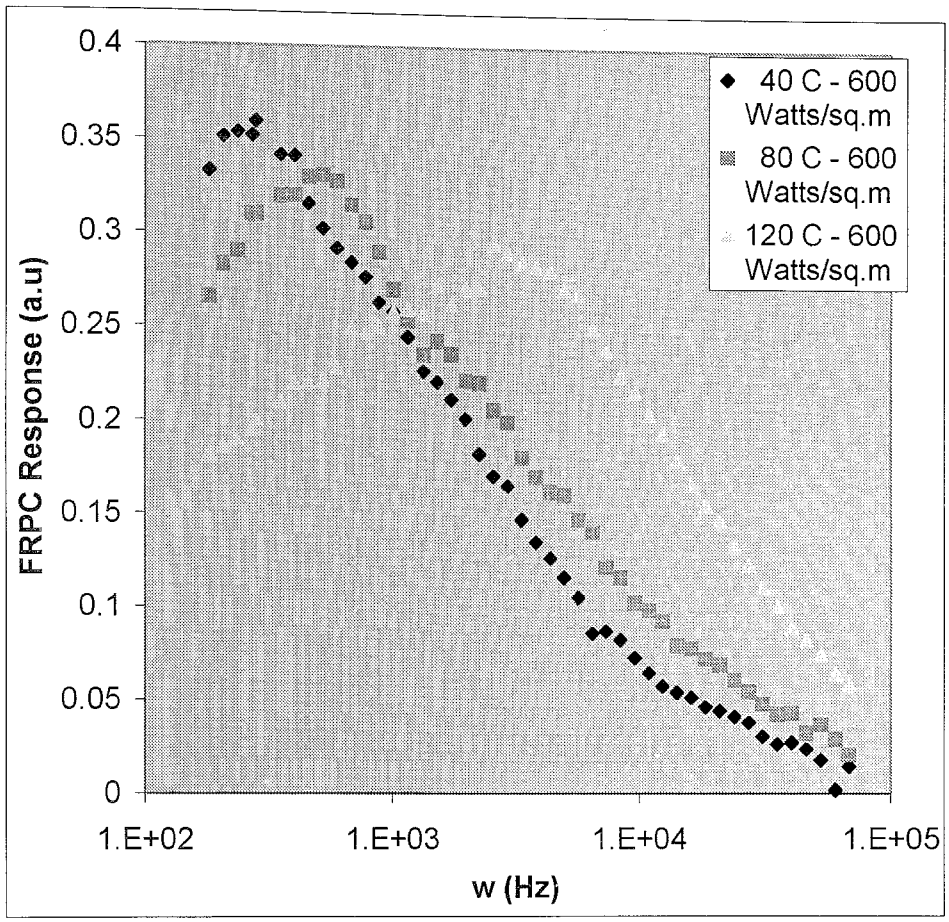

Figure 3.4. Frequency-resolved photocurrent (FRPC) response of an a-AsSeSb sample at temperatures of 40, 80 and 120 C and for the fixed illumination level of 600 Watts/m^2.

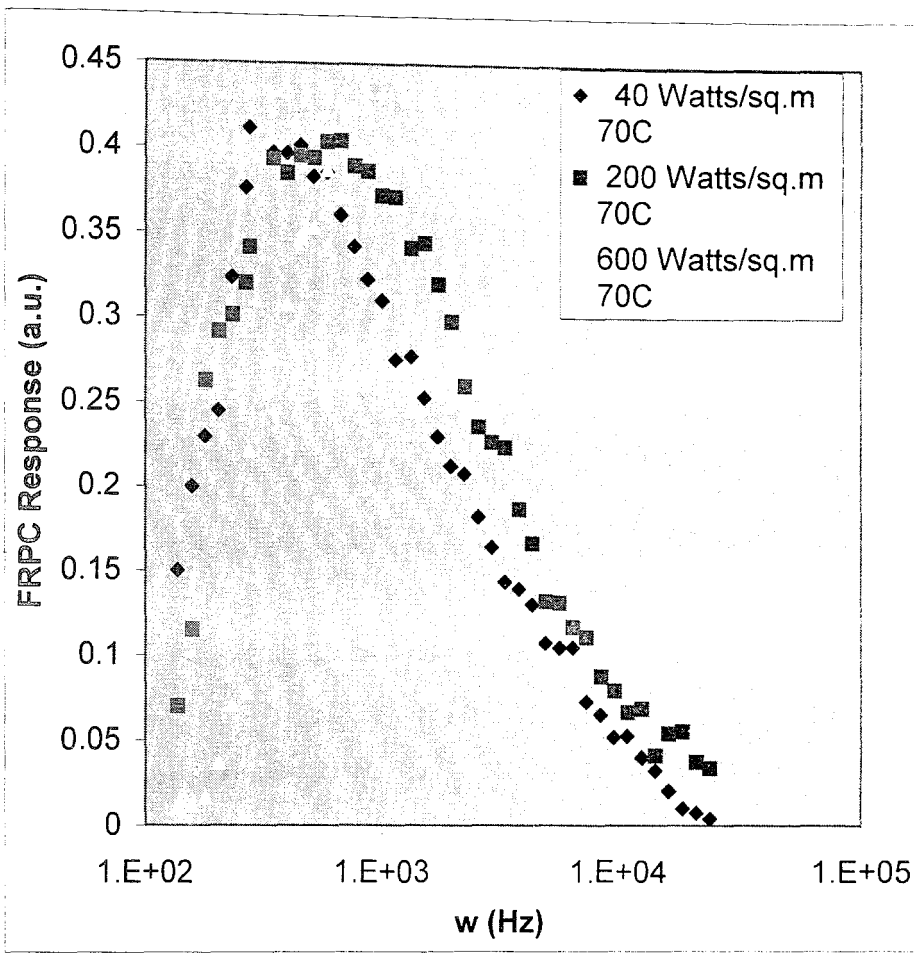

Figure 3.5. Frequency-resolved photocurrent (FRPC) response of an a-AsSe sample at the excitation intensities of 600, 200 and 40 Watts/m^2 and for a fixed temperature of 70C.

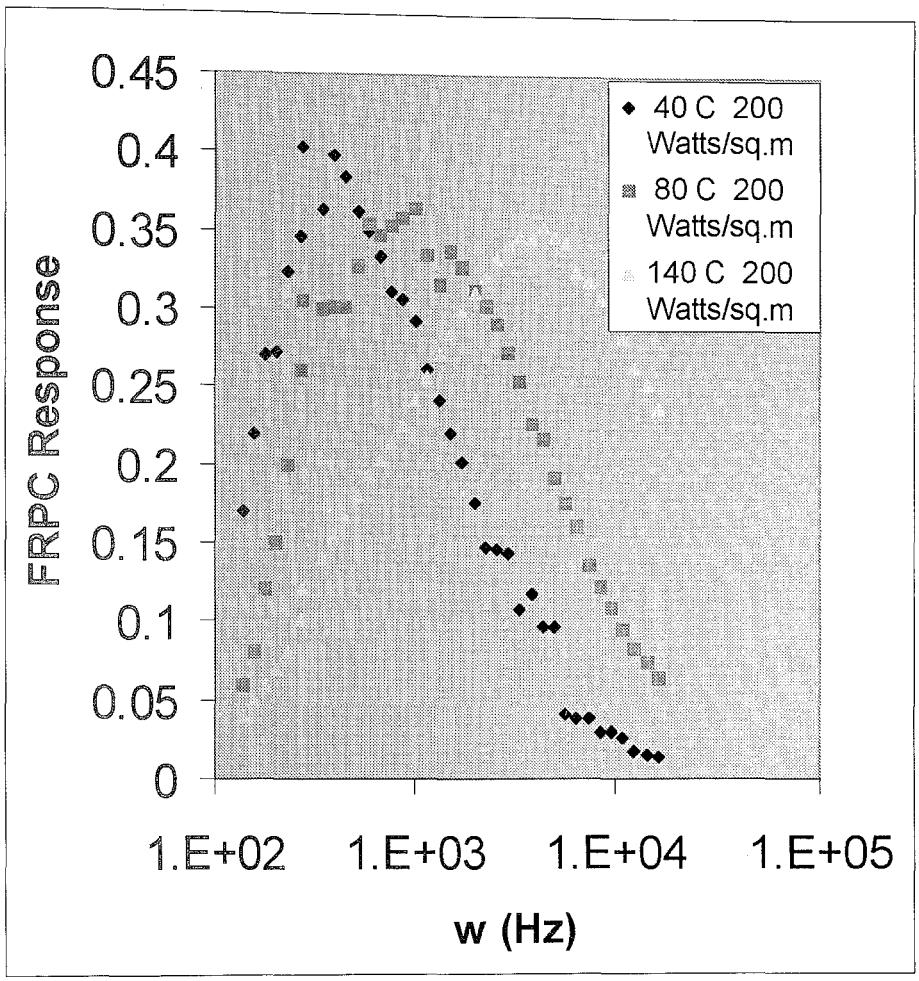

Figure 3.6. Frequency-resolved photocurrent (FRPC) response of an a-AsSe sample at temperatures of 40, 80 and 140 C and for the fixed illumination level of 200 Watts/m^2.

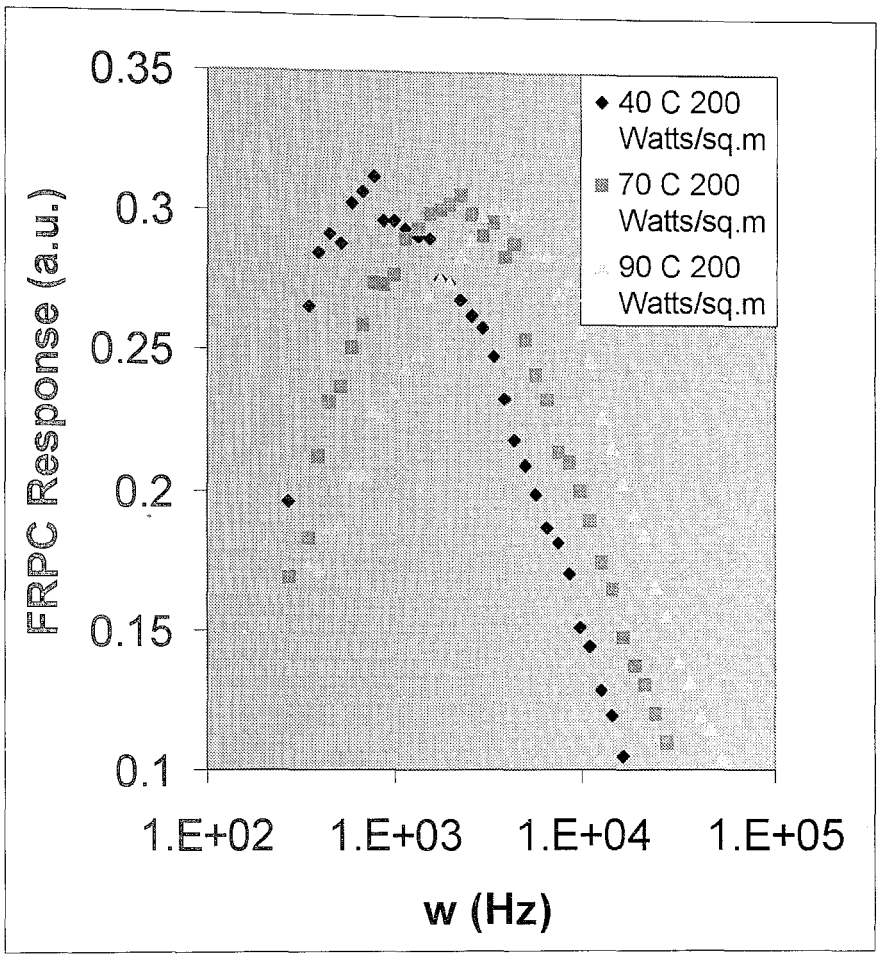

Figure 3.7. Frequency-resolved photocurrent (FRPC) response of an a-AsSeTe sample at temperatures of 40, 70 and 90 C and for the fixed illumination level of 200 Watts/m^2.

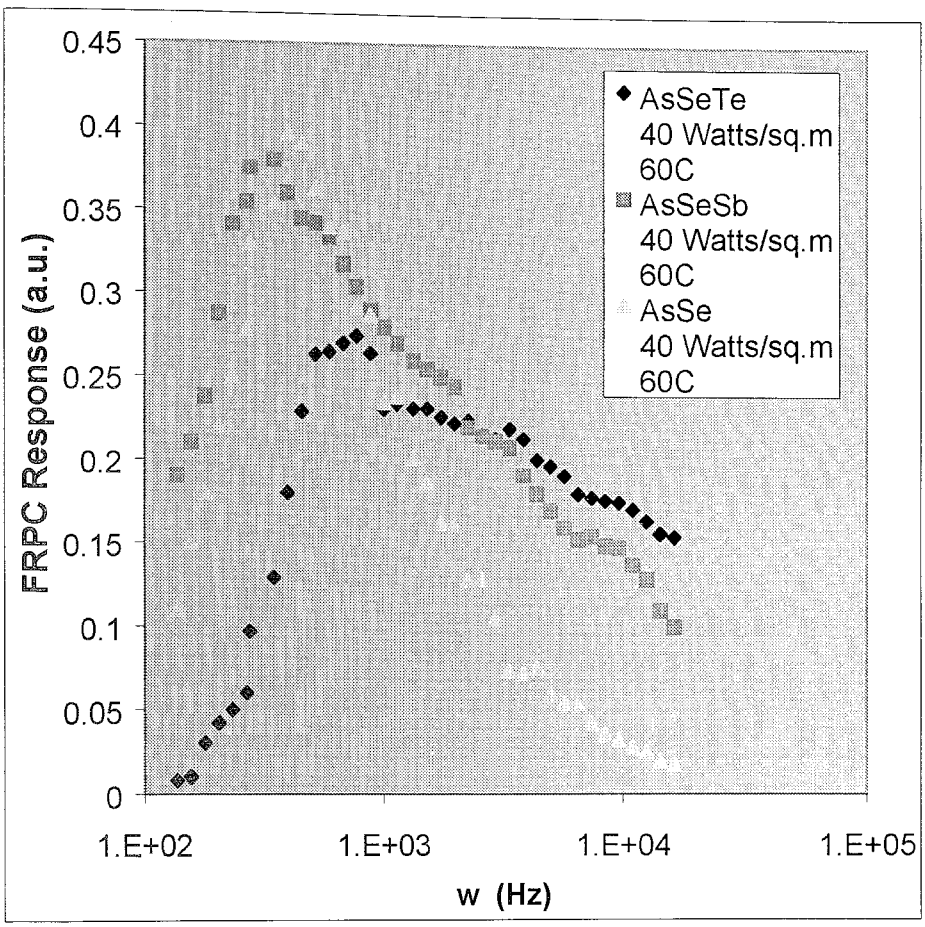

Figure 3.8. A comparison of the frequency-resolved photocurrent (FRPC) responses of samples of AsSeTe, AsSeSb and AsSe, at a temperature of 60 C and for the fixed illumination level of 40 Watts/m^2.

3.3. Dependence of Lifetime on Generation and Temperature

As explained above in Sections 2.4.6 and 2.4.7, for the *geminate recombination*, Tsang and Street (1979) describe in their recombinational model, a process in which each carrier of an e-h pair, after the formation, diffuses at most to a distance of $\approx 50A$ and eventually recombines with its original partner (geminate or twin) and where the pairs, above a density of $\sim 10^{18} cm^{-3}$, are supposed to overlap, hence causing recombination kinetics to become dependent on the pair density. Whereas in the *distant pair* model, where the recombination is assumed to be carried out between nearest available neighbours nongeminately, one cannot talk about the first mechanism.

Our data for the lifetimes of carriers in all these films are between ≈ 280 and $\approx 10^4$ microseconds. Using Eq. 3.2 and the parameters therein, these figures are found to give diffusion lengths around $60A\langle r\langle 85A$ (all greater than 50A, the maximum value assumed in the references, for the geminate recombination case) which enable us to state that the recombination kinetics for the chalcogenide samples we measured, are through distant pairs.

Figure 3.9 displays the excitation (illumination) intensity dependence of the lifetime plotted on a logarithmic scale. This relationship can be expressed as

$$\tau = AG^{\nu} \tag{3.3}$$

where τ is the lifetime, A is a constant, G is the generation rate (excitation intensity) and ν is the exponent whose value could reveal the type of recombination.

Since in the case of AsSeSb, the slopes of the lines in Figure 3.9 are -0.46 and –0.77 at respectively 295 K and 390 K; we can infer, by the help of a second clue that the recombination kinetics in these films is through *distant pairs*. The ν values for the a-SeTe and a-AsSe samples were respectively found to be –0.87 and –0.81 by Kaplan [15] and [16], which are in good agreement with our results.

The inverse relationship between lifetime and intensity of excitation is reinforced by the temperature. The lifetimes calculated are drawn in Figure 3.10 as a function of temperature, for the light intensities of 600 and 200 Watts/m^2, indicating that the lifetime which seems to rise almost linearly at first, levels off as the temperature is reduced (the slope getting down to almost one-fifth), the value for lower intensity being higher at each T, but the gap between the two lifetime values becoming less and less, as one goes to lower temperatures. From the formula

$$\tau = \tau_0 \exp\left(\frac{E_\omega}{kT}\right) \tag{3.4}$$

that gives the temperature dependence of lifetime; the activation energy E_ω is calculated to be around 0.7 eV, placing the quasi-Fermi level in AsSeSb around midgap, which for this type of materials was supposed to be around 1.6 eV [17].

Figures 3.11 and 3.12 drawn respectively for AsSeTe and AsSe reflect almost the same trend for these films, namely, an increase in the lifetime as one goes to lower temperatures and for each value of T, a longer lifetime for weaker illumination. But this general tendency becomes less apparent as one reaches lowest temperatures (that is, highest $1000/T$ values). As Figure 3.13 exhibits, the slope n (in the relationship $I_{ph} \propto T^n$) between the ln of photocurrent lifetime versus ln(T) in an a-AsSe sample, at three excitation intensities, 600, 200 and 40 Watts/m^2 is, on the average, the same, excluding the limiting values.

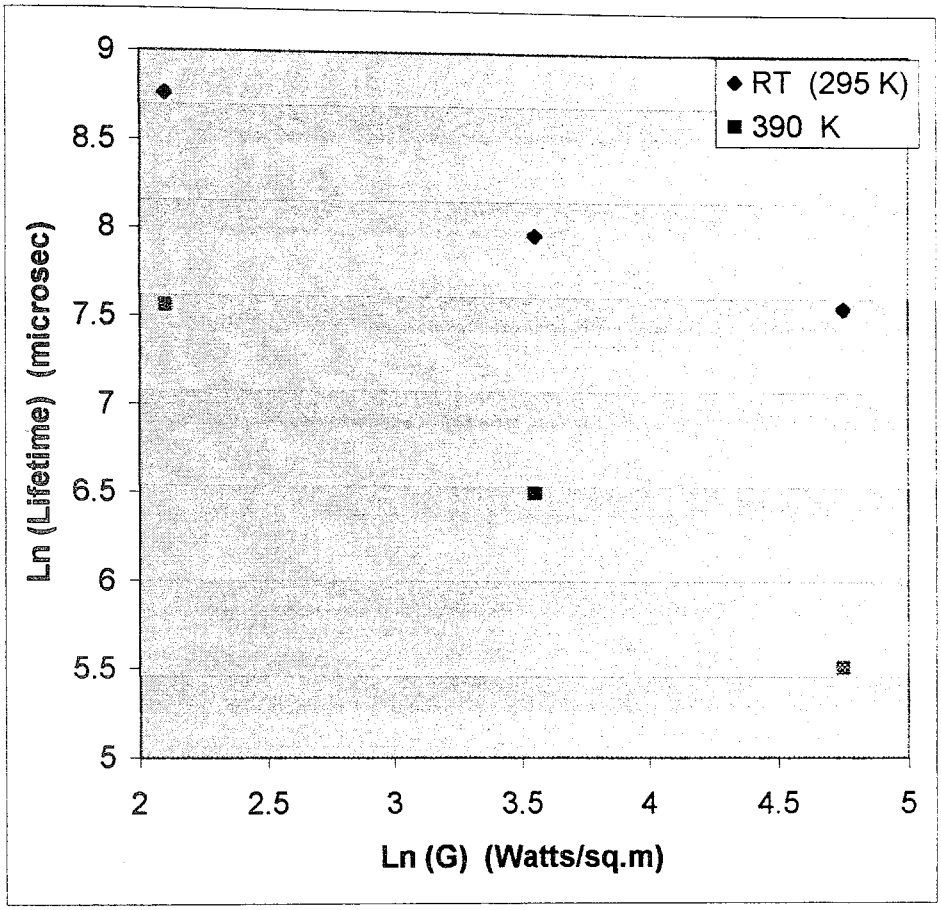

Figure 3.9. Photocurrent lifetime versus excitation intensity in an a-AsSeSb sample at 295K and 390 K.

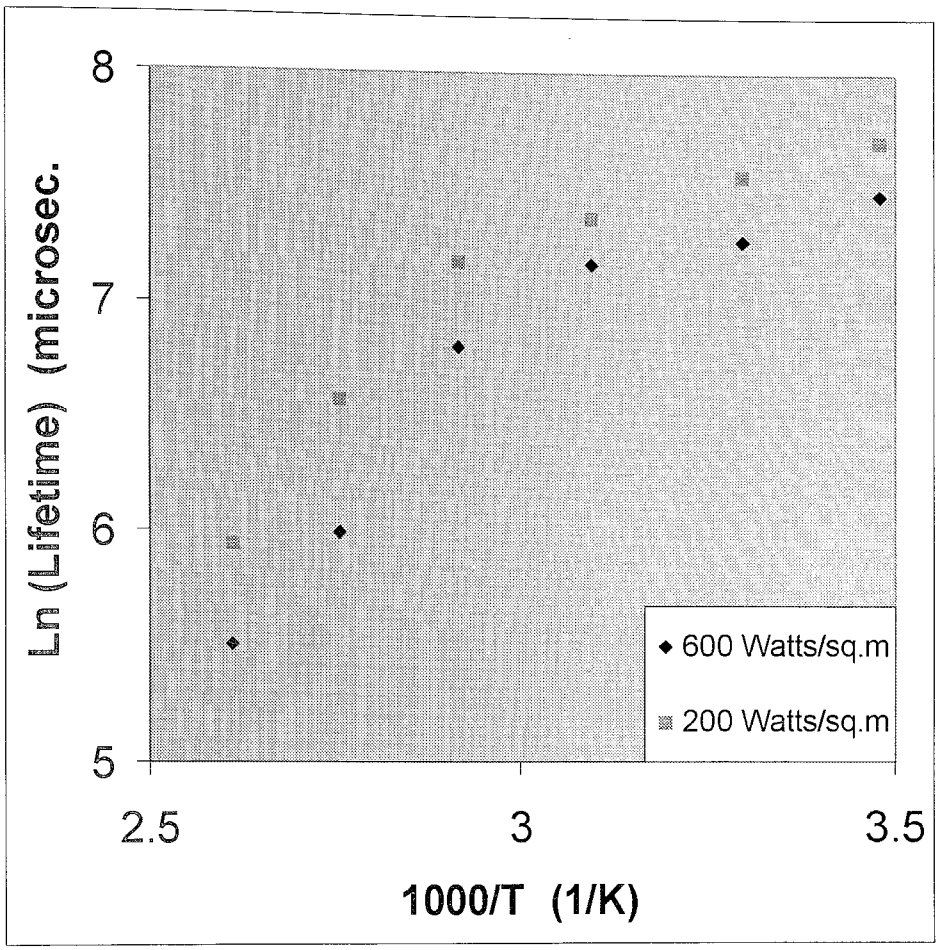

Figure 3.10. Photocurrent lifetime versus 1000/T in an a-AsSeSb sample, at two excitation intensities, 600 and 200 Watts/m^2.

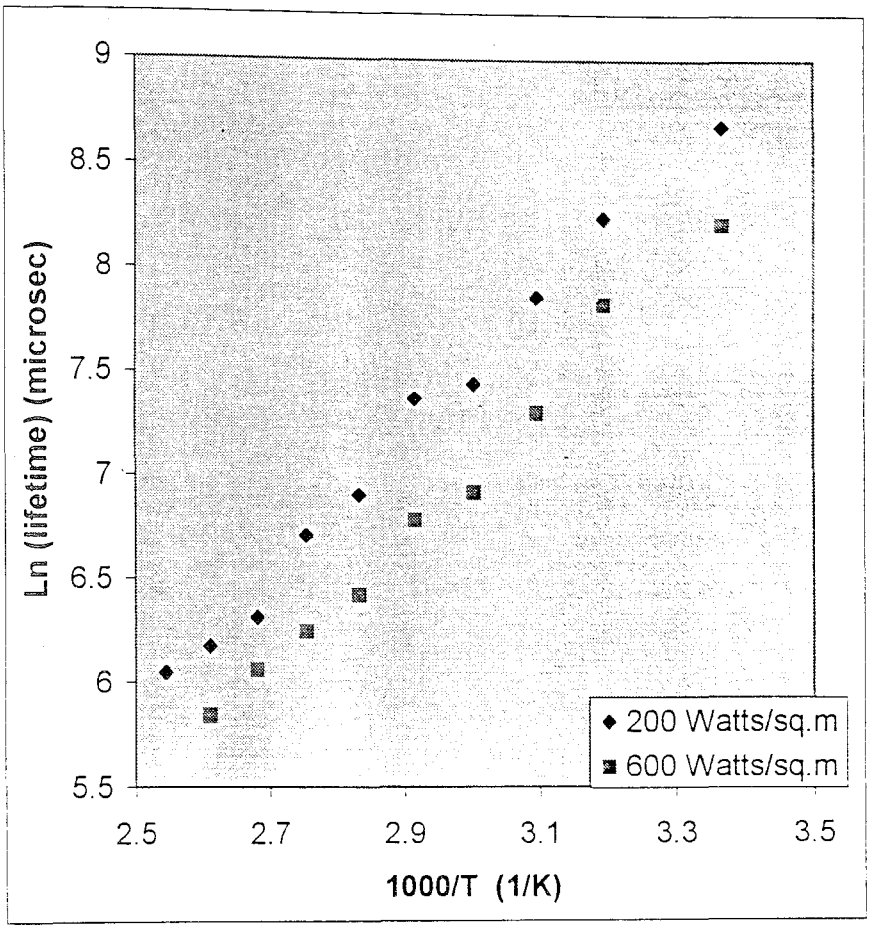

Figure 3.12. Photocurrent lifetime versus 1000/T in an a-AsSe sample, at two excitation intensities, 600 and 200 Watts/m^2.

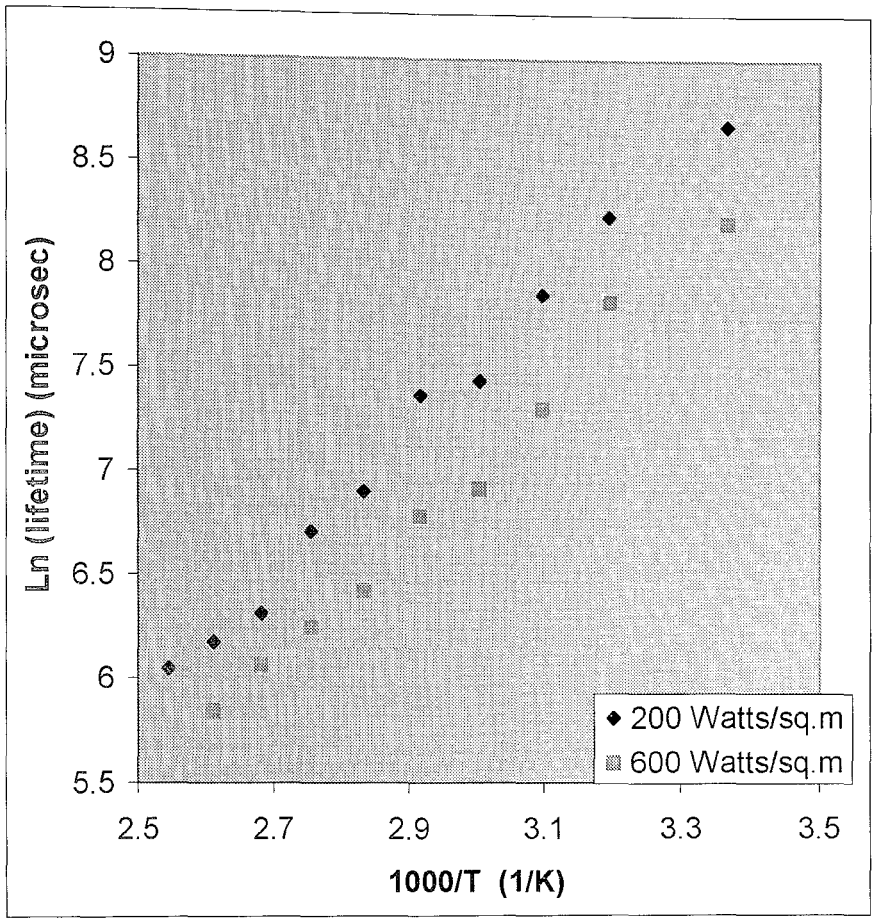

Figure 3.12. Photocurrent lifetime versus 1000/T in an a-AsSe sample, at two excitation intensities, 600 and 200 Watts/m^2.

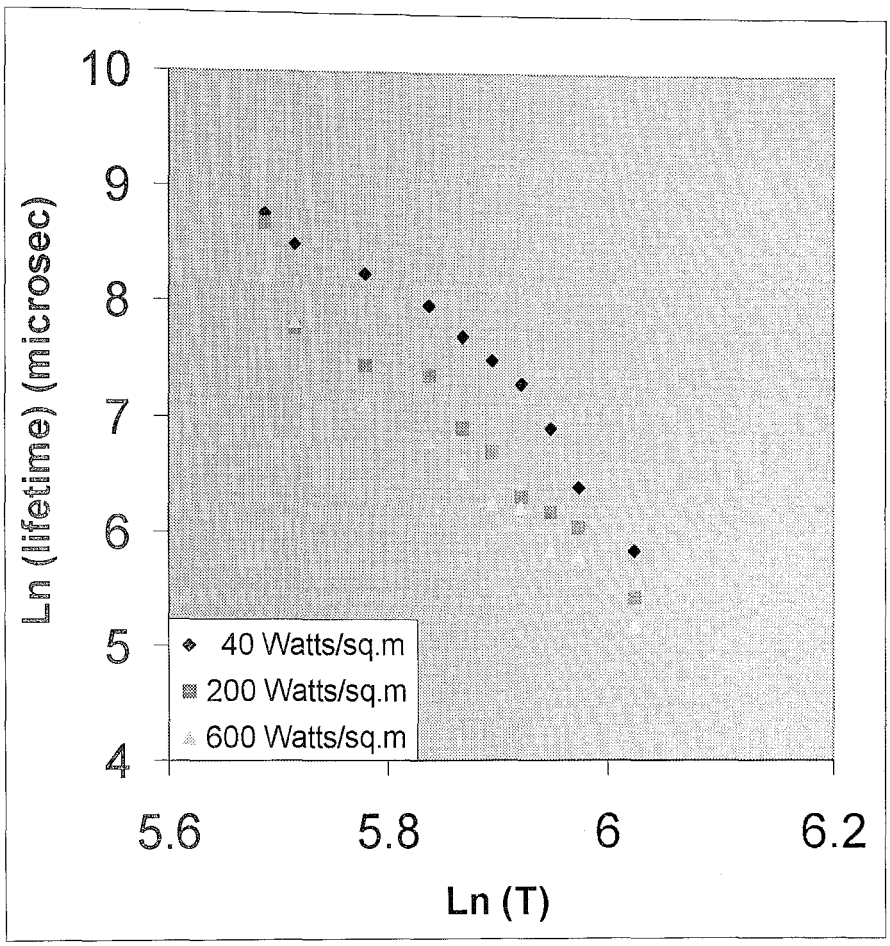

Figure 3.13. Photocurrent lifetime versus ln(T) in an a-AsSe sample, at three excitation intensities, 600, 200 and 40 Watts/m^2.

3.5. Dependence of Photocurrent on Generation, Temperature and Frequency

Figure 3.14 displays the temperature dependence of photocurrent for three excitation intensities, namely 40, 200 and 600 Watts/m^2, all taken at 200 Hz. This entirely linear dependence between the ln of the photocurrent and inverse temperature $(1000/T)$, as Table 1 shows, depicts a similar behaviour up to the frequencies of 10^4 Hz, but having a slowly increasing exponent of temperature at fixed excitation as the frequency is increased or a slightly decreasing exponent as the excitation is enhanced. So n is a function of G_0 and ω, increasing at constant G_0 with ω, decreasing at constant ω with G_0, falling from 9.6 to 7.0 for some ω_0 (200 Hz), shows a similar but about 30% less steep drop, namely from 13.0 down to 11.0 for $17\omega_0$ (3322 Hz).

The intensity of the current was determined to depend on the frequency ω and the intensity of the excitation light G_0. Table 3.2 displays almost the same attitude but at a slightly lower level; n the exponent in the relationship $I_{ph} \propto T^n$ takes somewhat smaller values in the case of AsSeTe than in AsSeSb films. Figure 3.17 shows the dependence of photocurrent in a-AsSeTe on illumination, at –110 C, a temperature which is extremely difficult to get any sensible data for the other two, namely AsSe and AsSeSb, whose photoconductivities are much below that of AsSeTe. At the root of this difference of conductivities might lie the fact that Sb, as is given initially in the Experimental part, has an electronic configuration ending with $5p^3$, that is, a half-filled orbital which is reluctant to give an electron (one of the three in the p-subshell) and distort its relatively stable configuration, whereas Te, ending with $5p^4$ can readily give the fourth sharing one of the three p orbitals with another.

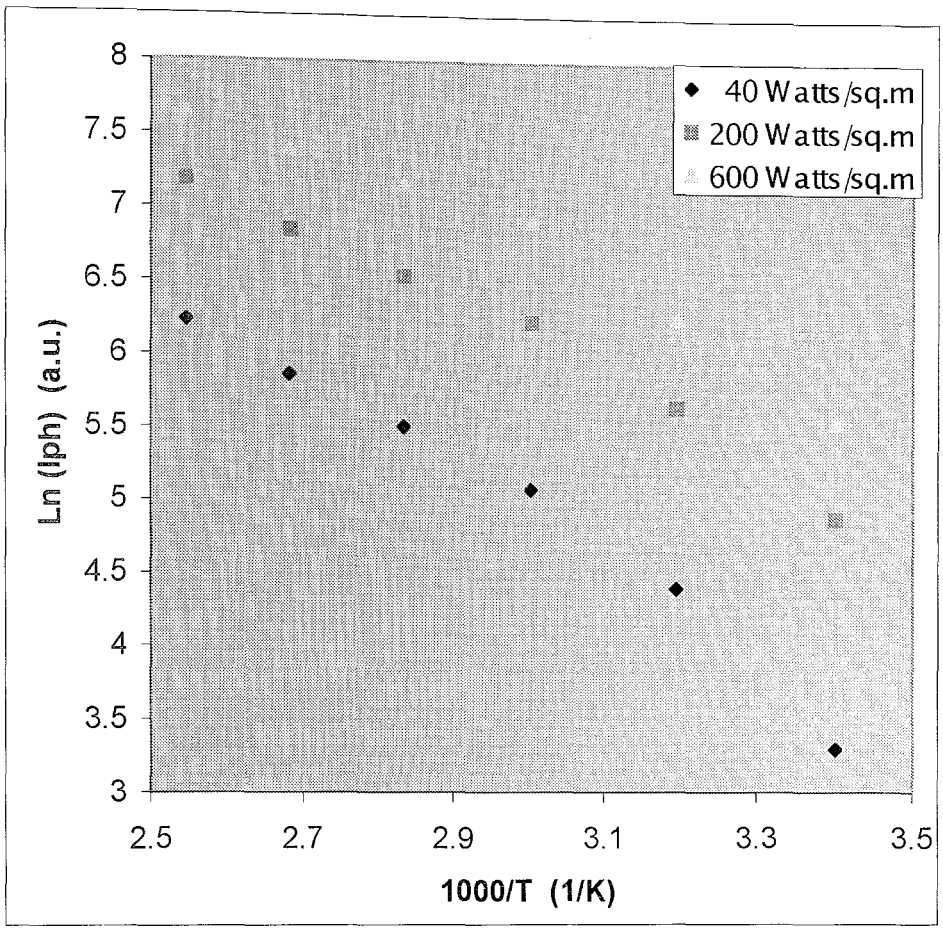

Figure 3.14. Temperature dependence of photocurrent in an a-AsSeSb sample for three excitation intensities, 600,200 and 40 Watts/m^2, taken at $\omega = 200$ Hz.

Exponent n ($I_{ph} \propto T^n$)	G_0 $(40 Watt/m^2)$	$5G_0$ $(200 Watts/m^2)$	$15G_0$ $(600 Watts/m^2)$
ω_0 (200 Hz)	9.6	7.6	7.0
$3.75\omega_0$ (762 Hz)	11.4	10.0	8.9
$(3.75)^2\omega_0$ (2911Hz)	13.4	11.4	10.8
$(3.75)^3\omega_0$ (10936Hz)	13.9	11.9	11.2

Table 3.1. The exponent n in the relation $I_{ph} \propto T^n$, for AsSeSb films, as a function of both the generation rate G and the frequency of excitation ω, within respectively 15-fold and 54-fold ranges.

Exponent n ($I_{ph} \propto T^n$)	G_0 $(40 Watt/m^2)$	$5G_0$ $(200 Watts/m^2)$	$15G_0$ $(600 Watts/m^2)$
ω_0 (45 Hz)	6.9	6.8	6.6
$6\omega_0$ (273 Hz)	7.7	7.6	7.2
$36\omega_0$ (1529Hz)	8.7	8.7	8.0
$200\omega_0$ (8488Hz)	10.4	10.1	8.7

Table 3.2. The exponent n in the relation $I_{ph} \propto T^n$, for AsSeTe films, as a function of both the generation rate G and the frequency of excitation ω, within respectively 15-fold and 200-fold ranges.

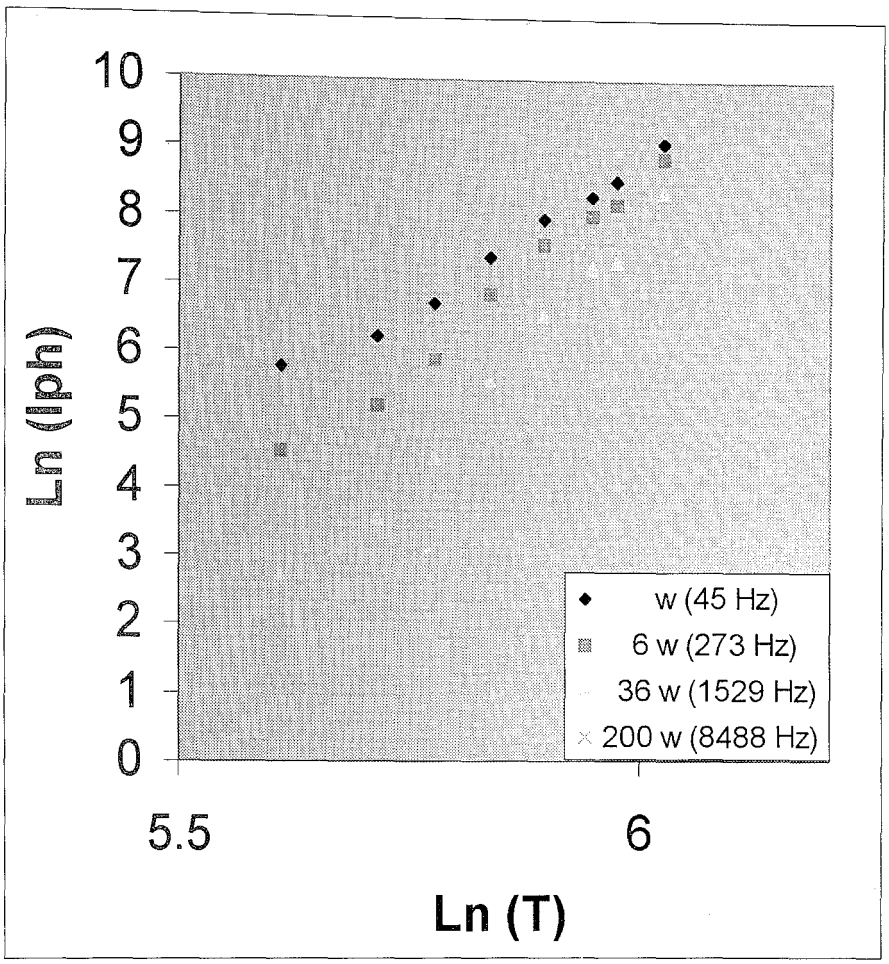

Figure 3.15. Temperature dependence of photocurrent in an a-AsSe sample at the excitation intensity of 600 Watts/m^2 and taken at four different frequencies.

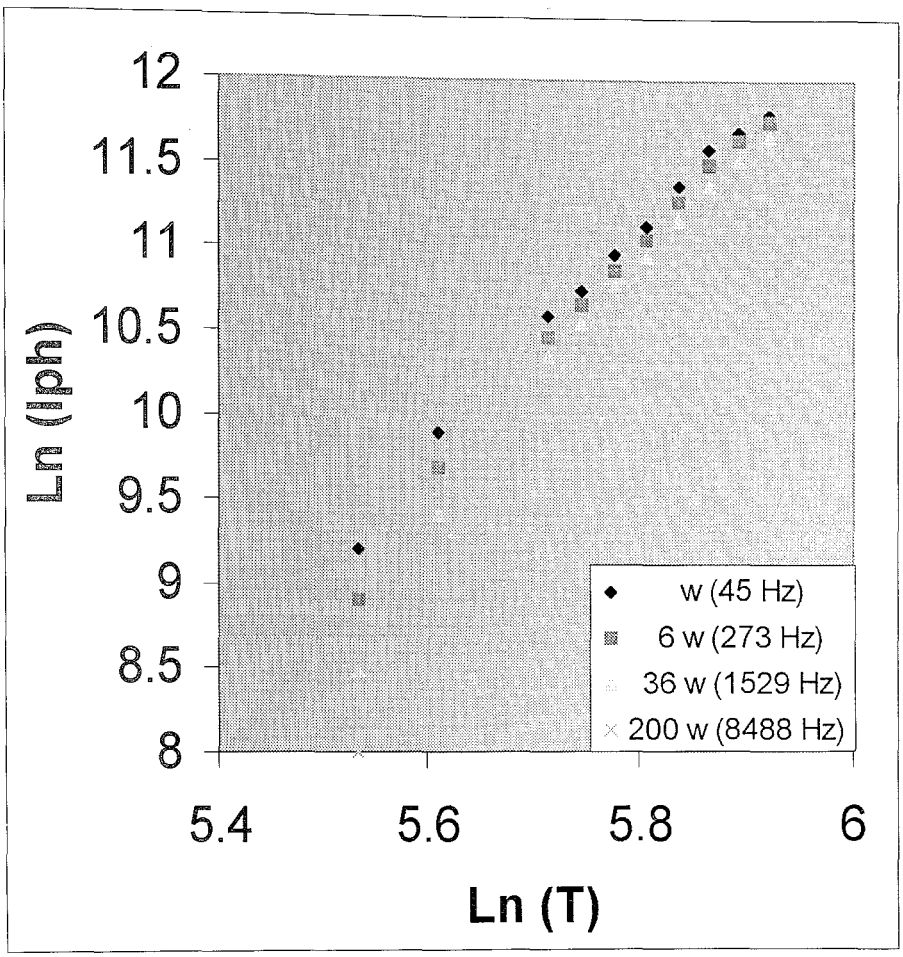

Figure 3.16. Temperature dependence of photocurrent in an a-AsSeTe sample at the excitation intensity of 600 Watts/m^2 and taken at four different frequencies.

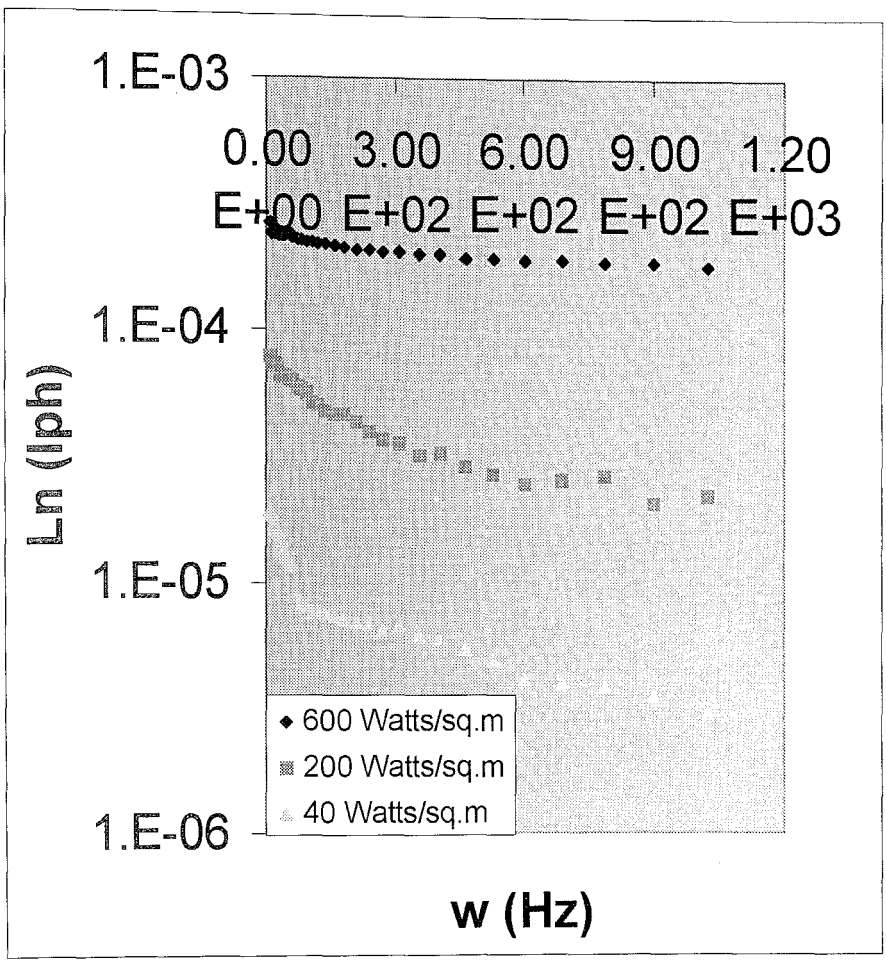

Figure 3.17. Frequency dependence of photocurrent in a-AsSeTe at –110 C, a temperature which is extremely difficult to get any sensible data for the other two, namely AsSe and AsSeSb, whose photoconductivities are much below that of AsSeTe.

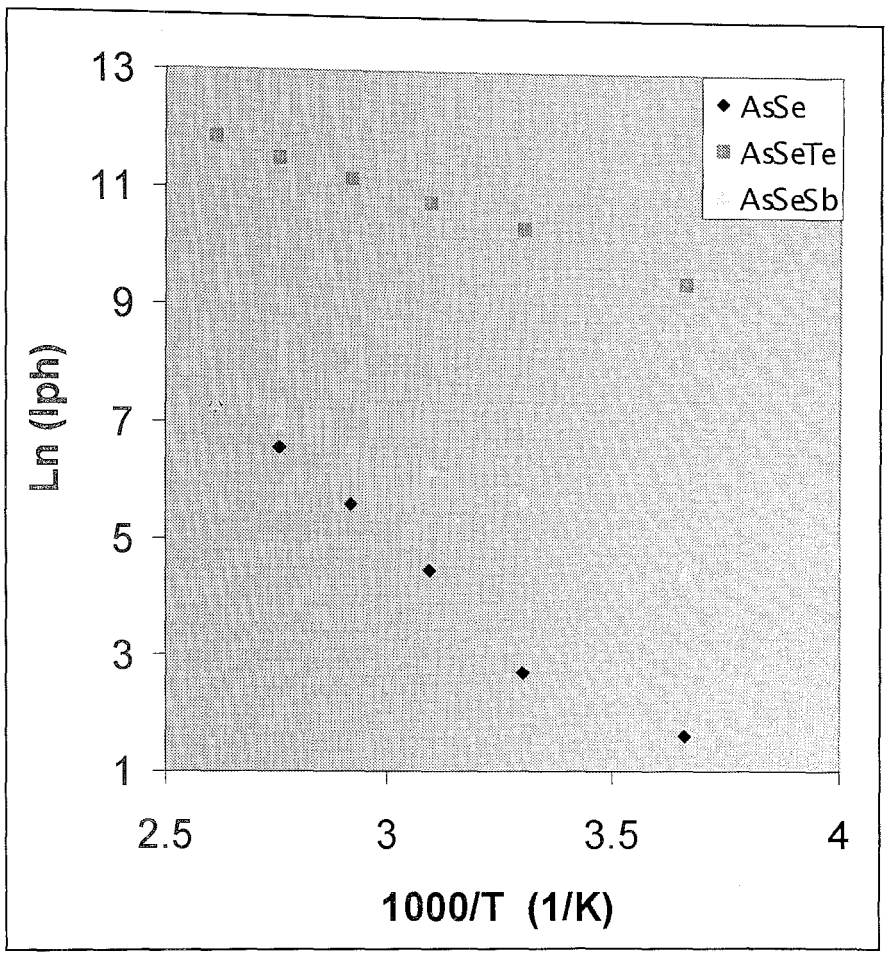

Figure 3.18. A comparison of the photocurrents in the three types of films, at the excitation intensity of 600 Watts/m^2 and ω=1529 Hz.

3.6. Dependence of Frequency Exponent on Generation and Temperature

As is seen from Figures 3.15 and 3.16, the photocurrent that shows an inverse relationship with frequency at each temperature value, drops logarithmically with temperature, the slope being slightly larger as the frequency of excitation is increased by equal ratios, namely, the slope decreases on the average, by 20% for each 3.75-fold rise in frequency for AsSeSb films. The photocurrent follows a relationship with temperature of the form $I_{ph} \propto G^{\gamma}$ and the exponent γ exhibits a gradual fall with T, from 0.92 down to 0.77 for the frequency of ω_0 (200 Hz), while from 0.69 down to 0.51 for $17\omega_0$ (3322 Hz), as depicted in Figure 3.19 for AsSeSb.

According to Rose (1978), an exponent of 1.0 in the relationship $I_{ph} \propto G^{\gamma}$, suggests that the recombination kinetics be *monomolecular,* while a 0.5 implies a *bimolecular* recombination. If the intensity dependence of the photocurrent is intermediate between 0.5 (*square root*) and 1.0 (*linear*), such as 0.72 as in the AsSeSb case, then it is indicative of a continuous and probably exponential distribution of traps in the gap. The values for the exponent γ lying between 0.56 and 1.0 for the a-AsSe samples were determined by Kaplan [16].

As can be observed from Figure 3.21, the photocurrent I_{ph} in AsSeSb varies as functions of both temperature T and frequency of modulation ω, at excitation intensities of 600, 200 and 40 Watts/m^2 and the exponent s in the relationship $I_{ph} \propto \omega^{s}$ (but not the photocurrent I_{ph}) increases proportionately with both the temperature and the intensity of excitation. The negative values of s grow as one goes to lower temperatures, namely, from -0.56 to -0.79 at respectively $390K$ and $280K$ for an excitation of 40 Watts/m^2; while they increase from -0.46 to -0.60 in the same range of T but for an excitation of 600 Watts/m^2.

The variation of the temperature dependence of the exponent n (in $I_{ph} \propto T^n$) can be seen in Figure 3.20, as a function of excitation for AsSeSb, at frequencies of 200 and 3322 Hz. The variation of n is nearly parallel for the two levels of generation but the values of the exponent being greater for the higher frequency meaning that the photocurrent becomes more temperature dependent as the frequency of the modulated excitation is increased.

Figure 3.21 depicts the temperature dependence of the exponent s (in $I_{ph} \propto \omega^s$) for AsSeSb, at excitation intensities of 600, 200 and 40 Watts/m^2. The variation of the frequency exponent s with temperature T is almost linear at a constant illumination but the slope of the exponent becomes less as the level of illumination is enhanced. It is also seen that the values of s are negative, that is, the photocurrent is inversely proportional to the frequency of the modulated signal, but that inverse proportinality gets less as the temperature increases and the rate of getting less grows as the level of illumination drops. Almost the same trend can be observed for AsSe in Figure 3.22.

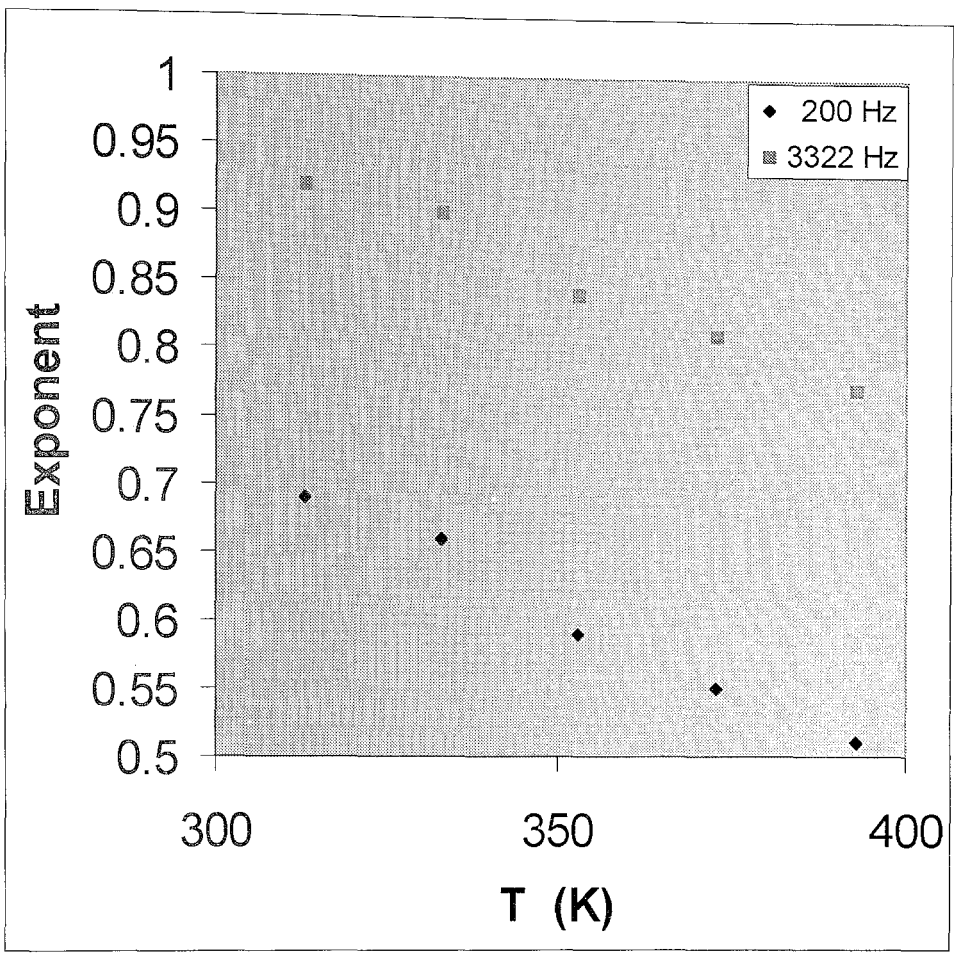

Figure 3.19. The temperature dependence of the exponent ν (in $I_{ph} = AG^{\nu}$) for AsSeSb, at frequencies of 200 and 3322 Hz.

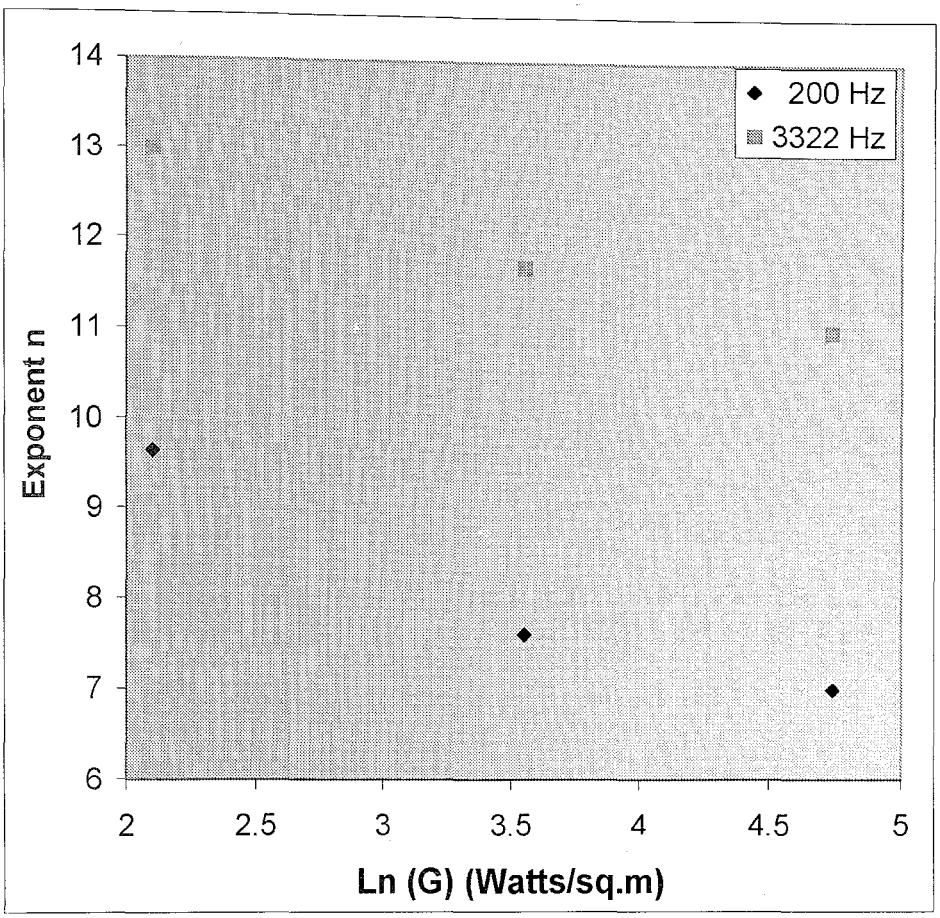

Figure 3.20. The variation of the temperature dependence of the exponent n (in $I_{ph} \propto T^{n}$) as a function of excitation for AsSeSb, at frequencies of 200 and 3322 Hz.

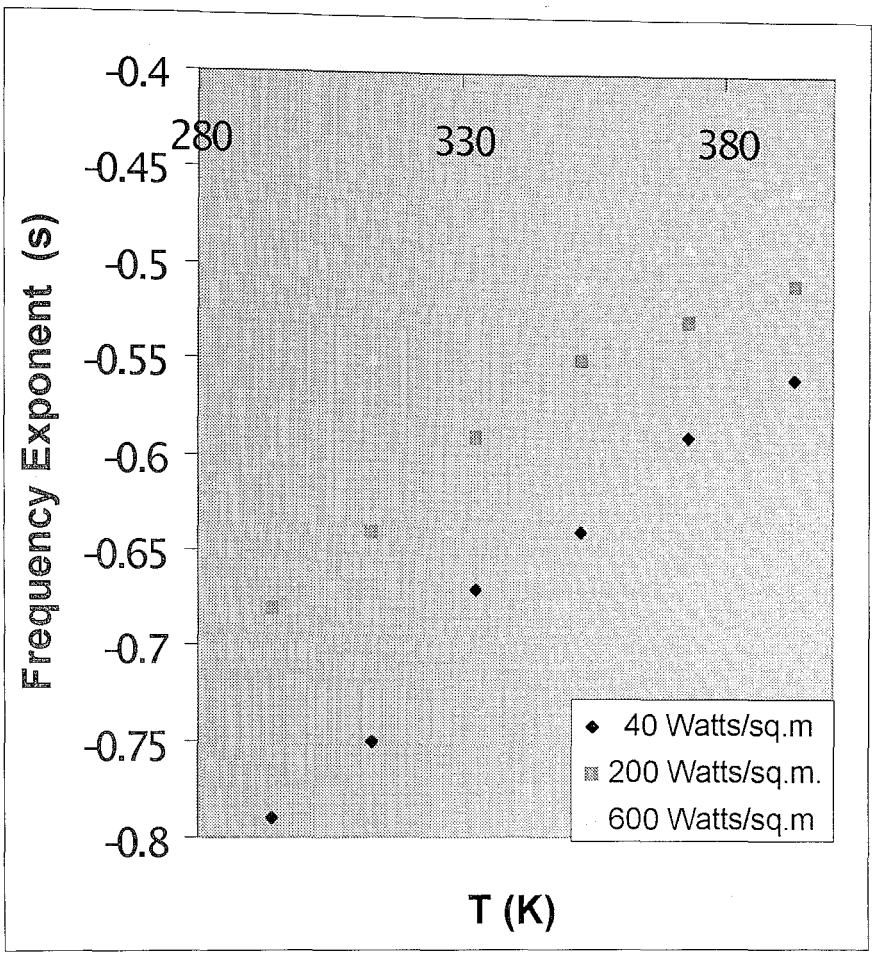

Figure 3.21. The temperature dependence of the exponent s (in $I_{ph} \propto \omega^{s}$) for AsSeSb, at excitation intensities of 600, 200 and 40 Watts/m^2.

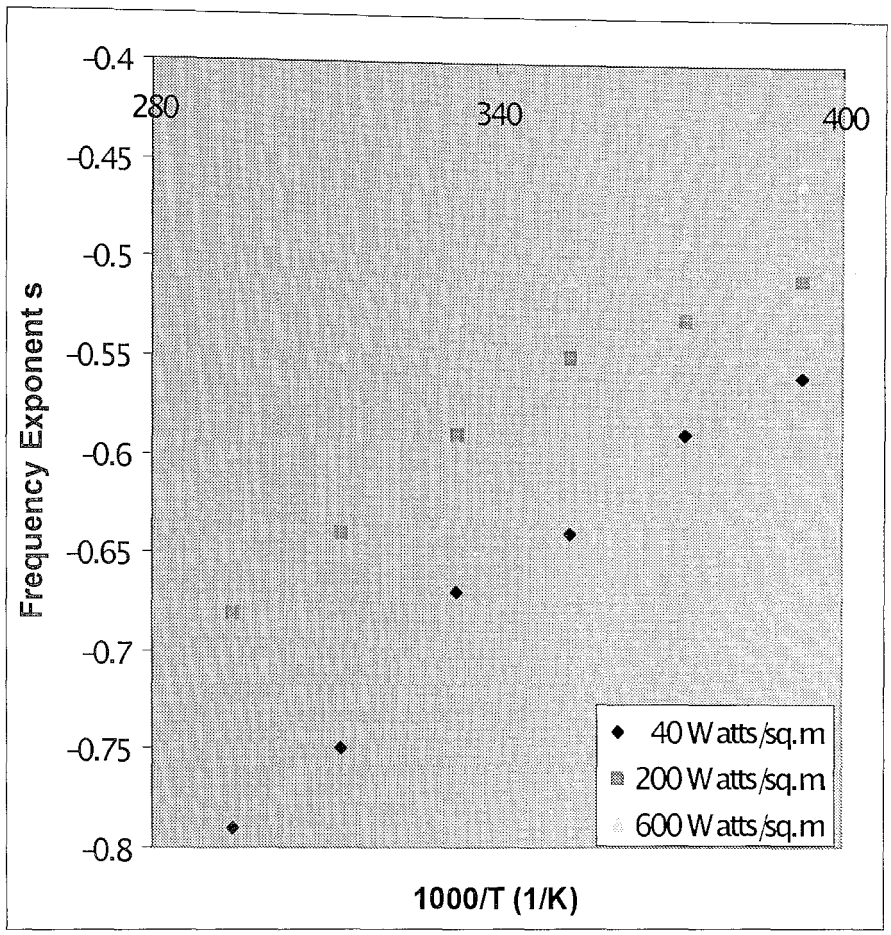

Figure 3.22. The temperature dependence of the exponent s (in $I_{ph} \propto \omega^{s}$) for AsSe, at excitation intensities of 600, 200 and 40 Watts/m^2.

4. CONCLUSION

The FRPC response of AsSeSb, AsSe and AsSeTe thin film samples was measured for the frequency range of 10 Hz to 1.1×10^4 Hz, (beyond which the data were not reliable), as a function of the intensity of the excitation and the temperature within a range of 230 K to 395 K, with the exception of the AsSeTe film at as low as 160 K. Since the carrier lifetimes turned out to depend on the intensity of the excitation light and the temperature, the recombination kinetics were decided to be performed by *distant pairs*. The lifetimes unveiled an activated behaviour with an activation energy of around 400 meV for an excitation intensity of 600 Watts/m^2, the dependence on the intensity being $\tau \propto G^{-0.46}$ at 295 K and $\tau \propto G^{-0.77}$ at 395 K. I_{ph}, the intensity of the photocurrent was found to depend on T (at fixed ω and G); on ω (at fixed T and G); and also on G (at fixed ω and T).

The photocurrent was measured to depend on the generation rate according to the formula $I_{ph} \propto G^{0.72}$, where the exponent 0.72 which is between 0.5 and 1.0 indicates that there are localized gap states in the mobility gap of the material. The temperature exponent n in the relationship $I_{ph} \propto T^n$ for AsSeSb has turned out to be between 7 and 10 for a frequency of some ω_0 (=200 Hz); and 11 and 13 for $17\omega_0$ (=3322 Hz); the value of the exponent showing a diminishing behaviour as the generation rate (intensity of excitation) is elevated. Similar results were obtained for the other films as well.

The photocurrent I_{ph} in the chalcogenide films varies as functions of both temperature T and frequency of modulation ω, at excitation intensities of 600, 200 and 40 Watts/m^2 and the exponent s in the relationship $I_{ph} \propto \omega^s$ (but not the photocurrent I_{ph}) increases proportionately with both the temperature and the intensity of excitation. The negative values of s grow as one goes to lower temperatures, namely, from -0.56 to -0.79 at respectively $390K$ and $280K$ for an excitation of 40

Watts/m^2; while they increase from –0.46 to –0.60 in the same range of T but for an excitation of 600 Watts/m^2.

APPENDIX A

Derivation of some of the results in the article "**Frequency-resolved Spectroscopy and its Application to the Analysis of Recombination in Semiconductors**" by Depinna, S.P. and Dunstan, D.J., *Phil. Mag. B*, Vol.50, 579, 1984.

$$I(\tau,t)=\int_{-\infty}^{t}\left(\frac{1}{\tau}\right)\exp\left[\frac{u-t}{\tau}\right]\left[G_0+g\sin(\omega u)\right]du=A+B \qquad (A.1)$$

where $A=\int_{-\infty}^{t}\left(\frac{G_0}{\tau}\right)\exp\left[\frac{u-t}{\tau}\right]du$ and $B=\int_{-\infty}^{t}\left(\frac{g}{\tau}\right)\exp\left[\frac{u-t}{\tau}\right]\sin(\omega u)du$

$$A=\int_{-\infty}^{t}\left(\frac{G_0}{\tau}\right)\exp\left[\frac{u-t}{\tau}\right]du=\frac{G_0}{\tau}\tau\exp\left[\frac{u-t}{\tau}\right]_{-\infty}^{t}=G_0(1-0)=G_0$$

and for B we can apply the method of integration by parts, setting

$z=\left(\frac{g}{\tau}\right)\exp\left[\frac{u-t}{\tau}\right]$ and $dv=\sin(\omega u)du$, then

$dz=\left(\frac{g}{\tau^2}\right)\exp\left[\frac{u-t}{\tau}\right]du$ and $v=-\left(\frac{1}{\omega}\right)\cos(\omega u)$

from $zv-\int vdz$

$$=\left(\frac{g}{\tau}\right)\exp\left[\frac{u-t}{\tau}\right]\left(-\frac{1}{\omega}\right)\cos(\omega u)\Big|_{-\infty}^{t}+\int_{-\infty}^{t}\left(\frac{g}{\omega\tau^2}\right)\exp\left[\frac{u-t}{\tau}\right]\cos(\omega u)du$$

$$=\left(-\frac{g}{\omega\tau}\right)\cos(\omega t)+\int_{-\infty}^{t}\left(\frac{g}{\omega\tau^2}\right)\exp\left[\frac{u-t}{\tau}\right]\cos(\omega u)du$$

applying the method of integration by parts to the second term as

$z=\left(\frac{g}{\omega\tau^2}\right)\exp\left[\frac{u-t}{\tau}\right]$ and $dv=\cos(\omega u)du$ then

$$dz = \left(\frac{g}{\omega\tau^3}\right)\exp\left[\frac{u-t}{\tau}\right]du \qquad \text{and} \qquad v = \left(\frac{1}{\omega}\right)\sin(\omega u) \qquad \text{it becomes}$$

$$\int_{-\infty}^{t}\left(\frac{g}{\omega\tau^2}\right)\exp\left[\frac{u-t}{\tau}\right]\cos(\omega u)du$$

$$=\left(\frac{g}{\omega\tau^2}\right)\exp\left[\frac{u-t}{\tau}\right]\left(\frac{1}{\omega}\right)\sin(\omega u)\Big|_{-\infty}^{t} - \int_{-\infty}^{t}\left(\frac{g}{\omega^2\tau^3}\right)\exp\left[\frac{u-t}{\tau}\right]\sin(\omega u)du$$

$$=\left(\frac{g}{\omega^2\tau^2}\right)\sin(\omega t) - \int_{-\infty}^{t}\left(\frac{g}{\omega^2\tau^3}\right)\exp\left[\frac{u-t}{\tau}\right]\sin(\omega u)du$$

now we see that, from the point where B was defined,

$$\int_{-\infty}^{t}\left(\frac{g}{\tau}\right)\exp\left[\frac{u-t}{\tau}\right]\sin(\omega u)du =$$

$$-\left(\frac{g}{\omega\tau}\right)\cos(\omega t)+\left(\frac{g}{\omega^2\tau^2}\right)\sin(\omega t) - \int_{-\infty}^{t}\left(\frac{g}{\omega^2\tau^3}\right)\exp\left[\frac{u-t}{\tau}\right]\sin(\omega u)du$$

therefore

$$\int_{-\infty}^{t}\left[\frac{g}{\tau}+\frac{g}{\omega^2\tau^3}\right]\exp\left[\frac{u-t}{\tau}\right]\sin(\omega u)du = -\left(\frac{g}{\omega\tau}\right)\cos(\omega t)+\left(\frac{g}{\omega^2\tau^2}\right)\sin(\omega t)$$

hence

$$\int_{-\infty}^{t}\exp\left[\frac{u-t}{\tau}\right]\sin(\omega u)du =$$

$$\left[-\frac{\cos(\omega t)}{\omega\tau}+\frac{\sin(\omega t)}{\omega^2\tau^2}\right]\frac{1}{\left[\frac{1}{\tau}+\frac{1}{\omega^2\tau^3}\right]} = \left[-\cos(\omega t)+\frac{\sin(\omega t)}{\omega\tau}\right]\left[\frac{\omega\tau^2}{1+\omega^2\tau^2}\right]$$

so that

$$\int_{-\infty}^{t}\exp\left[\frac{u-t}{\tau}\right]\sin(\omega u)du = \left[-\omega\tau\cos(\omega t)+\sin(\omega t)\right]\left[\frac{\tau}{1+\omega^2\tau^2}\right]$$

substituting this value in Eq. (A.1), the whole expression takes the form:

$$\int_{-\infty}^{t}\left(\frac{G_0}{\tau}\right)\exp\left[\frac{u-t}{\tau}\right]du+\int_{-\infty}^{t}\left(\frac{g}{\tau}\right)\exp\left[\frac{u-t}{\tau}\right]\sin(\omega u)du$$

$$=G_0+\left(\frac{g}{\tau}\right)\left[-\omega\tau\cos(\omega t)+\sin(\omega t)\right]\left[\frac{\tau}{1+\omega^2\tau^2}\right]$$

$$=G_0+\left(\frac{g}{1+\omega^2\tau^2}\right)\left[\sin(\omega t)-\omega\tau\cos(\omega t)\right] \qquad \text{(A.2)}$$

We set $\tan\phi=\omega t$ then

$$I(\tau,t)=G_0+\left(\frac{g}{1+\tan^2\phi}\right)\left[\sin(\omega t)-\tan\phi\cos(\omega t)\right]$$

$$=G_0+g\cos^2\phi\left[\frac{\sin(\omega t)\cos\phi-\sin\phi\cos(\omega t)}{\cos\phi}\right]$$

The lock-in output is

$$S(\tau)=\left(\frac{\omega}{2\pi}\right)\int_0^{2\pi/\omega}I(t)R(t)dt \qquad \text{(A.3)}$$

and for quadrature the lock-in response function $R(t)$ is given by

$R(t)=-\cos(\omega t)$ then

$$S(t)=\left(\frac{\omega}{2\pi}\right)\int_0^{2\pi/\omega}\{G_0+g\cos\phi[\sin(\omega t)\cos\phi-\sin\phi\cos(\omega t)]\}(-\cos(\omega t))dt$$

$$=\left(\frac{\omega}{2\pi}\right)\int_0^{2\pi/\omega}-G_0\cos(\omega t)dt-\left(\frac{g\omega}{2\pi}\right)\cos^2\phi\int_0^{2\pi/\omega}\sin(\omega t)\cos(\omega t)dt+\left(\frac{g\omega}{2\pi}\right)\sin\phi\cos\phi\int_0^{2\pi/\omega}\cos^2(\omega t)dt$$

$$=\left(\frac{\omega}{2\pi}\right)\left[-\frac{G_0}{\omega}\sin(\omega t)\right]_0^{2\pi/\omega}=\left(\frac{g\omega}{2\pi\omega}\right)\cos^2\phi\left(\frac{\sin^2(\omega t)}{2}\right)_0^{2\pi/\omega}+\left(\frac{g\omega}{2\pi}\right)\sin\phi\cos\phi\left(\frac{\pi}{\omega}\right)$$

$$=0-0+\left(\frac{g}{2}\right)\sin\phi\cos\phi=\left(\frac{g}{2}\right)\left(\frac{\omega t}{\sqrt{1+\omega^2\tau^2}}\right)\left(\frac{1}{\sqrt{1+\omega^2\tau^2}}\right)$$

$$=\left(\frac{g}{2}\right)\left(\frac{\omega t}{1+\omega^2\tau^2}\right) \qquad \text{(A.4)}$$

To obtain the response of the in-phase FRS method, it is merely necessary to replace $R(t)$ by

$R(t)=\sin(\omega t)$ then,

$S(\tau)=\left(\frac{\omega}{2\pi}\right)\int_0^{2\pi/\omega} I(t)R(t)dt$ becomes

$$S(\tau)=\left(\frac{\omega}{2\pi}\right)\int_0^{2\pi/\omega}[G_0+g\cos\phi\sin(\omega t-\phi)]\sin(\omega t)dt$$

$$=\left(\frac{\omega}{2\pi}\right)\int_0^{2\pi/\omega}G_0\sin(\omega t)dt+\left(\frac{g\omega}{2\pi}\right)\int_0^{2\pi/\omega}\cos^2\phi\sin^2(\omega t)dt-\left(\frac{g\omega}{2\pi}\right)\cos\phi\sin\phi\int_0^{2\pi/\omega}\cos(\omega t)\sin(\omega t)dt$$

$$=0+\left(\frac{g\omega}{2\pi}\right)\cos^2\phi\left(\frac{\pi}{\omega}\right)-0=\left(\frac{g}{2}\right)\cos^2\phi$$

$$=\left(\frac{g}{2}\right)\left(\frac{1}{1+\omega^2\tau^2}\right) \qquad \text{(A.5)}$$

REFERENCES

1. Madan, A. and Shaw, M. P., *The Physics and Applications of Amorphous Semiconductors*, Academic Press, Inc., 1988.

2. Ryvkin, S.M., *Photoelectric Effects in Semiconductors*, Consultants Bureau, 1964.

3. Oheda, H., "Phase Shift Analysis of Modulated Photocurrent: Its Application to the Determination of the Energetic Distribution of Gap States", *J.Appl. Phys*, Vol.**52** (11), November 1981.

4. Aktaş, G. and Skarlatos, Y., "Determination of the Gap Density of States in Amorphous Silicon by Phase Shift Analysis of the Modulated Photocurrent", *J.Appl. Phys*, Vol.**55** (10), May 1984.

5. Depinna, S.P. and Dunstan, D.J., "Frequency-resolved Spectroscopy and its Application to the Analysis of Recombination in Semiconductors", *Phil. Mag. B*, Vol.**50**, 579, 1984.

6. Dunstan, D.J., "Kinetics of Distant Pair Recombination I. Amorphous Silicon Luminescence at Low Temperature", *Phil. Mag. B.*, Vol.**46**, 579, 1982.

7. Kasap, S.O., *Principals of Electrical Engineering Materials and Devices*, McGraw-Hill, 1997.

8. Adler, D., *Amorphous Semiconductors*, CRC Press, Ohio, 1971.

9. Çil, C.Z., *Study of Evaporated Amorphous Silicon Films By Frequency Dependent Conductivity and Phase Shift Analysis of Modulated Photocurrent Methods*, Boğaziçi University, 1989.

10. Eşme, İ., *Hacimli Kalkojen Camlarının Elektriksel İletim Özellikleri*, Ph.D. Thesis, Yıldız Üniversitesi, 1983.

11. Rose, A., *Concepts in Photoconductivity and Allied Problems*, Interscience Publishers, 1963.

12. Dunstan, D.J., "Kinetics of Distant Pair Recombination II. Tunnelling Nonradiative Recombination", *Phil. Mag. B*, Vol.**49**, 191, 1984.

13. Tsang, C. and Street, R.A., "Recombination in Plasma-deposited Amorphous Si:H. Luminescence Decay ", *Physical Review B.*, **19**, 3027, March 1979.

14. Karabulut, Ö., *Film Halindeki Üçlü Amorf Kalkojen Alaşımlarında Elektriksel Özellikler ve İletim Mekanizmaları*, Yıldız Üniversitesi, 1983.

15. Kaplan, R., "Photoconductivity in a-SeTe ", *J. Phys. Condens. Matter* 7, 1995.

16. Kaplan, R., "Frequency-resolved Photoconductivity Studies in Amorphous As_2Se_3", *Philosophical Magazine B*, Vol 74, 1, 1996.

17. Eşme, İ., Çil, C.Z. and Aktaş, G., "Frequency Dependent Conductivity in As_2Se_3 and As_2Se_3+15% Sb ", *Appl. Phys. A.*, 51, 481, 1990.

REFERENCES NOT CITED

Bort, M., Fuhs. W., Liedtke, S., Stachowitz, R., "Geminate Recombination in a-Si:H", *Phil. Mag. Lett.*, Vol.**64**, 227, 1991.

Dunstan, D.J., Depinna, S.P., Cavenett, B.C., "A Direct Determination of the Lifetime Distribution of the 1.4 eV Luminescence of a-Si:H", *J.Phys.C: Solid State Phys.*, Vol.**30**, L425-L429, 1982.

Shockley, W., Read, W.T., "Statics of the Recombinations of Holes and Electrons", *Physical Review*, Vol 87, 5, September 1952.

Searle, T.M., "Quenching of Luminescence by Nonradiative Tunnelling", *Philosophical Magazine B*, Vol.**46**, 2, 1982.

Searle, T.M., "On Carrier Densities and Lifetimes in a-Si:H at Low Temperature", *Philosophical Magazine B*, Vol.**61**, 4, pp.251-258, 1990.

Searle, T.M., Nashashibi, T.S., Austin, I. G., "Radiative and Nonradiative Tunnelling in Glow-Discharge and Sputtered Amorphous Silicon", *Phil. Mag. B*, Vol.**39**, 389, 1979.

Simmons, J.G., Taylor, G,W., "Nonequilibrium Steady-State Statistics and Associated Effects for Insulators and Semiconductors Containing an Arbitrary Distribution of Traps", *Physical Review B*, Vol.**4**, 2, July 1971.